Final Report

Project 24-007

Texarkana Intensive Campaign

Prepared for:

Air Quality Research Program (AQRP)

The University of Texas at Austin

Prepared by:

University of Houston (UH)

Aerodyne Research, Inc.

Baylor University (BU)

August 29, 2025

QA Requirements: Audits of Data Quality – 10% minimum required; Report of findings in this report.

This study was supported by funding from the Texas Commission on Environmental Quality (TCEQ). The findings, opinions, or conclusions expressed do not necessarily represent those of the TCEQ.

EXECUTIVE SUMMARY

The goal of this project (24-007) was to investigate the sources of elevated particulate matter concentrations in the Texarkana area. A three-week field measurement campaign was conducted from February 10 to March 2, 2025 to characterize the chemical composition of both particle and gas phase species during high-loading events to provide insights into source contributions. The area surrounding the City of Texarkana has large pulp and paper industrial activities. This includes two independently operated plants: Domtar Ashdown Mill in Ashdown, AR, and the Graphic Packaging International Mill located south of Texarkana near Domino, Texas.

To conduct these measurements, the University of Houston deployed an instrumented mobile laboratory carrying a wide suite of trace gas and aerosol instrumentation from the University of Houston and Baylor University. This was performed in collaboration with Aerodyne Research, who deployed their miniature Aerodyne Mobile Laboratory instrumented with multiple volatile organic compound analyzers, including a Thermal Desorption Pre Concentration–Gas Chromatography system and a Vocus Proton Transfer Reaction – Time of Flight Mass Spectrometer in addition to global positioning and meteorological equipment.

Although the actual weather conditions were not as expected, with few persistent southerly winds and an unusual cold snap which brought snow and extended periods below freezing, the measurements were successful in isolating and characterizing plumes from the two large mill sources in the area as well as from several smaller point sources.

The data shows that the plume from the Domtar plant did reach the Texarkana C1031 monitoring site on at least one occasion during the measurement period, and the Graphics Packaging International plume persisted for distances that could impact C1031 under different wind conditions. Although both mills appear similar, they produce different products through a variety of practices and schedules, which results in their plumes presenting unique characteristics.

When not driving, the mobile laboratories were parked side-by-side at a location southwest of Texarkana, allowing the instruments to continue sampling while plugged into utility power. On several occasions, elevated aerosol and gas phase measurements were recorded while stationary. On the night of February 27–28, 2025 a broad plume bore the characteristics of the Domtar facility, which was supported with trajectory and dispersion modeling. Larger aerosol peaks also occurred during this time, but the mass spectra of the chemical composition indicated that these were likely more related to traffic emissions and were overlaid on top of the paper mill plume.

This project showed not only great success in characterizing aerosol emission sources impacting the Texarkana, TX area, but it also demonstrated the feasibility and benefits of pairing multiple mobile laboratories together to sample in tandem or in more complex route designs to address questions at a larger scale. The dataset generated by this project is ripe for deeper analysis to elucidate additional insights regarding aerosol chemistry and composition in Texarkana. Future sampling opportunities may include routine filter collections for positive matrix factorization analysis paired with aerosol optical properties, which can support the identification of biomass burning influence, crustal dust, and potential particulate matter from paper mills.

Table of Contents

List of Figures

List of Abbreviations and Acronyms

AAE	Absorption Ångström Exponent
AQRP	Air Quality Research Program
AR	Arkansas
AMS	Aerosol Mass Spectrometer
amp	ampere
BPP	Bivariate Polar Plot
BU	Baylor University
°C	Celsius
CAA	Clean Air Act
CBPF	Conditional Bivariate Probability Function
CE	Collection efficiency
Chl	Chloride
CLAP	Continuous Light Absorption Photometer
CO	carbon monoxide
CO_2	carbon dioxide
CPC	Condensation Particle Counter
DMA	Differential Mobility Analyzer
E	east
EPA	Environmental Protection Agency
ft	foot
GAW	Global Atmosphere Watch
GPI	Graphic Packaging International
GPS	Global Positioning System
GPT	Gas Phase Titration
HCHO	Formaldehyde
HEPA	High Efficiency Particulate Air
hr	hour
HR-ToF-AMS	High-Resolution Time-of-Flight Aerosol Mass Spectrometer
Hwy	Highway
IE	ionization-efficiency
jNO_2	Photolytic rate coefficient measurements of nitrogen dioxide
km	kilometer
kW	Kilowatt
Lidar	Light Detection and Ranging
LED	Light Emitting Diodes
LLOD	Lower Limit of Detection
LOD	Limits of detection
MAQL3	Mobile Air Quality Lab 3
mbar	millibars
MFC	mass flow controller
mi	miles
min	minutes
minAML	miniature Aerodyne Mobile Laboratory
ml	milliliters
mm	millimeters

mph	miles per hour
M/m^{-1}	inverse megameters
m/s	meters per second
m/z	mass-to-charge ratio of an ion
NE	northeast
NEMA	National Electrical Manufacturers Association
NH_4	Ammonium
NIST	National Institute of Standards and Technology
nm	nanometers
NO	Nitric Oxide
NOAA	National Oceanic and Atmospheric Administration
NO_X	Nitrogen Oxides
NOy	Reactive nitrogen compounds
NO_2	Nitrogen Dioxide
NO_3	Nitrate
NW	northwest
OD	outside diameter
Org	Organics
O_3	Ozone
PC	Ruggedized industrial computer
PFA	perfluoroalkoxy alkane
PID	proportional-integral-derivative
PM	Particulate matter
PM_1	Particulate matter 1 micron or less
$PM_{2.5}$	Particulate matter 2.5 microns or less
PMF	Positive Matrix Factorization
POPS	Portable Optical Particle Spectrometer
ppbv	parts per billion by volume
ppm	parts per million
psi	Pounds per square inch
PToF	particle time-of-flight
PTR-MS	Proton Transfer Reaction – Mass Spectrometry
PTR-TOFMS	Vocus Proton Transfer Reaction – Time of Flight Mass Spectrometer
QAPP	Quality Assurance Project Plan
QA/QC	Quality Assurance/Quality Control
RH	Relative Humidity
RRAD	Red River Army Depot
SAE	Scattering Ångström Exponent
sccm	standard cubic centimeters per minute
SE	southeast
SLPM	Standard Liters Per Minute
SO_2	Sulfur dioxide
SO_4	Sulfate
SW	southwest
TAP	Tricolor Absorption Photometer
TCEQ	Texas Commission on Environmental Quality

TDPC-GC	Thermal Desorption Pre Concentration – Gas Chromatography
TX	Texas
UH	University of Houston
UHP N2	ultra-high purity nitrogen
UV	Ultraviolet
VAC	volts alternating current
VOC	Volatile Organic Compound
W	west
wd	wind direction
ws	wind speed
ZAG	Zero Air Generator
µm	micrometer
σabs	aerosol light absorption coefficients
σscat	aerosol scattering coefficients
σbscat	particle back-scatter coefficients
#/cm^3	particle counts per cubic centimeter

1. INTRODUCTION

The University of Houston's Mobile Air Quality Lab 3 (MAQL3) and the miniature Aerodyne Mobile Lab (minAML) partnered to conduct mobile air quality measurements in the Texarkana area during a three-week field measurement study from February 10 to March 2, 2025. The Texarkana, Texas-Arkansas (TX-AR) metropolitan area has recently become an area of concern due to elevated levels of particulate matter 2.5 microns and smaller ($PM_{2.5}$). This area is forested and contains a few large paper mills, which are potential sources of PM in Texas, Arkansas, and Louisiana. There are other possible industrial sources of $PM_{2.5,}$ and it is possible that the $PM_{2.5}$ is being advected into the area from sources well outside of the area. The upcoming changes to the regulatorily acceptable $PM_{2.5}$ levels necessitate a better understanding of the cause of these enhanced $PM_{2.5}$ levels in the Texarkana area. A comprehensive study of the particles and gas phase chemical species associated with these $PM_{2.5}$ exceedance episodes can assist in interpreting the sources of these air pollutants.

The area surrounding the City of Texarkana has pulp and paper industrial activities. This includes two independently operated plants: Domtar Ashdown Mill in Ashdown, AR, and the Graphic Packaging International (GPI) mill located south of Texarkana near Domino, TX. These facilities were identified by signage visible from the road as well as online resources, but it is possible that other companies may operate adjacent to or in close proximity to these plants.

This project was focused on measuring aerosols, volatile organic compounds (VOCs), and trace gases, including sulfur dioxide (SO_2), carbon monoxide (CO), ozone (O_3), nitric oxide (NO), nitrogen dioxide (NO_2), and other reactive nitrogen compounds (NO_y) around the Texarkana area. To conduct these measurements the University of Houston deployed an instrumented mobile laboratory (**Figure 1** and **Figure 2),** carrying a wide suite of trace gas and aerosol instrumentation from the University of Houston and Baylor University. The MAQL3 team conducted targeted sampling as well as exploratory and stationary measurements. **Figure 3** displays the Global Positioning System (GPS) track of the MAQL3 throughout the campaign.

Aerodyne Research deployed the minAML instrumented with multiple VOC analyzers, including a Thermal Desorption Pre Concentration–Gas Chromatography (TDPC-GC) and Vocus Proton Transfer Reaction – Time of Flight Mass Spectrometer (PTR-TOFMS), in addition to global positioning and meteorological equipment. This platform provided mobile measurements with a smaller instrument footprint. Sample inlets collected ambient samples from a boom over the vehicle hood with instruments switching between real-time (i.e., 1 Hertz) and time-integrated measurements (i.e., Gas Chromatography sample collection). Real-time measurements allow for mobile plume detection, while stationary measurements can be used to further characterize the chemical makeup of the target plume.

Figure 1. *The UH Mobile Air Quality Lab-3 (left) parked at the Texarkana RV Park and Event Center for stationary measurements next to the Aerodyne minAML (right). Photo taken during the AQRP Texarkana Field campaign after a light snow shower.*

Figure 2. *Inside of MAQL3 while installing Baylor University instruments (left) and looking forward from the rear of the box at University of Houston instruments (right).*

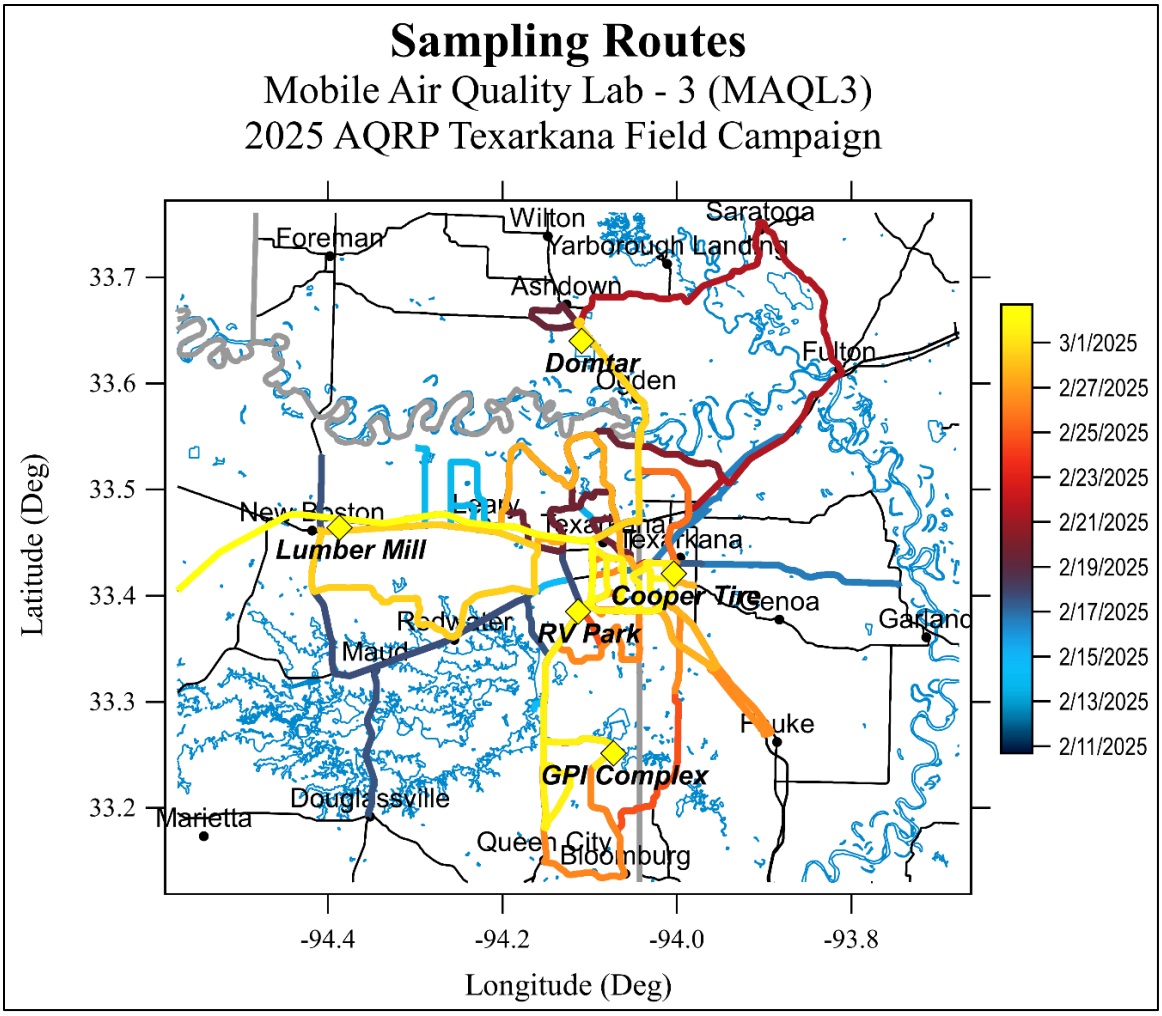

Figure 3. *Sampling routes for MAQL3 mobile measurements during the AQRP Texarkana field campaign are colored by time.*

2. OBJECTIVES

The goal of this project was to investigate the sources of elevated $PM_{2.5}$ concentrations in the Texarkana area during a three-week field measurement campaign from February 10 to March 2, 2025. The study characterized the chemical composition of both particle and gas phases during high-loading events to provide insights into source contributions and associated health risks. The findings will support policymakers in identifying effective mitigation strategies. The specific objectives of this study include:

- Characterization of selected $PM_{2.5}$ and VOC point sources in the Texarkana area.
- Assess background $PM_{2.5}$ levels near and upwind of the Texarkana TX-AR metropolitan area, including measurements beyond Texas state boundaries, without focusing on detailed emission factors from out-of-state sources.
- Investigation of any highly local effects that might be present and impacting the measurement of $PM_{2.5}$ at the Texarkana New Boston Station (C1031).
- Assessing the potential impacts of ozone in Texarkana, focusing on whether O_3 levels influenced air quality or indicated active photochemical processes during the monitoring period.

3. METHODOLOGY

3.1. Methodology Summary

The UH Mobile Air Quality Lab and the miniature Aerodyne Mobile Lab were equipped with instruments for near-continuous air sampling, producing 1-second data and supported by GPS and meteorological sensors. During the three-week campaign, both labs operated from a base at the Texarkana RV Park, using shore power or onboard generators. Mobile and stationary measurements were guided by prevailing meteorological conditions, with plume transects conducted upwind of Texarkana to track emissions. Wind profiles were used to target specific sources, and instrument operation resumed within minutes after any power transitions.

3.2. Stationary Sampling Site

Texarkana RV Park, the primary base location for this study, was located in the southwestern corner of Texarkana. This site was selected due to its accessibility to 30 and 50-ampere (amp) electrical connections and its relatively low background interference from industrial sources. Its geographic position also provides a favorable upwind sampling location for Texarkana under prevailing southwest wind conditions. Overnight monitoring at the RV Park provided background data, while daytime efforts focused on source characterization throughout the region.

3.3. Field Campaign

Mobile sampling was conducted on days where wind and precipitation conditions were favorable for sampling targeting potential aerosol sources, the vicinity of monitor C1031 (approximately 5 miles away), and additional upwind locations. Depending on meteorological conditions and daily objectives, the two mobile laboratories operated either together or independently to maximize spatial coverage.

MAQL3 conducted mobile operations on 15 days during the campaign, and the Aerodyne minAML was mobile on 16 days. While MAQL3 and the minAML usually conducted mobile operations simultaneously, due to the size and operating requirements of the larger MAQL3, there were occasions when the minAML was able to perform mobile sampling while MAQL3 remained stationary. These occasions were typically a result of a narrow window of favorable conditions or a lack of known traversable roads in the sampling area where large trucks were allowed.

3.4. Instrumentation

The deployment utilized the MAQL3, a highly modified 2018 Freightliner M2-106 crew cab straight truck with a 24-foot (ft) cargo box converted to a laboratory. Instrumentation racks and supplies were secured via aircraft seat track-style mounting strips, which allowed for a variety of attachment options and were adjustable in 1-inch increments. The floor tracks were standardized side to side and front to rear to ensure that racks and equipment could be easily and securely

repositioned within the space. The walls, ceiling, and exterior roof were also equipped with the same tracks to facilitate mounting power outlets, routing of cabling and sample lines, and to secure supplies such as gas cylinders and ladders. All data acquisition systems were networked and accessible from the front seats, allowing the operators to monitor and control the instrumentation from the safety of the cab and provide real-time feedback to each other and the driver to guide the next steps during the sampling activities. Power was supplied by a 20-kilowatt (kW) diesel generator mounted under the cargo box. This generator drew fuel from the main fuel tanks on the truck, allowing for extended run times. Power was fed to the lab space via two 50-amp 120/240 volts alternating current (VAC) load centers, which could be operated from the generator or powered by separate shore power connections from any standard National Electrical Manufacturers Association (NEMA) 14-50R, such as is commonly found in RV parks and event spaces.

The inlet system, meteorology, and GPS sensors were mounted at the end of a horizontal tower structure overhanging the front of the truck such that measurements were made at approximately 10 ft above the ground. The length of the structure places the inlet system roughly 2 ft forward of the front bumper of the truck, which helped ensure the samples were not impacted by the vehicle itself or the exhaust from the diesel generator. The photolysis rate of nitrogen dioxide (jNO_2) was measured by a radiometer mounted on the roof of MAQL3, pointing straight upward.

MAQL3 measured trace gases, meteorological parameters, and aerosol optical properties. Trace gases measurements included O_3 by chemiluminescence with NO, nitric oxide by chemiluminescence with O_3, nitrogen dioxide by chemiluminescence with O_3 after reduction to NO by Ultraviolet Light Emitting Diodes (UV-LED) photolysis, total reactive nitrogen by chemiluminescence with O_3 after reduction by a 300 degree Celsius (°C) molybdenum converter at the sample inlet, CO by off-axis cavity ringdown, and SO_2 by ultraviolet (UV) pulsed fluorescence. Formaldehyde (HCHO) was measured by using the Hantzsch reaction and fluorescence light technique. All gases (except NO_y) were sampled through weekly-changed 47 millimeters (mm) Teflon filters on perfluoroalkoxy alkane (PFA) lines. Aerosol number and size distributions were measured with a Handix Portable Optical Particle Spectrometer (POPS). Aerosol light absorption was quantified at 365, 528, and 652 nanometers (nm) using a Brechtel Tricolor Absorption Photometer (TAP), while scattering and backscattering at 450, 550, and 700 nm were measured with a TSI 3563 nephelometer. The non-refractory PM_1 chemical composition was determined using an Aerodyne Aerosol Mass Spectrometer (AMS), calibrated regularly for ionization efficiency and air beam signal. Collection efficiency (CE) was assumed as 0.5 for sulfate, nitrate, and ammonium, and 0.7 for organics based on size distributions.

Meteorological and GPS parameters were measured continuously on MAQL3 with an Airmar 220WX with a relative humidity (RH) module. This sensor measured wind speed, wind direction, temperature, pressure, relative humidity, as well as GPS data, which was used to calculate parameters such as vehicle speed and direction internally and was used to correct the measured wind directions. These data were recorded in the trace gas data system and

synchronized to those measurements upon collection. Winds while in motion are less likely to be representative of the mean wind field, as the measured winds are subject to the wake of passing vehicles, obstructions from signs, trees, and buildings. Therefore, only stationary winds (vehicle speed < 1 miles per hour (mph)) were reported for this project as they were more representative of the overall flow. Additional measurements of the planetary boundary layer height by aerosol Light Detection and Ranging (Lidar) backscatter and photolysis rate of nitrogen dioxide by filter radiometer were also included in this measurement package.

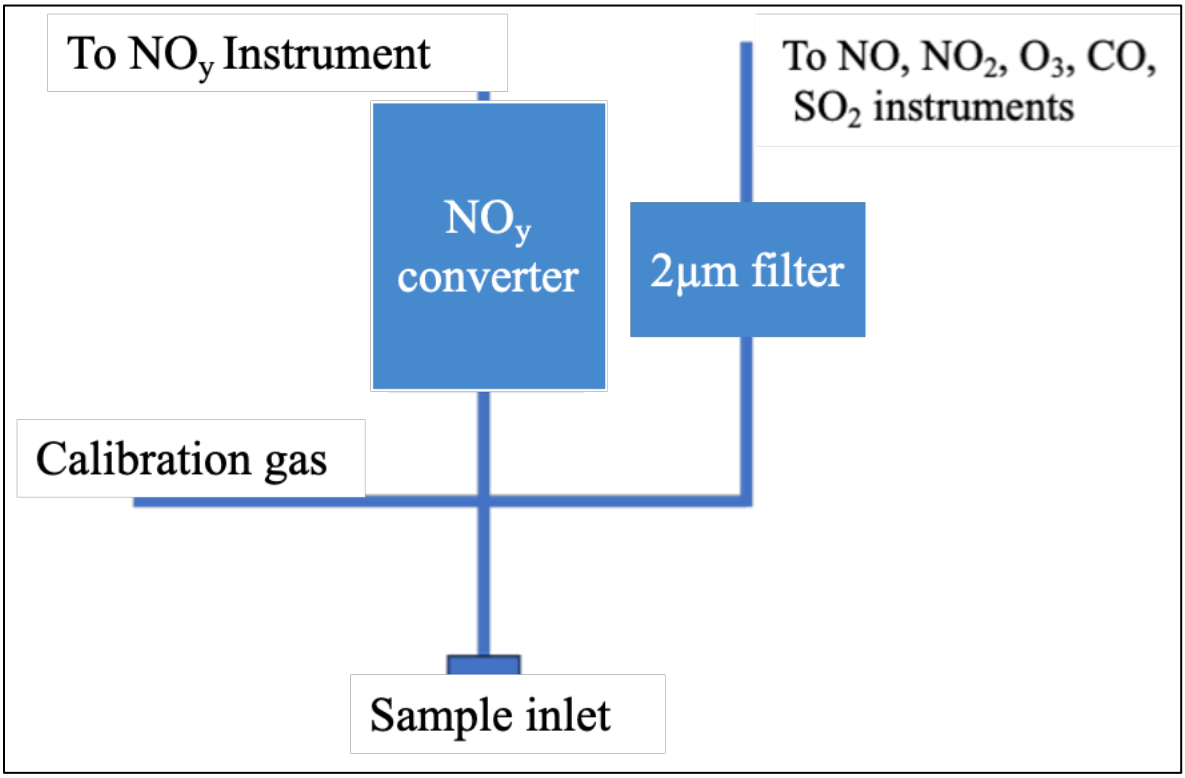

Figure 4. *Simplified schematic of the trace gas inlet system on MAQL3.*

Figure 4 shows a simplified schematic for the trace gas inlet system. Other gas inlet systems followed similar methodologies. A 47-millimeter Teflon filter support grid was installed on the inlet tube to prevent bugs and water from entering the sample lines and extended approximately 2–3" outside of the inlet box. Immediately inside the box, a Teflon cross union (four ports) was used to connect the molybdenum converter for the NO_y instrument, trace gas line to the instrumentation, and calibration line. Calibration gas was delivered to the inlet upstream of the converter and a 1.2 micrometers (µm) particle filter to calibrate through as much of the sample system as possible. This method of calibration allowed for verification that there were no leaks in the sample system and to account for any losses that may occur in the sample lines or filters.

VOC speciation was conducted using a Proton Transfer Reaction–Mass Spectrometry (PTR-MS) and a Thermal Desorption Pre Concentration–Gas Chromatography (TDPC-GC) system onboard the mobile lab. PTR-MS provided real-time VOC data with automated zero/calibration modes.

The two-channel TDPC-GC enabled offline analysis of high- and mid-volatility VOCs, operating in ambient, zero, and calibration modes with 4–10 hours (hr) cycles depending on platform status. For details on PTR-MS, see Krechmer et al. [2018].

The rapid measurement of VOCs on board the miniAML was key to assist in the attribution of overall enhanced particle and gas phase signals to specific sources. Vehicular, biomass burning, and industrial VOC markers are all rapidly quantified and displayed in real-time, informing decisions regarding placement of both mobile laboratories to better determine sources.

3.4.1. Proton Transfer Reaction Mass Spectrometer (PTR-MS) Instrument Assessment

The PTR-MS instrument provides a measurement of a selected set of organic gases possessing proton affinities greater than water. Most unsaturated VOCs possessing more than 2 carbons can be detected using the PTR-MS. This instrument is located immediately behind the driver in the mobile laboratory to minimize the length of the sampling inlet.

The PTR-MS parameters drift tube pressure, detection region pressure, drift tube temperature, and reagent ion intensity should always be within the following specifications:

Drift tube pressure = 2.1 (± 0.05) millibars (mbar)
Detection region pressure < 45 x 10^{-6} mbar
Drift tube temperature 60 (± 1) ^{o}C

The drift tube pressure and temperature are automatically controlled and maintained via a proportional-integral-derivative (PID) feedback loop.

The PTR-MS used a tap from the VOC sample inlet – shared with the TDPC-GC through a short length, ~ 4 feet, of 1/4” outside diameter (OD) PFA tubing, with a sample pump pulling at 2.2 standard liters per minute (SLPM) to minimize residence time but maintain laminarity. The PTR-MS draws 0.25 SLPM of this flow into the instrument for analysis and the rest is exhausted through the sample pump.

The PTR-MS has three modes of operation: measure, zero and calibrate. Zero and calibration periods are automatically actuated at pre-defined intervals using electronically controlled solenoid valves. The measure, calibrate and zero modes are fully automated.

Instrument zeros were software-controlled and scheduled to occur at a regular specified interval using an on-board zero air generator (ZAG). The PTR-MS uses a 3-way solenoid valves to overflow the instrument inlet with zero air at a flow rate (nominal 0.4 SLPM) greater than the instrument draw. The excess zero gas was vented via the PTR-MS sample pump, and therefore the zero (and calibrate) mode did not affect the TDPC-GC, which was also on the VOC sample inlet.

VOC free air was produced by pulling filtered ambient air through a heated oxidation catalyst. A ¾" OD stainless steel tube packed with a 50:50 mix of Platinum and Palladium coated alumina

beads is housed within a small oven that is heated to 400 °C and oxidizes any VOCs to carbon dioxide (CO_2). Instrument background is mass-dependent, with some ions having non-zero values. Atmospherically persistent compounds such as acetone (m/z 59) exhibited discernible decreases in their ion intensities when the PTR-MS was sampling zero air.

Instrument calibrations were performed automatically at regular intervals (generally every hour when the PTR-MS was in direct measurement mode) by serially diluting the PTR-MS multi-component calibration gas (see section **3.5.3**) with VOC free air from the on-board ZAG. The calibration gas was added to the zero air stream via a 3-way solenoid valve, upstream of the PTR-MS inlet, to allow sufficient mixing. Excess diluted calibration gas was vented to the PTR-MS sample pump, similar to zero-mode, so that the calibration procedure does not affect the TDPC-GC measurements. The flows of the calibration gas and the VOC free dilution gas were controlled via mass flow controllers. Serial dilutions were performed by mixing 2–5 milliliters per minute (ml/min) of the calibration gas into a zero-gas dilution flow of 250–400 ml/min.

3.4.2. Gas Chromatography Instrument Assessment

The Thermal Desorption Pre-Concentrator (TDPC)-GC instrument is a 2-channel Gas Chromatography system that provides semi-continuous quantitation of trace organic gases within the volatility ranges of each chromatograph channel. The instrument has a “high-volatility” VOC and a “mid-volatility” VOC channel as configured for this field campaign. Each channel relies upon a two-stage adsorbent / thermal desorption pre-concentration system to provide adequate analyte for separation and analysis by the Vocus PTR-TOFMS.

The GC system shared a common inlet with the PTR-MS and was located next to the PTR-MS inside the mobile laboratory to reduce the inlet length, and to allow for simpler temporal correlation with real-time VOC measurements made with the PTR-MS system.

The GC system pulled approximately 0.5 SLPM of ambient air from the main inlet via 1/4” OD PFA tubing, typically less than 4 feet in length. A subset of this sample flow (200 standard cubic centimeters per minute (sccm)) was directed to the GC inlet for analysis, with the rest of the flow vented. The gas sample was split to separate multibed sample tubes, which were held at a fixed temperature (typically 20 °C) during sample collection. The flow to each tube was controlled by calibrated mass flow controllers (MFCs) to provide known sample volumes. After sample collection (typically 100 sccm for 10 min), the sample tubes were forward-flushed with carrier gas to reduce the water-loading in the tubes. The tubes were then heated with a controlled temperature ramp to 300 °C in 60 seconds to transfer analyte to narrow-bore focusing traps (Markes International U-T15ATA-2S) held at 20 °C, using low flow-rate carrier gas (typically 2 sccm). The analyte was held on the focus trap until flash-heated and injected upon the respective separation column, for separation and detection. Separation and detection took 20 minutes and required that the Vocus was offline from ambient measurements to analyze the GC effluent.

The GC system was used differently depending on whether the mobile lab was actively driving or stationary, either to investigate a source site or in off-hours while at the RV park. While

mobile, the GC remained in standby state but could be manually triggered by the field scientist to collect an ambient sample. This sample could then be immediately injected into the GC system and into the PTR-MS for analysis or held until the scientist identifies a time period when direct PTR-MS measurements can be missed. This also allowed for stationary collection of the ambient sample (for 10 minutes), and then the lab could be driven during the subsequent 20-minute analysis period.

When the mobile lab was stationary (e.g., at the RV park overnight), the GC and Vocus were switched to a 10-hr cycle, where the GC collected an ambient sample and then a zero sample every five hours. This produced 240 minutes of direct ambient measurements via PTR-MS, followed by a pair of 20-minute chromatograms. The PTR-MS was offline from direct measurement for the full hour of GC measurement.

The TDPC-GC was operated in three modes: ambient sampling, calibration (cal) mode, and zero mode. The calibration and zero modes enable internal solenoid valves to overflow the GC inlet with a mixture of calibrant gas and zero gas, or just zero gas, respectively. The calibrant used for this campaign was a gas cylinder purchased from Apel-Riemer Environmental Inc. (see section 3.5.3). The GC flowed this calibrant gas continuously at nominally 0.4 sccm via a critical orifice and was occasionally directed to the GC inlet. This flow rate was controlled by the gas cylinder regulator pressure and was checked routinely via a mass flow meter (Alicat).

Sample tubes were changed routinely to maintain quantitative instrument response. For the Texarkana field campaign, sample tubes were replaced every 7th day to maintain <100 samples collected per tube.

The TPDC-GC system recorded temperatures, flows, and pressures relevant to the sample collection and chromatographic analysis. The following parameters were maintained throughout the campaign:

Sample flow rate = 100 sccm (± 1 sccm)
Sample tube temperature = 20 (± 1) °C during sample collection
Focus trap temperature = 20 (± 1) °C during sample focusing

3.5. Discussion of Quality Assurance/Quality Control (QA/QC) Activities and Results

3.5.1. University of Houston

3.5.1.1. Calibration Methods

A blended cylinder of CO, SO_2, NO, and propene was used to challenge the CO, SO_2, NO, NO_2, and NO_y instrumentation aboard the MAQL3. Additionally, the NO_2, and NO_y were challenged with NO_2 generated by a Teledyne T700U gas-phase titration (GPT) system. The blended gas challenges in the MAQL3 were introduced with the T700U dilution system and valves to the

inlet of the sample line upstream of the filter to best represent ambient conditions and account for and/or identify potential losses in the inlet lines and filter.

Two instruments measured O_3. The measurements from the faster instrument were reported in the final data, but the backup instrument was used in the field as another means to verify that the measurements were accurate. While the backup instrument showed greater signal noise, the instrument averages agreed well. The O_3 instruments were also challenged regularly with O_3 generated by a Thermo Primary Standard ozone generator. Ozone from the O_3 generator was supplied through a valve that, when triggered, allowed the O_3 instruments to sample directly from the O_3 generator output rather than the sample inlet system.

The HCHO instrument was challenged with an HCHO gas cylinder and a dilution system. Similar to the calibration methods used for the trace gases discussed above, the HCHO dilution was introduced to the VOC sample inlet, upstream of the filter.

3.5.1.2. Baseline Evaluation Methods

A combination of internal pre-reactor, catalyst, or zero air overflow methods were used to evaluate trace gas instrument baselines as appropriate for the specific instrument measurement methods. All trace gas instruments were regularly zeroed using zero air overflow at the inlet. This zero air was supplied by a Teledyne zero air generator with internal scrubbers.

The MAQL3 POPS and nephelometer instruments were on the aerosol inlet and sample line (separate from the trace gas and NO_y sample lines) along with the Baylor University TAP and AMS instrumentation. The baselines for the POPS and nephelometer were evaluated by flowing a sample through a particle filter upstream of the instruments.

3.5.1.3. Calibration Frequency

Trace gas multipoint calibrations using the blended cylinder occurred two to three times per week throughout the field campaign. Calibrations with NO_2 were performed once per week. The trace gas instruments (except O_3) were typically spanned twice per day—before and after drives. All spans were followed by zero air overflows (which included O_3). The O_3 instruments were calibrated one to three times per week.

The HCHO instrument was zeroed before and after each drive and was calibrated after each tubing change, which is part of the weekly maintenance of the instrument. The instrument was also calibrated after changing batches of the Hantzsch solution it used. Calibrations took place one to two times per week.

All UH trace gas and VOC instruments were also calibrated before and immediately after the campaign. The results from calibrations and spans were used to correct the final data, and the standard deviations of calibration slopes were used as a factor in the final uncertainties reported in **Section 3.6.1** below.

3.5.1.4. Completeness

All measurement data have been screened for invalid or non-ambient datapoints, baseline corrected, and slope corrected where applicable. Completeness of the data delivered was assessed by calculating the percentages for each measurement using the following equation:

$$Completeness = \frac{(datapoints\ delivered) + (calibration\ \&\ zeroing\ datapoints)}{(total\ possible\ datapoints\ during\ campaign)} \times 100\%$$

The 10 s average data were used for the completeness calculations, and the results are displayed in **Table 1**. All measurements exceeded the required 90 % completeness except for the particle scattering measurements from the nephelometer, which was 88.1 %. The data logger error which caused the nephelometer data to be displayed on screen but not saved to the data file at the beginning of the field campaign, significantly impacted the data completeness, as the error was not found and fixed until 6:26 p.m. on February 12. This amounted to approximately 9 % of the raw data being lost.

Table 1. *Data Completeness for University of Houston Measurements*

Measurement Parameter		Completeness	Measurement Parameter	Completeness
NO		99.5 %	O_3	98.6 %
NO_2		98.6 %	Particle Scattering	88.1 %
NO_y		98.7 %	Particle Rate (POPS)	95.2 %
SO_2		99.9 %	HCHO	94.7 %
CO		99.9 %		

3.5.1.5. Platform Intercomparison

The POPS instruments (one inside MAQL3 and the other mounted on top of the minAML) were used as aerosol plume indicators and for intercomparison between the two mobile labs. Periods where both mobile labs were parked next to each other at the RV park with inlets separated by approximately 10 meters, were compared to determine whether both POPS instruments were able to measure similar variability in particle rates. The instruments observed very similar plume structures and compared well overall in terms of the variability. Particle rate values from each instrument were normalized to the maximum values each one measured, creating a data wave with values between 0 and 1, where 1 corresponds to the highest particle rate that the POPS instrument measured during the field campaign. This PM plume indicator represents the relative strength of PM plume signals throughout the campaign.

3.5.2. Baylor

3.5.2.1. Realtime Aerosol

The real-time aerosol instruments sampled downstream of a $PM_{2.5}$ cyclone operated at 16.7 liters per minute and, was checked weekly. Flows to each instrument were controlled with mass flow controllers or via a critical orifice. A 90 mm quartz-fiber filter was installed upstream of each controller to prevent clogging of the MFC. Instruments were calibrated as follows: the nephelometer every 15 days (via CO_2 gas), the TAP with each filter change (i.e., white filter check), and the AMS weekly (ionization efficiency). Baseline (zero) checks for all aerosol instruments were performed daily using a 30-min High Efficiency Particulate Air (HEPA) filtered measurement. Data completeness exceeded 90% and was calculated using ambient measurements (stationary and mobile), zero periods, and calibration periods.

3.5.2.2. Optical Absorption and Scattering Measurements

Tricolor Absorption Photometer

A tricolor absorption photometer (TAP; Model 2901, Brechtel Inc., Hayward, CA) was used to measure the aerosol light absorption coefficients (σ_{abs}) at UV (365 nm), green, (520 nm) and red (640 nm) wavelengths. The TAP is the commercially available version of the National Oceanic and Atmospheric Administration's (NOAA) continuous light absorption photometer (CLAP) and uses 10 solenoid valves to consecutively sample through eight sample filter spots and two reference filter spots (Ogren et al., 2017). LED light sources simultaneously shine light through the sample and reference spots. The reference spot allows a differential measurement approach in the TAP so the increase in light attenuation due to deposited particles on the sample spot can be largely separated from filter effects. A transmittance threshold for light attenuation was set to 50% to change the sampling filter spot. Each of the eight (8) sample spots is separated from the other by O-rings that clamp the filter material to prevent any inter-spot leakage. The air flow passes through the filter and into a solenoid valve controlled by the TAP Reader software. For spot loading effect, TAP automatically performs the correction using its inbuilt methodology (based on the filter correction method discussed by Ogren, 2010), and the instrument output is real-time, corrected absorption coefficients. TAP data acquisition is performed using the TAP software provided by Brechtel.

Nephelometer

Aerosol scattering coefficients (σscat) at three different wavelengths (450 blue, 525 green, and 635 red) were measured using an Ecotech Aurora 3000 nephelometer. Ecotech Aurora 3000 nephelometer uses a white light source to illuminate the air sample, and the light scattered by the aerosol particles (and gases) at a particular wavelength is measured using a photomultiplier tube. Additionally, this nephelometer provides a separate measurement of particle backscatter (σbscat). The instrument automatically calculates Rayleigh scattering from internally measured

temperature and pressure and corrects the reported signal for those factors. Calibration of the nephelometer was performed prior to the instrument being set up at the site and then every 15 days using CO_2 as a span gas. Zero checks are performed once every week by using internally filtered particle-free air passed through a HEPA filter. The chamber temperature inside the nephelometer was set to 40 °C. This helped to maintain a relative humidity <40% for scattering measurements as per the Global Atmosphere Watch (GAW) recommendations (GAW, 2011). Scattering measurements are corrected for angular truncation errors following the procedure described by Müller et al. (2011). The averaging time was set to a five-minute average. Nephelometer data acquisition is performed using the DAQFactory software.

Optical Calculations - Ångström Exponents Calculations

The TAP and nephelometer measurements were used to calculate the Ångström (Absorption and Scattering) exponents for characterization of the wavelength dependency of aerosol absorption and scattering, respectively. The Ångström exponent is calculated as the negative slope of the linear fit of the optical parameter versus the wavelengths on a log-log plot (Moosmüller and Chakrabarty, 2011). The Ångström exponents for three wavelength bands can be represented using the following equation (Bergstrom et al., 2007; Kirchstetter et al., 2004; Schnaiter, 2005; Schnaiter et al., 2006).

$$\text{Absorption Ångström Exponent} = - \frac{log\ (\sigma abs_{\lambda 1,}\ \sigma abs_{\lambda 2,}\ \sigma abs_{\lambda 3,})}{log(\ \lambda 1, \lambda 2, \lambda 3)}$$

The absorption Ångström exponent (AAE) is calculated with the absorption coefficient data measured using the TAPs at 640, 520, 365 nm (λ_1, λ_2, and λ_3, respectively). The Scattering Ångström Exponent (SAE) is calculated with the scattering coefficient measured using the nephelometer at 450, 525, and 635 nm (λ_1, λ_2, and λ_3, respectively).

$$\text{Scattering Ångström Exponent} = - \frac{log\ (\sigma scat_{\lambda 1,}\ \sigma scat_{\lambda 2,}\ \sigma scat_{\lambda 3,})}{log(\ \lambda 1, \lambda 2, \lambda 3)}$$

SAE is an intrinsic property of the aerosol derived based on the wavelength dependency of the aerosol scattering. SAE is inversely related to the particle size which indicates that larger particles will have smaller SAE and vice versa (Schmeisser et al., 2017).

High-Resolution Time-of-Flight Aerosol Mass Spectrometer

The High-Resolution Time-of-Flight Aerosol Mass Spectrometer (HR-ToF-AMS) size calibration was performed using monodisperse ammonium nitrate particles to ensure accurate characterization of particle time-of-flight (PToF) and sizing through the aerodynamic lens. Calibrating an HR-ToF-AMS typically includes (i) a daily 30-min zero/span, a size calibration

(prior to the campaign), and (iii) weekly ionization-efficiency (IE) calibration. For the daily zero/span, sample particle-free, dry (HEPA-filtered) air for ~30 minutes in the same PToF modes used for ambient measurements to quantify electronic and gas-phase backgrounds and verify flows. For size calibration, atomize and dry ammonium nitrate (80 to 700 nm), classify it with a differential mobility analyzer (DMA) to produce monodisperse particles across the lens transmission range, and record PToF to map mobility diameter to vacuum aerodynamic diameter and align chopper timing, updating lens velocity and PToF bins. For IE, use 300-nm ammonium nitrate selected by the DMA.

3.5.3. Aerodyne

The calibration standard used for the field campaign was a compressed gas mixture of nominal 1 ppm VOCs in nitrogen, with one component at 100 ppb due to low volatility, supplied by Apel-Reimer Environmental, Inc. [Miami, FL]. The standard was gravimetrically prepared in an aluminum cylinder with 1800 pounds per square inch (psi) ultra-high purity nitrogen (UHP N2) gas balance pressure. Accuracy is certified to ±5% via comparison to National Institute of Standards and Technology (NIST) and NIST-traceable standards for all compounds in the cylinder. The gas cylinder calibration is certified to remain within ±5% for 12 months from the date of analysis (September 2024). **Table 2** shows species in the calibration cylinder:

Table 2. *Calibration cylinder species.*

Compound	CAS Reg #	Concentration (ppb)
Ethanol	64-17-5	1056
Acetonitrile	75-05-8	921
Acetone	67-64-1	1008
Acrylonitrile	107-13-1	971
Isoprene	78-79-5	988
Methacrolein	78-85-3	1033
Methyl Ethyl Ketone	78-93-3	1014
Benzene	71-43-2	967
o-Xylene	95-47-6	980
α-Pinene	80-56-8	972
1,2,4-Trimethylbenzene	95-63-6	987
Octamethylcyclotetrasiloxane (D4)	556-67-2	963
Decamethylcyclopentasiloxane (D5)	571-02-6	1001
β-Caryophyllene	87-44-5	103.6

As described previously, the Vocus and GC-Vocus measurements were alternated throughout the campaign. Instrument calibration strategies were dependent upon which acquisition mode in use, see **Table 3**. When the Vocus was operating in direct-measurement mode, instrument zeros were performed every 30 minutes for 60 seconds by overflowing the inlet with VOC-free air (zero air)

generated via a heated catalyst. Instrument sensitivities were performed every hour for 90 seconds via the addition of pre-mixed calibration gas mixed with zero gas overflowing the instrument inlet. Each calibration period is bracketed by instrument zeros, 60 seconds before and 120 seconds after, to ensure that the calibration signal is measured in a clean background and that the calibration gas has cleared from the Vocus inlet before switching back to ambient measurements. Both calibration and zero gas flows are controlled by a mass flow controller, with zero flow typically 375 sccm and calibration gas typically 3.0 sccm during the campaign. When the instrument was in GC-Vocus mode, the instrument typically only collected zero and ambient data automatically with manual measurement of sensitivity performed four times throughout the campaign. The GC collects a zero chromatogram via overflow of the GC inlet with UHPN2 at nominal 250 sccm. During each calibration event, the instrument measures a set of samples of calibration gas (nominal 0.4 sccm diluted) into the zero gas flow. For the first three calibration events, the GC collected a set of 3 replicates at a single mixing ratio. For the fourth calibration, the GC collected sets of 3 replicates at 3 different sample collection lengths, equivalent to three different mixing ratios. The zero and calibration modes of the GC can be programmed via instrument sequencing and, therefore, were typically performed overnight while the mobile lab was parked at the RV park.

Table 3. *Procedures to Assess QA objective for Additional Measurements.*

Measurement Parameter	Analysis Method	Assessment Method
Ion count of protonated VOCs	Sample reaction with protonated water	Dedicated sampling of VOC-free air with matched humidity every 30 minutes. Hourly calibration using standards to determine instrument response.
Speciated VOC ion counts	Gas Chromatogram with Mass Spectrometer Detector	Daily measurement of UHP nitrogen. Weekly calibration standards to track retention times. Post-campaign determination of the ion count/ppb VOC using multiple standard calibration tanks. In-field checks of the response per ppb VOC are done with the calibration chromatograms.
Wind Speed and Direction	Airmar 200WX WeatherStation Instrument	The anemometer direction is checked against a coordinated manual fan blowing on the anemometer along the four quadrants (ahead, driver, passenger, rear). Wind speed calibration is compared by looking at the GPS velocity signal during a mobile condition with light ambient wind.
Position	Global Position System Airmar 200WX WeatherStation Instrument	Examining the output from the GPS compared to an online source, such as Google Maps, verifies the function. All mobile ground tracks are mapped into the UTM coordinate space to put traces onto a georeferenced image of the roadway, terrain, and facility boundaries.

3.6. Audit of Data Quality - Detection Limits and Uncertainties

3.6.1. University of Houston

Table 4 shows the combined uncertainty and lower limits of detection (LLODs) for key measurements during this measurement project. The NO_y instrument also has a fixed upper limit of detection due to the manufacturer's firmware design of approximately 400 ppbv. These values, however, are only seen in strong plumes of vehicle exhaust when quite close to the source.

The uncertainty is calculated in quadrature i.e., the square root of the sum of the squares of the major contributors to the sensitivity calculations. These include individual uncertainties such as from flow controllers used to blend the calibration cylinder gas flows with zero air (2% each), calibration gas cylinder manufacturer uncertainty (NIST traceable standards: 1% for CO and NO, 2% for SO_2 and NO_2, 5% for HCHO), and the relative variability of the calibration responses over the course of the project. The lower limit of detection is determined by flowing zero air, or air free of the species of interest, to the instrument for an extended evaluation of the instrument response. The data is then averaged to the reporting time, in this case, 10 seconds, and the standard deviation of the noise in the data is considered the precision of the measurement. Three times, the standard deviation is used as the lower limit of detection in order to give subsequent data users confidence that the values reported are sufficiently larger than zero and that the measurements can be utilized. LLODs for longer averaging times (30, 60, and 300 seconds) are also reported in **Table 4**, should data users further average the reported data.

Table 4. *Summary of uncertainty and lower limits of detection (LLODs) for the full sampling period using different averaging times.*

Measurement	Uncertainty	LLOD 10 s averaging (ppbv)	LLOD 30 s averaging (ppbv)	LLOD 60 s averaging (ppbv)	LLOD 300 s averaging (ppbv)
NO	5%	0.6	0.3	0.27	0.12
NO_2	7%	0.9	0.5	0.38	0.18
NO_y	4%	0.3	0.2	0.19	0.15
O_3	7%	0.3	0.3	0.24	0.09
CO	4%	<5	<5	<5	<5
SO_2	4%	0.6	0.3	0.23	0.10
HCHO	8%	0.4	0.3	0.29	0.22

3.6.2. Baylor

This was performed at the beginning of the campaign. HR-ToF-AMS detection limits (1 min averages) for submicrometer aerosol ranged between 0.04 to 0.082 $\mu g/m^{-3}$ and were calculated using the methodology described by DeCarlo et al 2006. The campaign's average detection limits of organics (Org), sulfates, nitrates, ammonium, and chloride were 0.069, 0.067, 0.067, 0.066,

and 0.056 μg m^{-3}. The detection limits were determined as three times the standard deviation of the mass concentration of HEPA-filtered air (sampled for 30 minutes). The Condensation Particle Counter (CPC) detection limit was ~0.26 particle counts per cubic centimeter (#/cm^3), and the detection limit of the TAP was 0.5 M/m^{-1}.

3.6.3. Aerodyne

Limits of detection for the Vocus PTR-TOFMS are defined as three times the standard deviation of the ion signal average for each analyte ion when the system was measuring zero air. The PTR-MS measures at 1-Hz sample rate and the data were averaged to 10-sec, the reporting rate. As zero measurements were performed throughout the campaign, the data collected was used at the start of the campaign, February 12, 2025. For GC-PTRMS data, limits of detection (LOD) were defined as three times the standard deviation of the baseline signal adjacent to the chromatographic peak multiplied by the instrument sensitivity and the peak width (defined as full width at half-maximum peak height [FWHM]). For GC data, LODs for individual peaks can be reported, which represent assigned compounds, while for direct PTR-MS data, only the measurement of the ion associated with those compounds can be reported. **Table 5** shows the limit of detection for the full campaign.

Table 5. *Summary of limits of detection for the full sampling campaign.*

Ion(s) of interest	Potential assignments	Vocus PTR-TOFMS LOD [ppb]	TDPC-GC PTRMS LOD [ppb]
$C_2H_6OH^+$	Ethanol	0.200	0.027
$C_2H_3NH^+$	Acetonitrile	0.04	0.004
$C_3H_6OH^+$	Acetone; propanal	0.05	0.005
$C_3H_3NH^+$	Acrylonitrile	0.008	<0.001
$C_5H_8H^+$	Isoprene	0.02	0.003
$C_4H_6OH^+$	Methacrolein; methyl vinyl ketone	0.03	0.001
$C_4H_8OH^+$	Methyl Ethyl Ketone	0.15	<0.001
$C_6H_6H^+$	Benzene	0.03	0.002
$C_7H_8H^+$	Toluene	-	-
$C_8H_{10}H^+$	C8-aromatic species (e.g., o-Xylene)	0.014	<0.001
$C_{10}H_{16}H^+$	Monoterpenes (e.g. α-Pinene)	0.009	<0.001
$C_9H_{12}H^+$	C9-aromatic species (e.g., 1,2,4-TMB)	0.024	<0.001
$[(CH_3)_2SiO]_4H^+$	D4-Siloxane	0.006	0.001
$[(CH_3)_2SiO]_5H^+$	D5-Siloxane	0.005	<0.001

4. DISCUSSION

4.1. General Campaign Conditions

4.1.1. Major Frontal Passages and General Weather Pattern Discussion

Figure 5 shows the meteorological conditions measured by MAQL3 throughout the field campaign. The NO_2 photolysis rate, measured by a radiometer mounted to the MAQL3 roof, provides an indicator for sunlight reaching the surface each day. The temperature and humidity data (measured by an Airmar mounted near the sample inlets) show the strong cold front that passed through on the evening of February 17, causing temperatures to fall below freezing on February 18 and remain low for multiple days, accompanied by light snow.

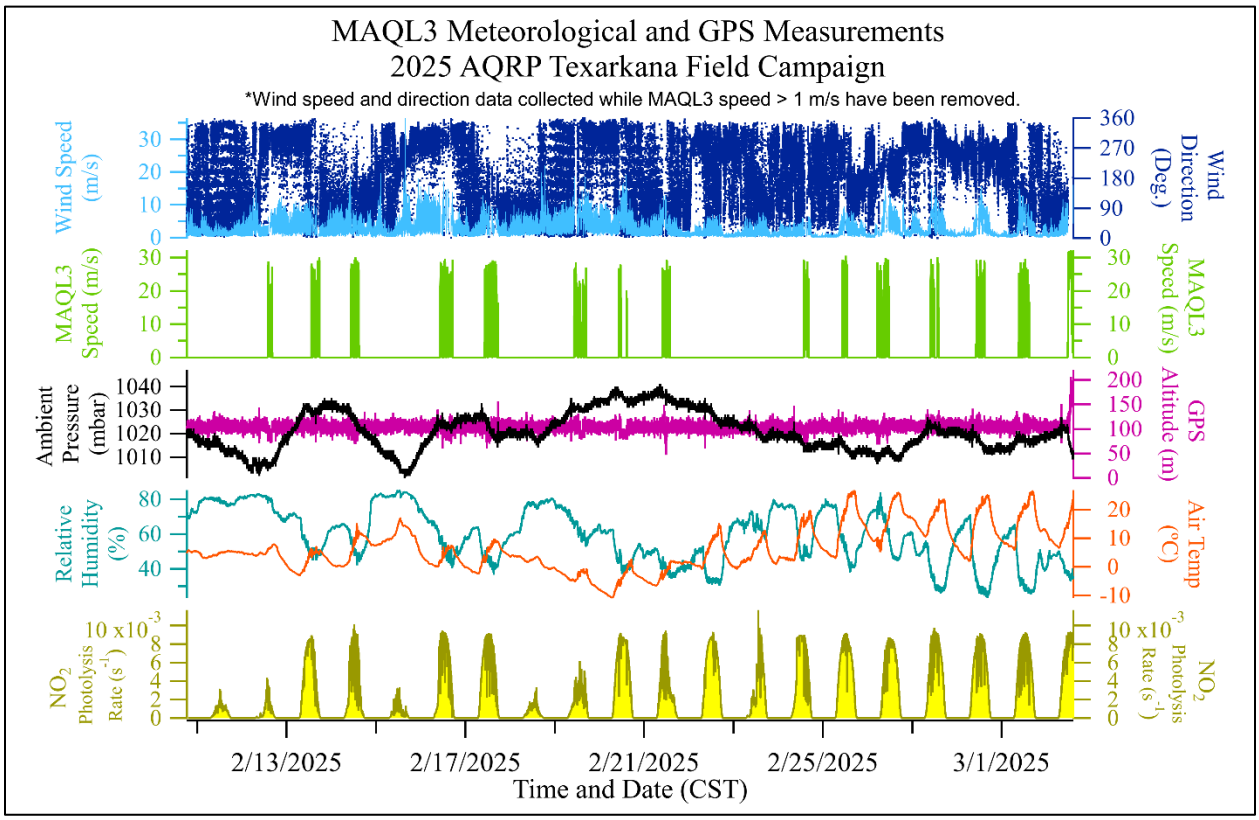

Figure 5. *Meteorological and GPS measurements from MAQL3 throughout the Texarkana field campaign. Data has been averaged to 10 s.*

4.1.2. Climatological vs Campaign Conditions

Climatological data show that winds in February (**Figure 6**, left) are typically from the South (https://mesonet.agron.iastate.edu/sites/windrose.phtml?station=TXK&network=AR_ASOS) where significant sampling targets are located. This influenced the decision to run the mobile measurement campaign from February 10 to March 2, 2025. However, the 2025 conditions

differed from typical wind patterns and southerly winds were rare (**Figure 6**), and a strong cold front brought well below normal temperatures from February 18–21 (**Figure 7**)

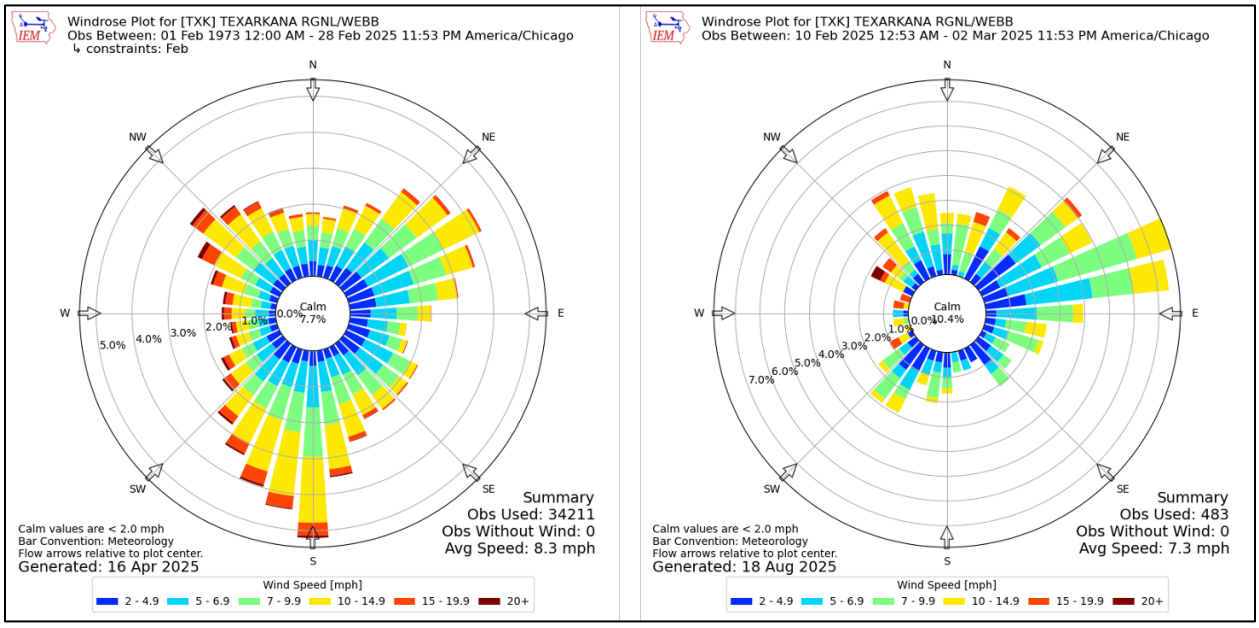

Figure 6*. Wind rose at Texarkana Regional Airport for February 1973 to 2025 (left) and only February 10 to March 2, 2025 (right).*

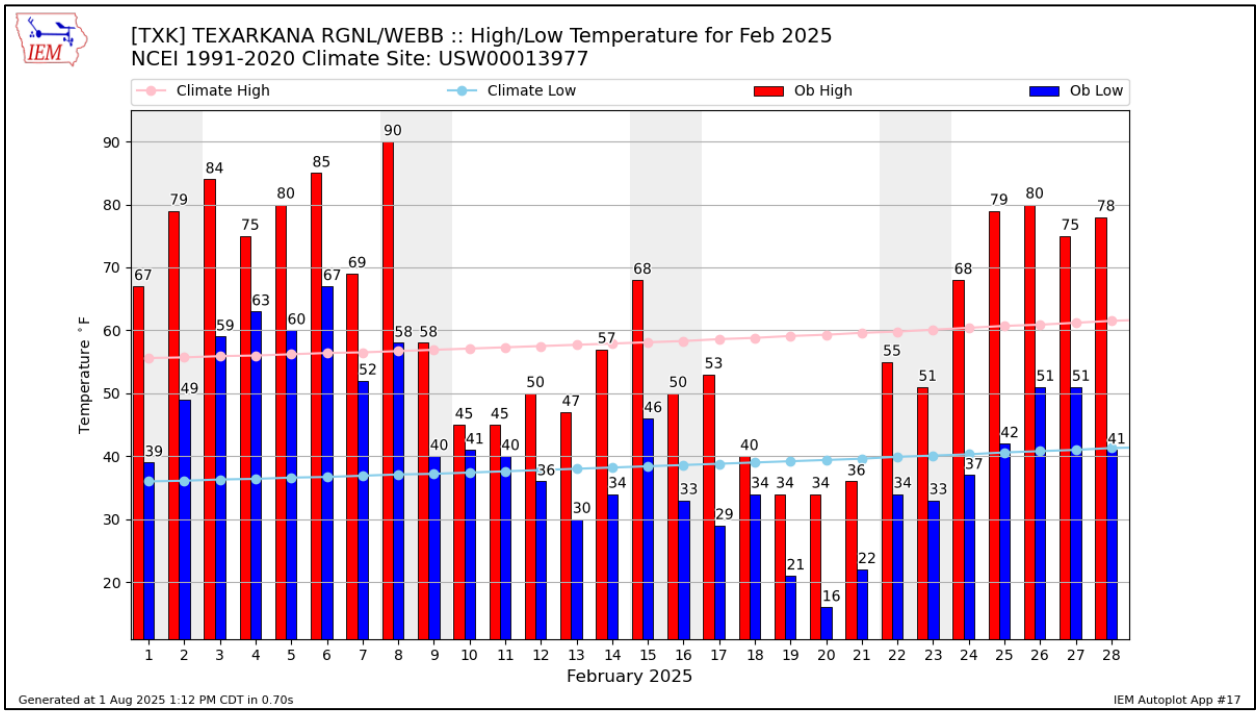

Figure 7. *Texarkana Regional Airport high and low temperatures for February 2025.*

The pollution rose plot **(Figure 8)** shows TCEQ data from C1031 from February 10 to March 2, 2025 and offers valuable insight into how wind patterns influence $PM_{2.5}$ concentrations at the

TCEQ monitoring site. It combines wind data and pollutant concentrations by averaging pollution levels for each wind direction, then displaying them as colored bars pointing in the direction the wind came from. Winds from the east to northeast (E–NE) direction are frequently associated with elevated $PM_{2.5}$ levels, suggesting that sources in that sector are significant contributors to the fine particulate pollution in the area.

Interestingly, although winds from the southwest (SW) occurred less frequently, only about 8% of the time, they are still linked to high $PM_{2.5}$ concentrations. This smaller percentage is by no means negligible; it signals the potential presence of a recurring, localized $PM_{2.5}$ source situated within the SW quadrant of the monitoring site.

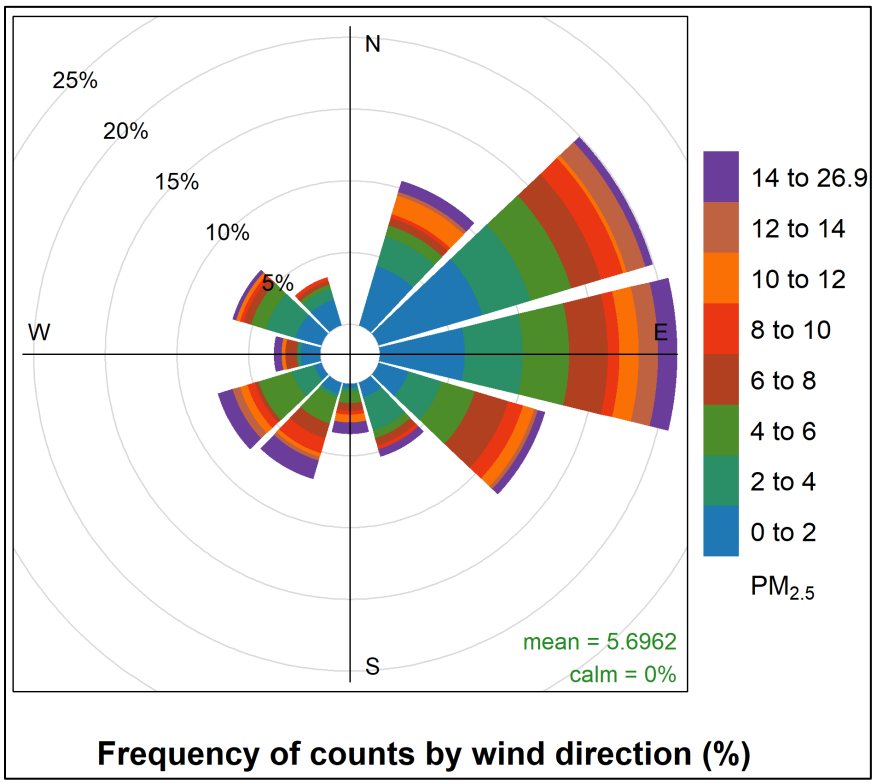

Figure 8. *Pollution rose plot for $PM_{2.5}$ (units in $\mu g/m^3$), TCEQ CAMS 1031 data from February 10 to March 2, 2025.*

The Bivariate Polar Plot (BPP), **Figure 9**, is another variation of a rose plot, illustrating how pollutants, in this case $PM_{2.5}$ concentrations, vary by both wind direction (wd) and speed (ws). Wind direction is shown around the circle, wind speed increases outward from the center, and pollutant concentration is represented by color. This plot helps identify the wind conditions for varying pollution levels and under what wind conditions the pollutant tends to be highest. The plot (TCEQ data from C1031 from February 10 to March 2, 2025) shows elevated $PM_{2.5}$ levels extending toward the east (E), southeast (SE), northeast (NE), and northwest (NW) sectors, particularly during low to moderate wind speeds. The BPP can be scaled and overlaid on a map by calculating the distance using the equation $s=v\times t$, where s is distance, v is wind speed, and t is travel time. The distance the air parcel traveled can be estimated based on wind speed and

transport time. This helps infer the potential location of emission sources relative to the sampling site. In this analysis, a 1-hour transport time was assumed to estimate the upwind distance of potential emission sources influencing pollutant concentrations observed in the BPP to align with the 1-hour averaging interval of the TCEQ $PM_{2.5}$ data. This ensures consistency between the temporal resolution of the pollutant measurements and the estimated upwind source influence. Because $PM_{2.5}$ particles are relatively stable in the atmosphere and can persist for hours to days, allowing them to travel long distances without rapid chemical transformation or loss, it is important to consider transport into the area. Therefore, using a 1-hour averaging period in BPP analysis can also capture the influence of upwind sources from both local and regional scales. If the PM is assumed to be from local sources, this could reflect contributions from sources located within approximately 4 to 9 miles of the site. The hotspots identified near the center (i.e., calm winds) may be linked to nearby activities typical of that area. Furthermore, a pronounced central hotspot within the BPP suggests contributions from highly localized sources. According to the Environmental Protection Agency Toxic Release Inventory (EPA-TRI) (https://www.epa.gov/enviro/tri-search), a few registered industries within this immediate area are marked as ongoing $PM_{2.5}$ emitters.

Moreover, the elongated $PM_{2.5}$ hotspot to the SW was identified when the wind speed was around 10 meters per second (m/s) may indicate that transport to the region from this direction was occurring, as there is no fall-off in concentrations at the extents of the BPP results. Additionally, because a specific source under the hotspot area has not been identified, it is possible that the higher PM levels are being transported into the Texarkana area. At least 70–80 kilometers (km) southwest of Texarkana, there are two power plants, one coal and one natural gas, as well as a steel mill with a power plant on site that should be noted.

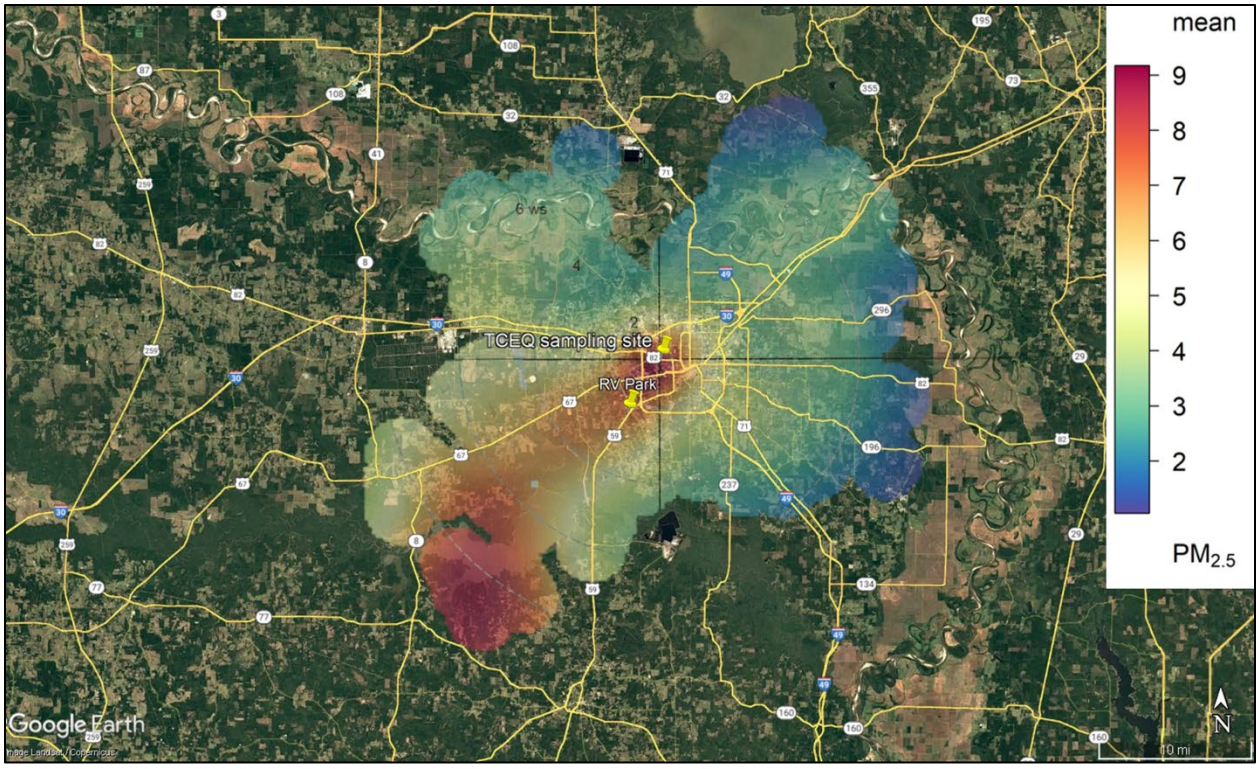

Figure 9. *Bivariate Polar Plot (BPP) for $PM_{2.5}$ (units in mg/m^3), TCEQ CAMS 1031 data, from 02/10/2025 to 03/02/2025.*

4.1.3. General Sampling Observations

Figure 10 shows the timeseries of ten-second averages for O_3, NO, NO_y, SO_2, CO, HCHO, and the normalized $PM_{2.5}$ plume strength for both mobile and stationary measurements aboard MAQL3 during the field campaign. Elevated $PM_{2.5}$, SO_2, CO, NO_X, and HCHO were indicative of distinct pollution events that were likely caused by industrial activity and combustion sources. High $PM_{2.5}$ and SO_2 may indicate either local emission events or plume transport, whereas O_3 showed typical daily photochemical variability.

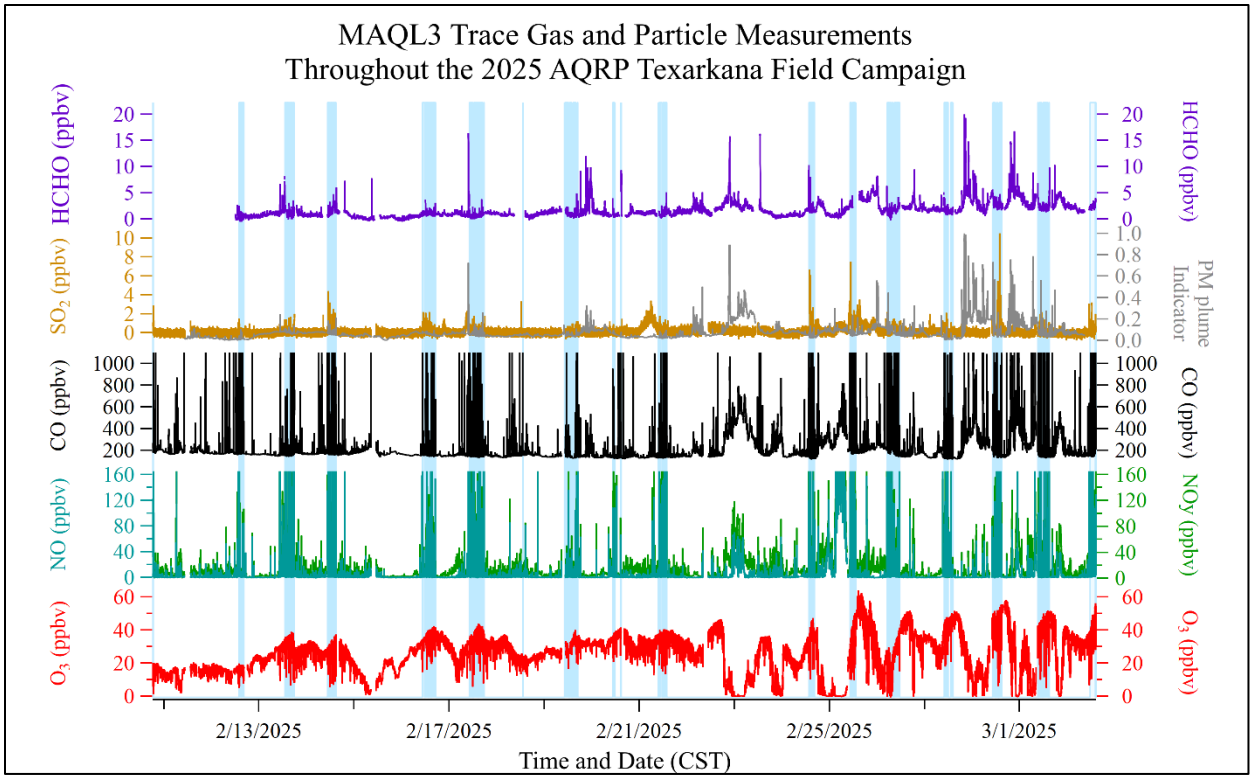

Figure 10. *Data summary of several of the MAQL3 UH measurements made during the AQRP Texarkana campaign. Ten-second averages for O_3, NO, NO_y, SO_2, CO, HCHO, and the particulate matter relative plume strength indicator (with a maximum of 1, calculated from POPS instrument measurements) are plotted against Central Standard Time. Mobile sampling periods are indicated by blue shaded regions.*

Figure 11 displays the MAQL3 POPS data ($PM_{2.5}$ particle rate normalized to the highest measured value) compared to the daily $PM_{2.5}$ maximums and averages reported by the TCEQ C1031 New Boston Monitor during the campaign. Periods where MAQL3 was moving and often sampling very close to sources are highlighted in blue. **Figure 11** shows that despite the distance from the monitor, the MAQL3 data showed similar trends to C1031, with PM levels increasing later in the campaign. The majority of the MAQL3 data were collected while stationary at the RV Park and these measurements are discussed further in section **4.5**.

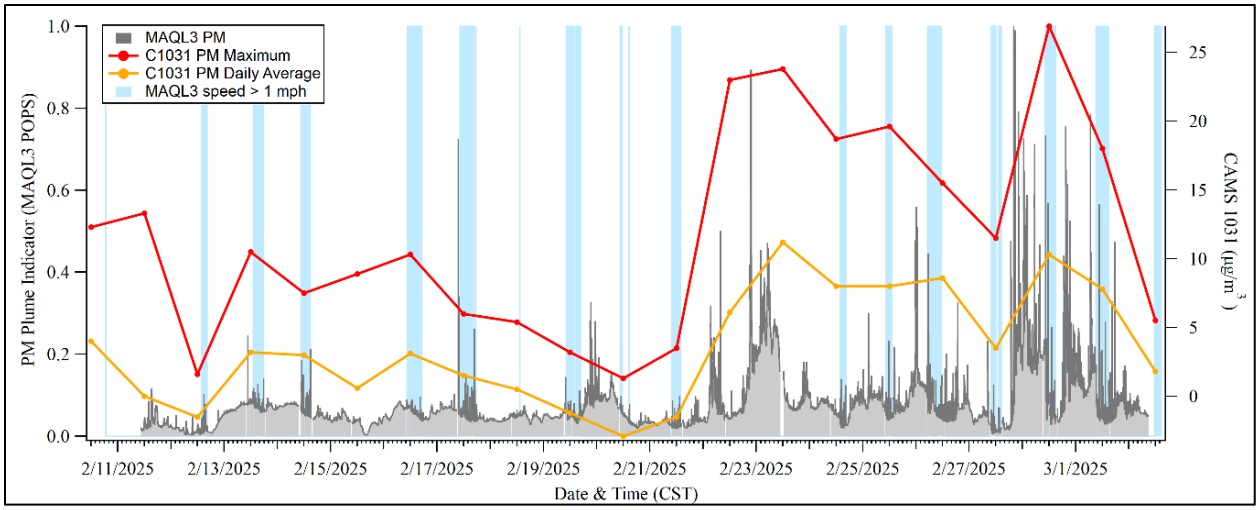

Figure 11. *The MAQL3 particulate matter relative plume strength indicator (with a maximum of 1, calculated from POPS instrument measurements) and the TCEQ C1031 monitor $PM_{2.5}$ daily averages and maximums. Periods where MAQL3 was mobile are highlighted in blue.*

4.2. Graphic Packaging International Complex

Graphic Packaging International's Texarkana Mill is an integrated bleached kraft paperboard facility that produces solid bleached sulfate (i.e., virgin grade paperboard) (Graphic Packaging, 2025). TCEQ's identifies Kraft pulping with Low Volume, High Concentration/High Volume, Low Concentration non-condensable gas systems and a bleaching system. The mill's kraft lines include corresponding bleaching, chemical recovery, and utility systems—two recovery boilers (RB01/RB02, with electrostatic precipitators), two lime kilns (LK01/LK02, with wet scrubbers), and smelt dissolving tanks with scrubbers—as well as onsite wastewater management typical for the sector.

Besides reporting to the EPA-TRI, **Figure 10**, this facility submits Clean Air Act (CAA) data which shows this facility emits PM <10 µm, NO_2, and a few VOCs as minor emissions, with SO_2 reported as a major emission. Although GPI reports PM as a minor pollutant under the CAA and TRI programs, the TCEQ 2023 Point Source Emissions Inventory (https://www.tceq.texas.gov/airquality/point-source-ei/point-source-emissions-data) shows the facility emitted 408 tons per year of $PM_{2.5}$, classifying it as a major source. This discrepancy highlights how TRI and CAA reports often reflect permitted or potential emissions, while TCEQ's inventory provides actual emissions data, which in this case is significantly higher.

During mobile sampling periods where MAQL3 and minAML were sampling together, the minAML was generally leading MAQL3. As the minAML is smaller, it was able to traverse roads ahead of MAQL3 and look for potential impediments (low-hanging branches, low bridges, weight limits, etc.) that could pose a hazard to the MAQL3 while presenting no risk to the minAML.

The lesser emissions from the minAML vehicle and generator exhaust also meant that it was easier for MAQL3 to avoid minAML exhaust contamination of the sample than it would be for the reverse situation. **Figure 12** shows a photo taken from the cab of MAQL3 where the minAML is visible ahead. The picture was taken as the two mobile laboratories approached the GPI complex. MAQL3 generally followed the minAML no closer than this, using the real-time CO measurements as an indicator for minAML exhaust contamination. The separation distance was frequently much greater than what is shown in **Figure 12**. Depending on wind conditions and the surroundings, CO measurements often showed lingering exhaust on the roadway for 30 seconds or more after the minAML had passed through. This was especially true in areas where dense forest lined either side of the road, creating a canyon for emissions to linger. At times, due to conditions such as the minAML driving upwind of MAQL3, the exhaust was not avoidable if the two platforms were to remain together. In those cases, MAQL3 backed off as much as reasonable to minimize contamination and noted that the CO emissions were primarily from the minAML. Fortunately, in most cases, CO was not the primary identifying component of the target plume and therefore did not interfere with the goals of the sampling effort.

Figure 12. *Picture of GPI Paper Mill along sampling route, taken from inside the MAQL3 cab. The MinAML is in front of MAQL3, as was typical during mobile sampling.*

To ensure that adequate measurement data were collected and to examine the variability of the GPI plume, multiple close-in passes were made during mobile sampling on the morning of February 14, 2025. The mobile laboratories used a truck pull-off area approximately 1.5 miles SW of the GPI facility as a turnaround, and a Love's Travel Stop (or nearby parking lot) approximately 4.5 miles west (W) of GPI at the other end of the passes. Three passes were made approaching from the west, and three from the southwest. **Figure 13** shows a view of the GPI complex as MAQL3 approached the mill entrance from the southwest. Visible plumes can be seen blowing over the roadway.

Figure 13. *Photo of GPI complex taken from the MAQL3 cab.*

Trace gas and some of the particulate matter measurements (particle rate from the MAQL3 POPS and green scattering from the nephelometer) are shown for each of the six passes in **Figure 14.**

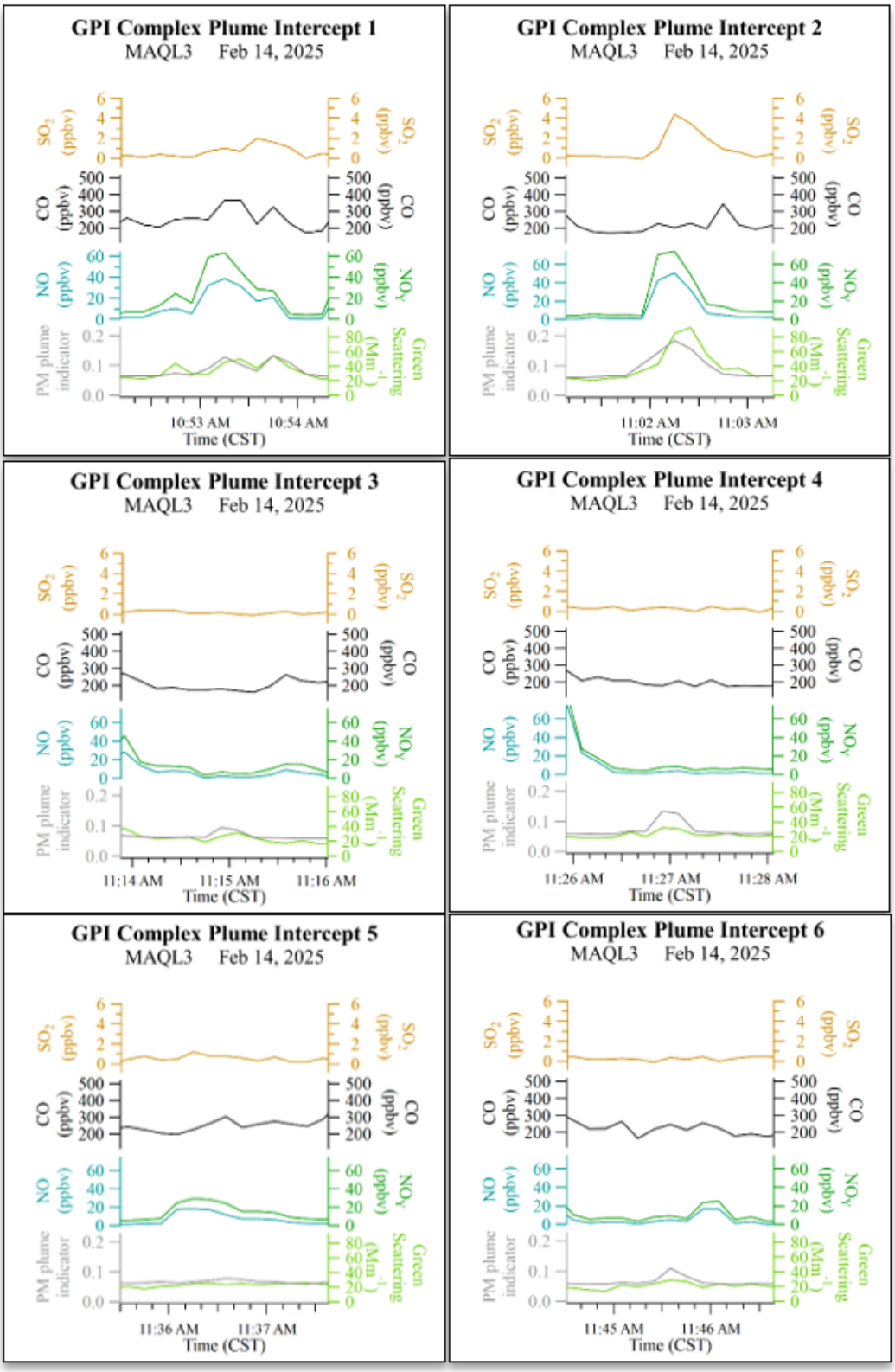

Figure 14. *MAQL3 data displayed as a timeseries for each of the six passes of the GPI complex on February 14, 2025. The PM plume indicator was calculated from POPS instrument measurements representing plume strength relative to the maximum particle rate measured.*

While the plume always included an enhancement in the PM, the proportions of other trace gases varied. The plume intersected at each pass may have contained emissions from different parts of the plant operations. As shown in **Figure 12**, visible plumes were emitted from several different stacks. Additionally, the GPI complex had significant logging truck activity producing NO_X emissions that can mix into the surrounding air and affect the NO_X to other pollutant ratios. The pass-to-pass variability measurements show that emissions are regular enough to be measured multiple times over the course of an hour, but due in part to the variability of the plume composition, structure, and similarity other possible sources, it was useful to have accompanying VOC and speciated aerosol measurements from the BU and Aerodyne instruments that could more clearly identify plume components that could be distinguished as GPI plant emissions, as shown in **Figure 15**–**Figure 17**.

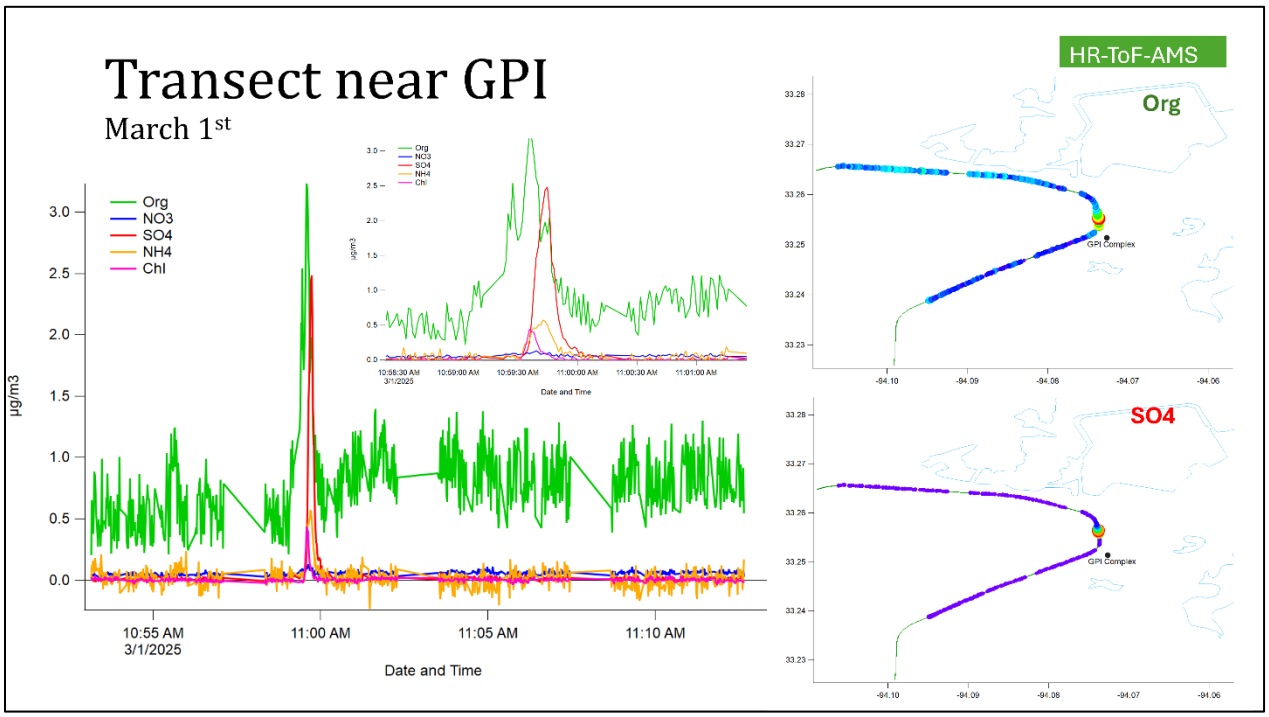

***Figure 15**. HR-ToF-AMS time-series of mobile transect near GPI on March 1, 2025, with unit mass resolution of Organics (Org), Nitrate (NO_3), Sulfate (SO_4), Ammonium (NH_4), and Chloride (Chl) species. The MAQL3 transect route, colored by Org (top right) and SO_4 (bottom right) concentration.*

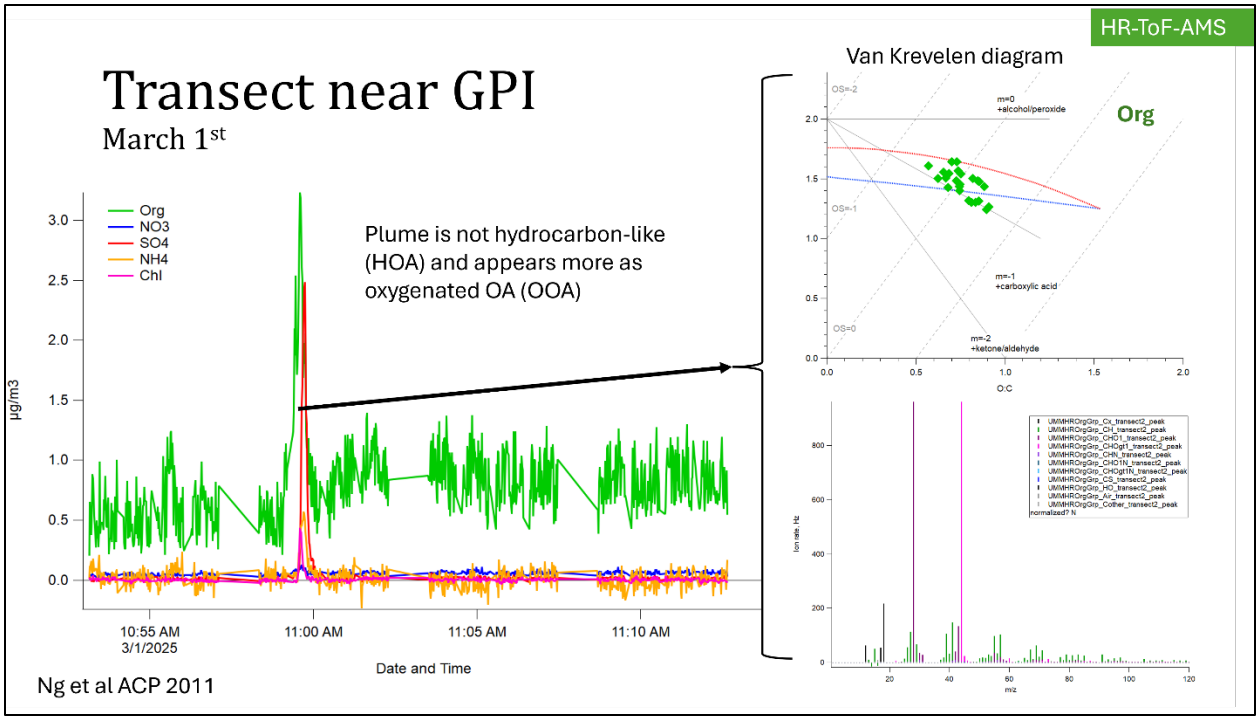

Figure 16. *HR-ToF-AMS time-series of mobile transect near GPI on March 1st, 2025, with unit mass resolution of Org, NO_3, SO_4, NH_4, and Chl species. Van Krevelen plot (top right) and HR Org mass spectrum (bottom right).*

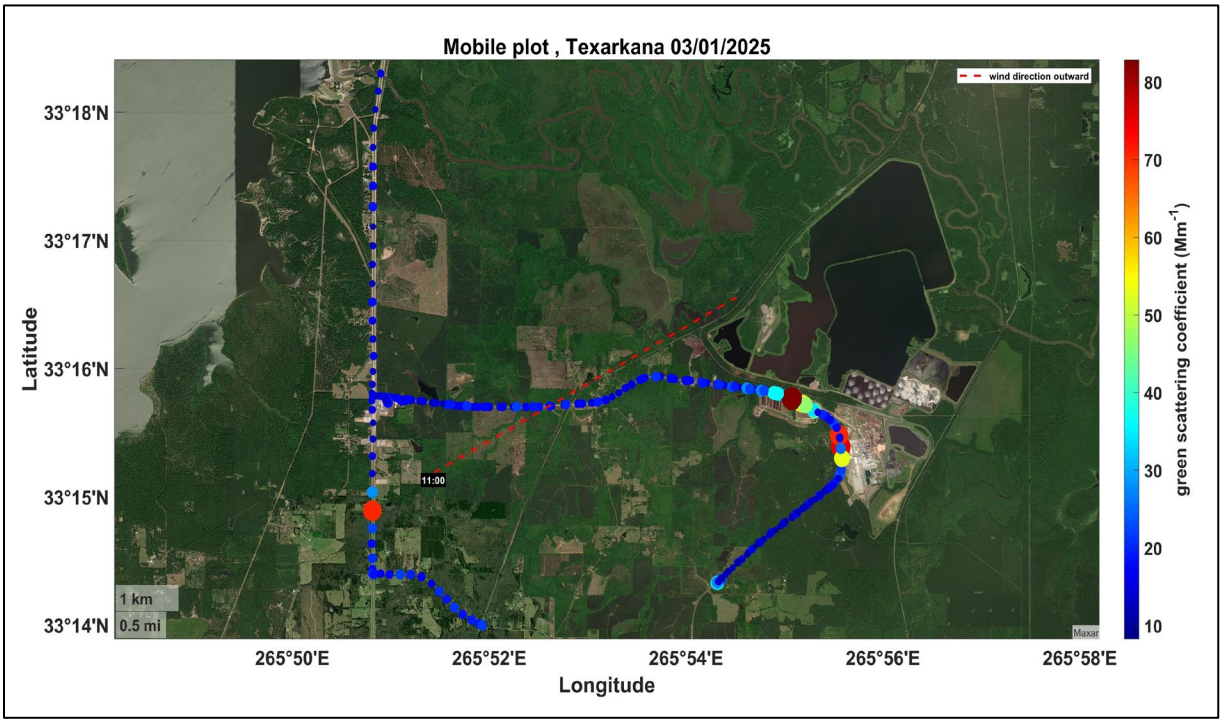

Figure 17. *Aerosol scattering coefficient (green wavelength) time-series of mobile transect near GPI on March 1, 2025.*

4.3. Domtar

The Domtar Ashdown Mill (https://www.domtar.com/our-location/ashdown-mill/) is a large fluff pulp and southern bleached softwood kraft pulp facility. The Arkansas Energy & Environment Department describes the Ashdown plant as a kraft mill with three pulp lines that use sodium hydroxide and sodium sulfide (white liquor) to digest wood chips into pulp in batch or continuous digesters (Arkansas Department of Energy and Environment, 2022). These operations can generate particulate matter. The resulting pulp, or "brownstock," is washed to remove spent cooking chemicals (black liquor), and this washing process can release volatile organic compounds. Each of the three pulp lines has corresponding bleaching, chemical recovery, and wastewater storage/treatment systems. Besides reporting to the USEPA-TRI, this facility submits Clean Air Act (CAA) data showing major emissions of CO, particulate matter (PM_{10}), SO_2, NO_2, and VOCs. However, no data on $PM_{2.5}$ emissions are provided.

On February 28, MAQL3 made a total of eight passes along U.S. Highway (Hwy) 71, which runs along the NE side of the Domtar Ashdown Mill. Over approximately two hours, the MAQL3 traveled back and forth along Hwy 71 using a Walmart parking lot in Ashdown, and a U-turn area between Ashdown, AR and Ogden, AR as turnaround points.

Winds were favorable along this route and plumes from the mill (as identified by PM, SO_2, NO_X, and NO_y signals, as well as a distinct smell) were intercepted. However, plume signatures were highly variable from pass to pass. Plumes were noted by the distinct smell present on each pass, but distinguishable increases in trace gas and PM measurements were not always observed. Additionally, some measurements could not be confidently tied to the Domtar facility due to nearby vehicles on the road and passing trains that run between Hwy 71 and Domtar. **Figure 18** shows four plots from passes where notable plumes were identified. For three of these intercepts, MAQL3 was able to stop for stationary sampling off to the side of the road in order to stay in the plumes for longer.

Even within this sample of four plumes, variability in the plume composition was present. Some plumes had significantly higher amounts of SO_2, for example. The variability can be demonstrated through the ratio of the maximum $PM_{2.5}$ particle rate to the maximum SO_2 mixing ratio for each pass. For intercepts one through four shown in **Figure 18**, the ratios of peak PM to SO_2 vary significantly and similar variation is present in the CO, NO_X, and NO_y data.

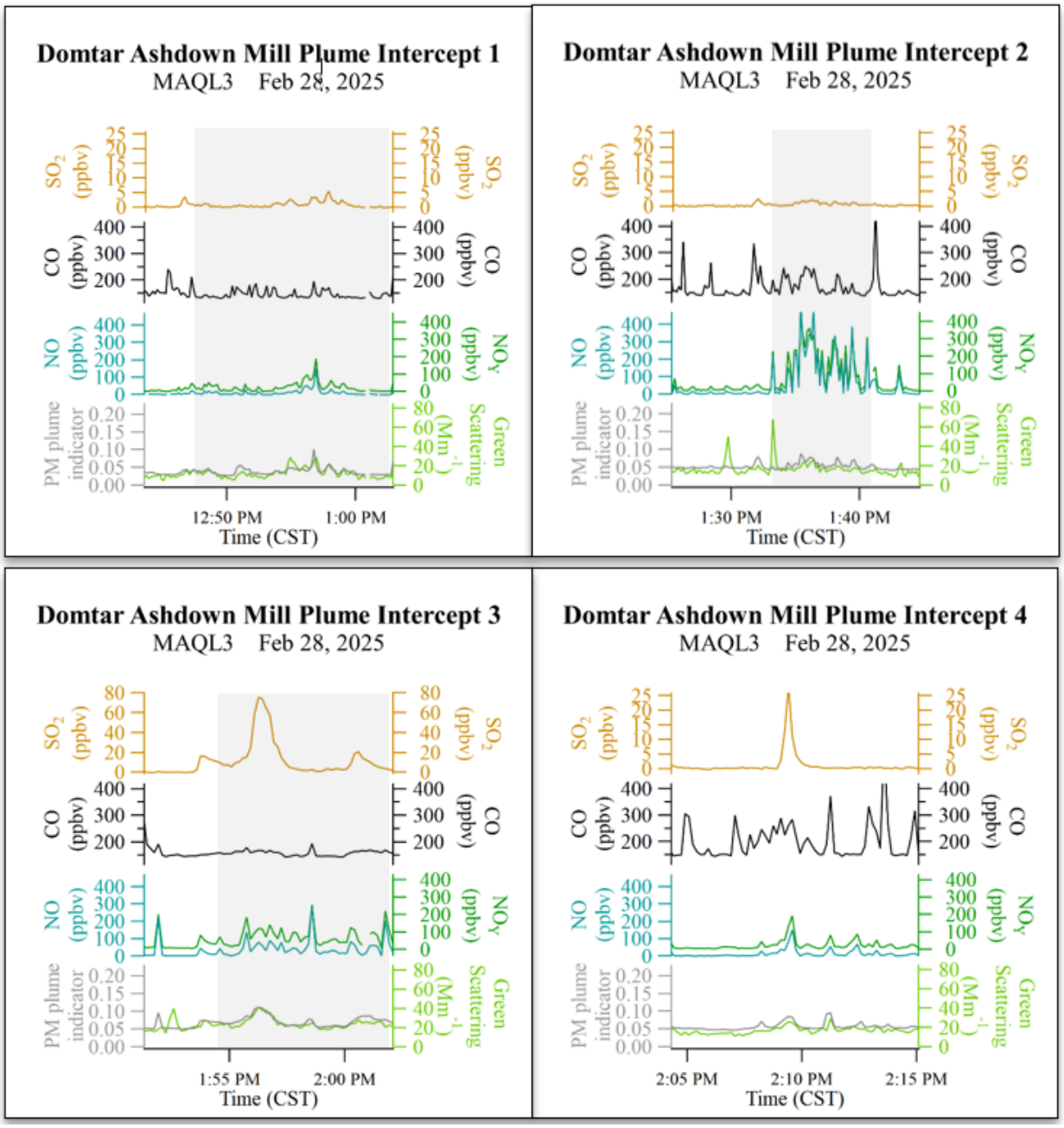

Figure 18. *MAQL3 data displayed as a timeseries for each of the four interceptions of plumes from Domtar Ashdown Mill on February 28, 2025. Shaded grey regions indicate time when MAQL3 was stopped for stationary sampling. The PM plume indicator was calculated from POPS instrument measurements representing plume strength relative to the maximum particle rate measured.*

The variability may have been caused by small wind changes, causing different emissions from within the facility to be sampled. **Figure 19** shows a picture of the Domtar Ashdown Mill taken during the stationary sampling period shown in the intercept 1 graph (**Figure 18**). Several stacks located throughout the mill are visible, as well as a large dust cloud from the surface (left side). Not shown in the photo, there are also several different industrial ponds located on the south side of the facility. Different emission sources are likely to have different compositions as they are

generated by different parts of the mill process. The BU HR-ToF-AMS also observed increases in pollutant (e.g., total organics and sulfates) during close passes downwind of the mill (**Figure 20**–**Figure 21**).

Figure 19. *Photo of the Domtar Ashdown Mill taken from the cab of MAQL3 while parked on the side of Hwy 71 near the plant entrance. Several emission sources are visible.*

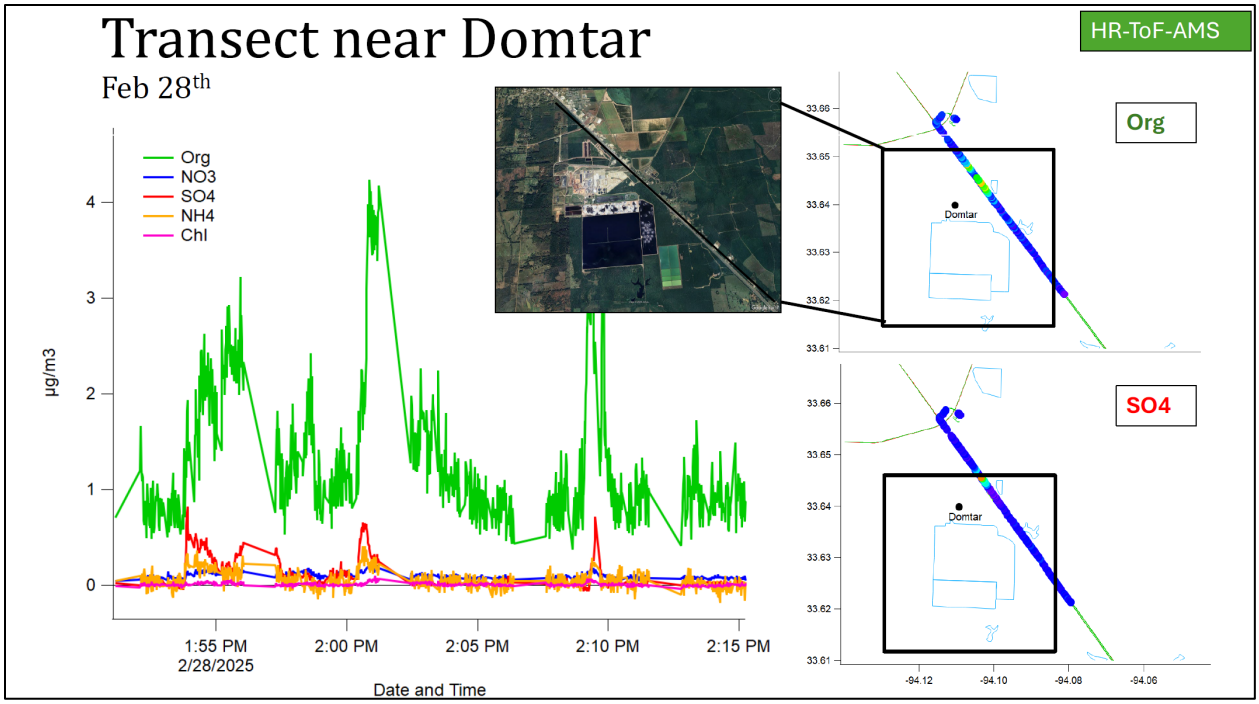

Figure 20. *HR-ToF-AMS time-series of mobile transect near Domtar on March 1, 2025, with unit mass resolution of Org, NO_3, SO_4, NH_4, and Chl species. The MAQL3 transect route, colored by Org (top right) and SO_4 (bottom right) concentration.*

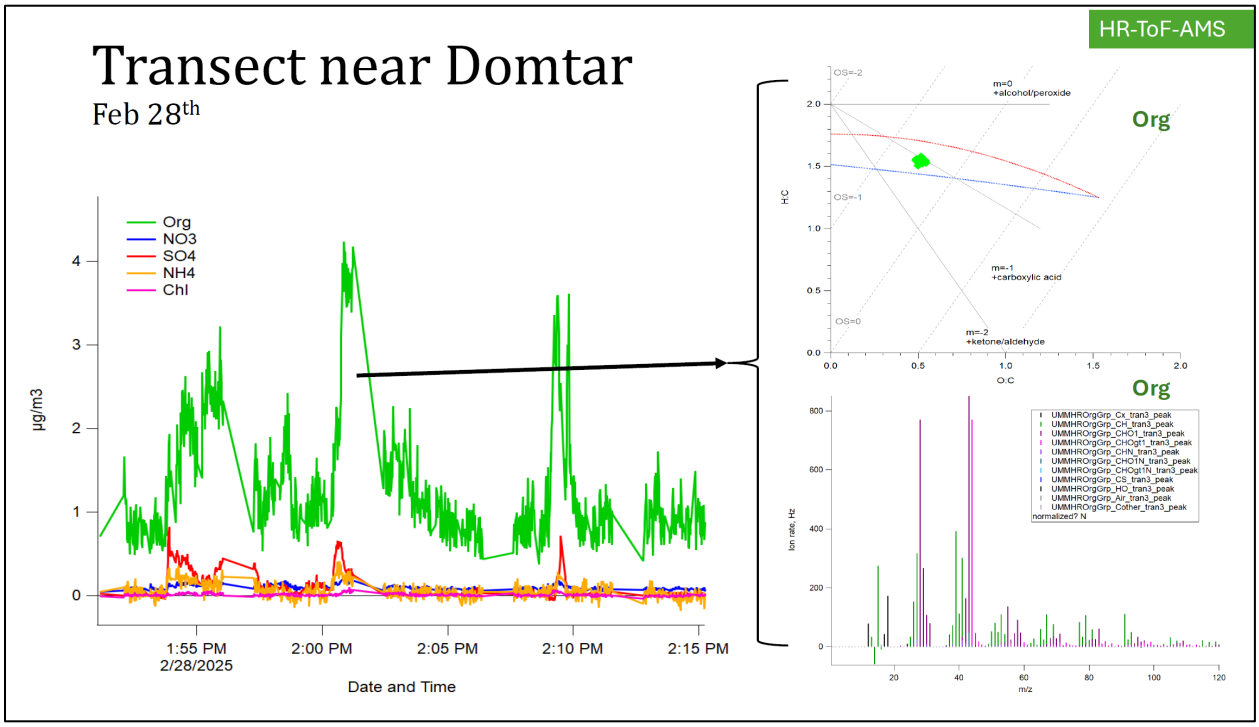

Figure 21. *HR-ToF-AMS time-series of mobile transect near Domtar on March 1, 2025, with unit mass resolution of Org, NO_3, SO_4, NH_4, and Chl species. Van Krevelen plot (top right) and HR Org mass spectrum (bottom right).*

On February 19, the decision was made to focus on the paper mill facility in Ashdown, AR and follow any detected plumes to determine if there was any transport into the Texarkana metropolitan area from this plume. This was actually the third day of focusing on plumes emanating from that area following measurements done on February 13 and 16. Winds on February 13 were out of the NE and on February 16 were out of the NW. On February 19, with a moderate, predominantly N wind, the minAML detection of the C10H17+ ion associated with pinenes was instrumental in determining the path of plumes from this paper mill source. Pinenes are known to be emitted in the combustion of pine wood, which does occur at paper mills. **Figure 22** depicts the loading of C10H17+ ions colored by signal intensity over the route of the minAML on that day. The plume was first captured on Pine Prairie Rd, a dirt road approximately 2 miles south of the Ashdown, AR plant (**Figure 23**). A GC scan was done at this point to better speciate the plume.

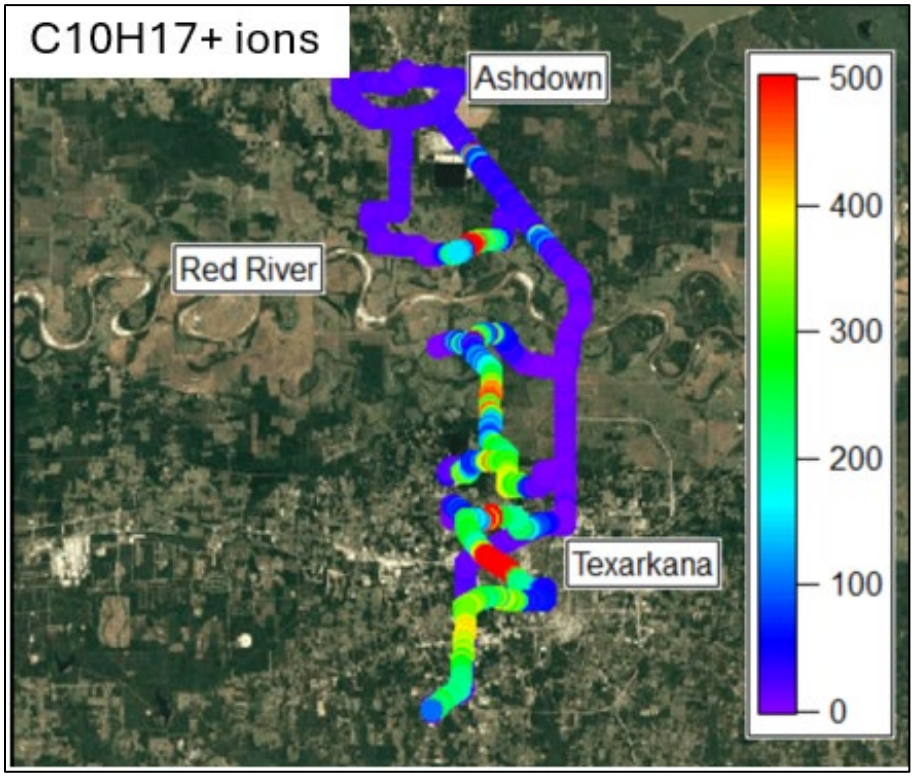

Figure 22. *The route of minAML is depicted colored by C10H17+ ions associated with pinene.*

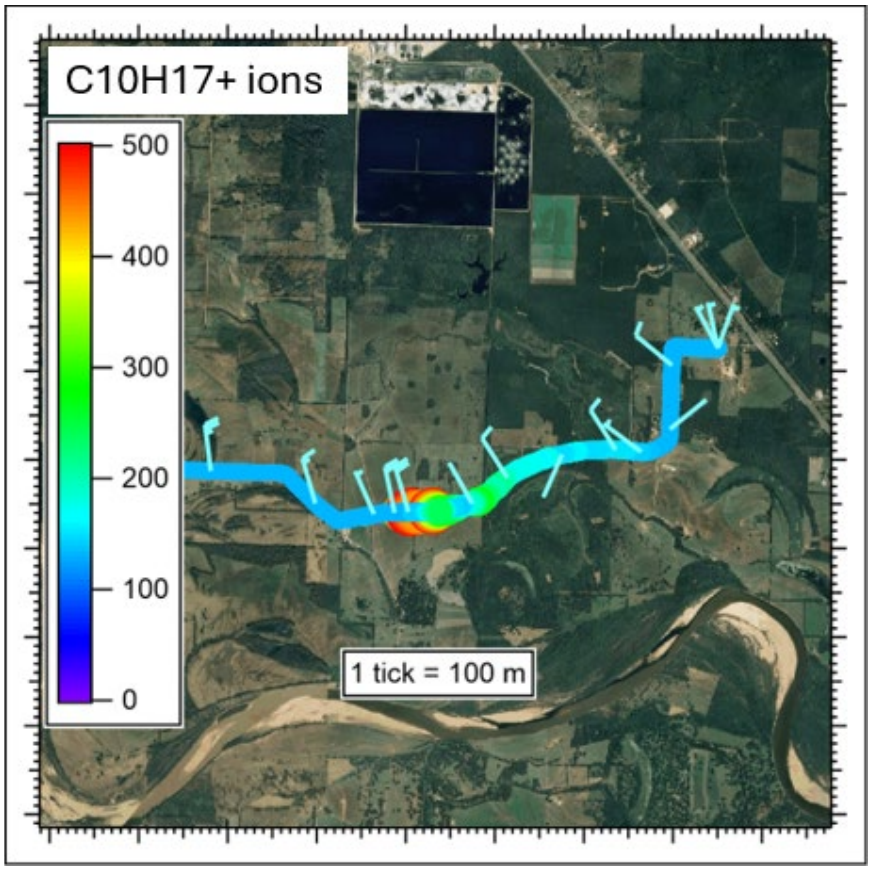

Figure 23. *Close C10H17+ ions plume crossing on Pine Prairie Rd, approximately 2 miles south of Ashdown AR facility. Wind barbs indicate a NNW wind on this transect.*

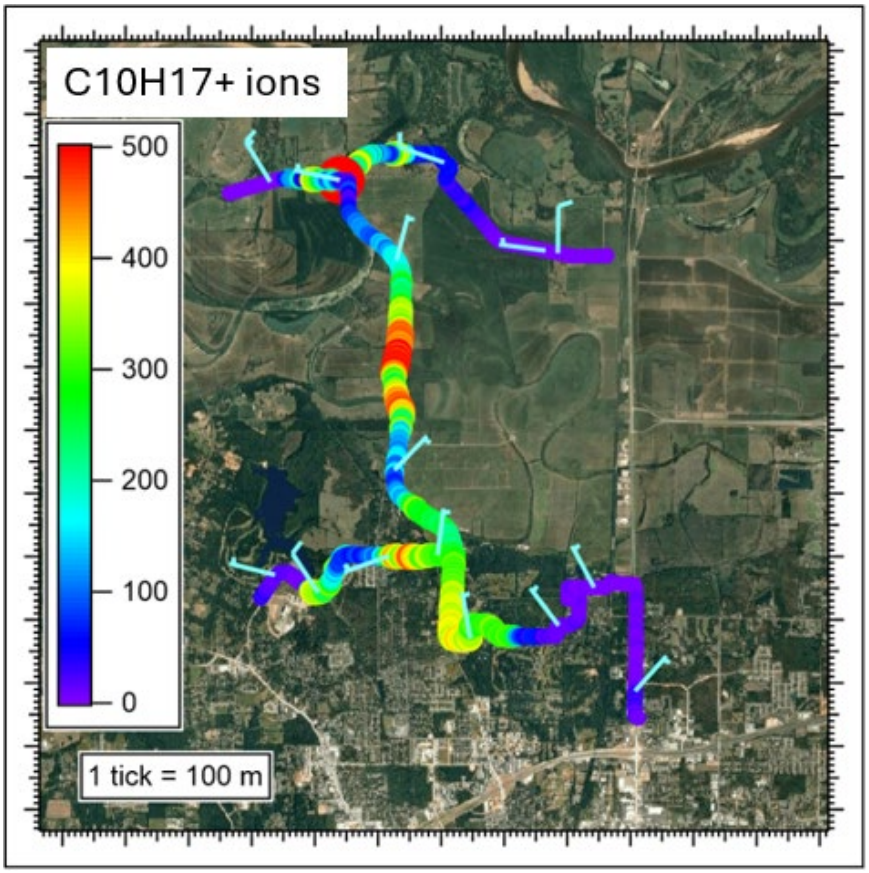

Figure 24. *Intermediate C10H17+ ions plume crossings occurring in the area North of Texarkana South of the Red River in the state of Texas.*

This plume was later tracked at intermediate locations in the state of Texas between the Red River and Texarkana (**Figure 24**). Winds were generally out of the North during this period.

The plume was eventually tracked into the city of Texarkana (**Figure 25**). It passed over the C1031 monitoring site and the RV park. Winds remain predominantly out of the North and there are quite defined edges to the plume. Downtown Texarkana is out of the plume. However, areas slightly to the west including the C1031 monitoring site are in the plume.

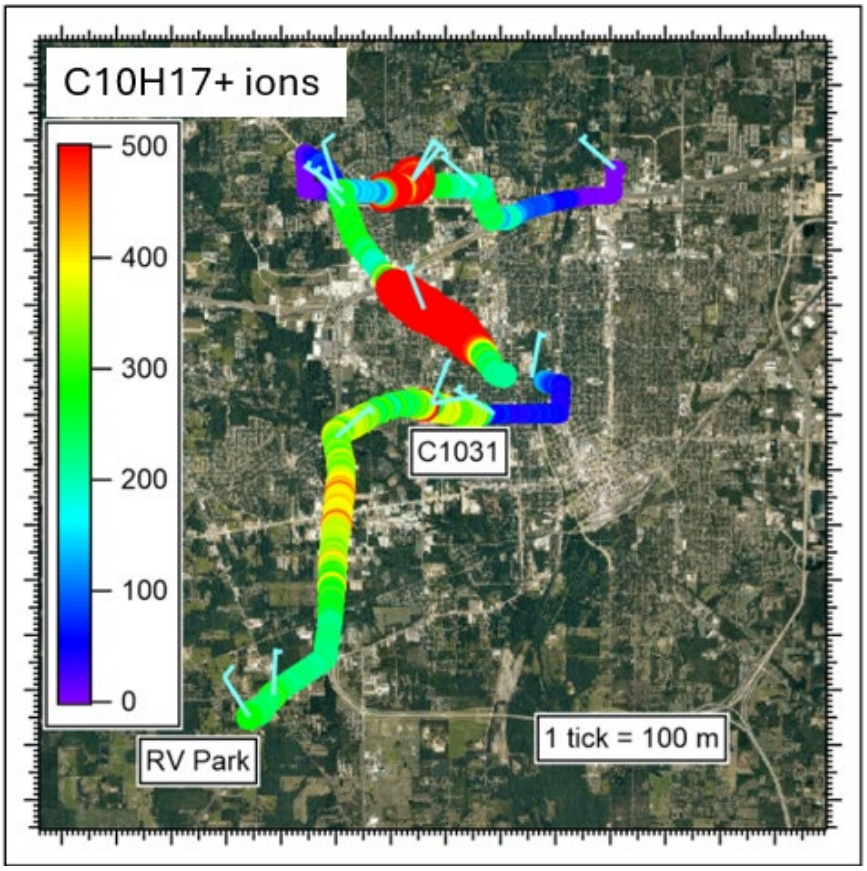

Figure 25 *C10H17+ ions plume crossings in Texarkana.*

4.4. Other Sources Surveyed and Associated Weather Conditions

4.4.1. Lumber Mill New Boston

Along with US-TRI reporting, this facility's CAA data indicates minor emissions of CO, PM<10 μm, SO_2, NO_2, and VOCs. Plumes of C10H17+ (pinene) were detected with the VOCUS in the minAML in this vicinity of the mill on two occasions. **Figure 26** depicts transects conducted when winds were out of the north-northeast. The trace is colored by the ion counts of C10H17+, and it's apparent that the plume emanating from the lumber mill is crossed twice on the map.

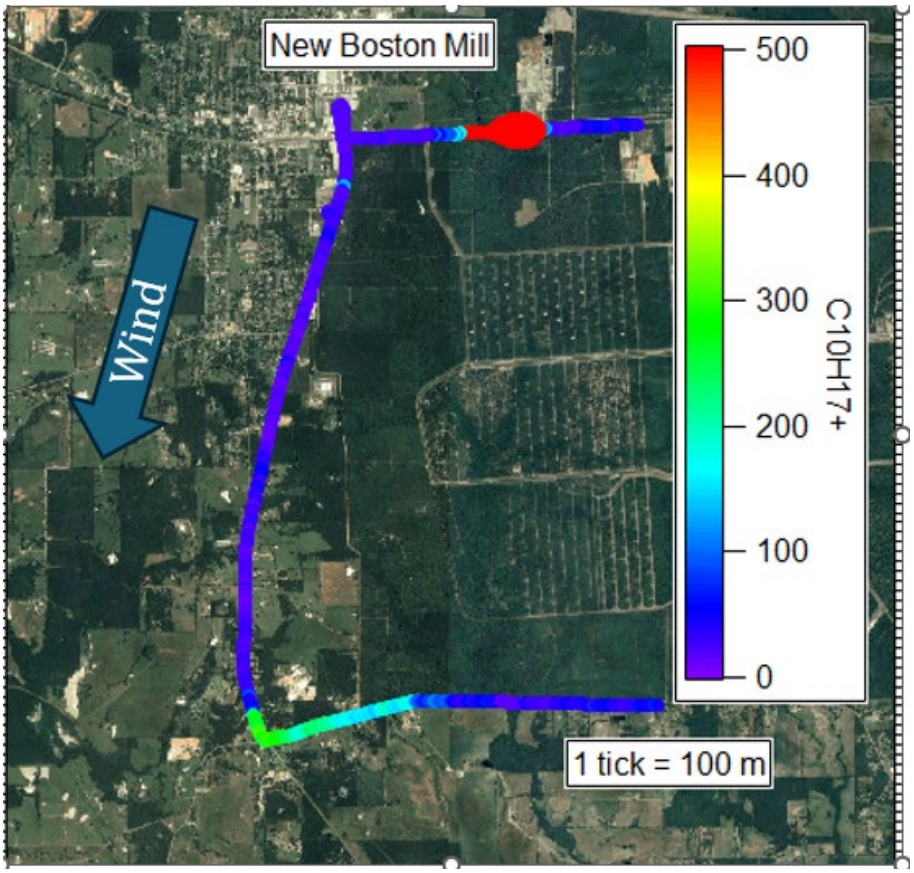

Figure 26. *Transects conducted with the minAML downwind of the New Boston Lumber Mill, colored and sized by the C10H17+ ion intensity.*

4.4.2. Cooper Tire Plant Texarkana, Arkansas

The cooper tire plant in Texarkana Arkansas was investigated by conducting transects downwind of its location on multiple occasions and plumes were never detected emanating from this facility.

4.5. Overnight Plumes with Associated Particle Loading Observed at RV Park

Plumes were frequently observed while the mobile labs were parked for the evening, conducting stationary sampling at the RV park. **Figure 27** shows the location of the RV park relative to the New Boston Monitor (C1031), as well as the Domtar and GPI facilities.

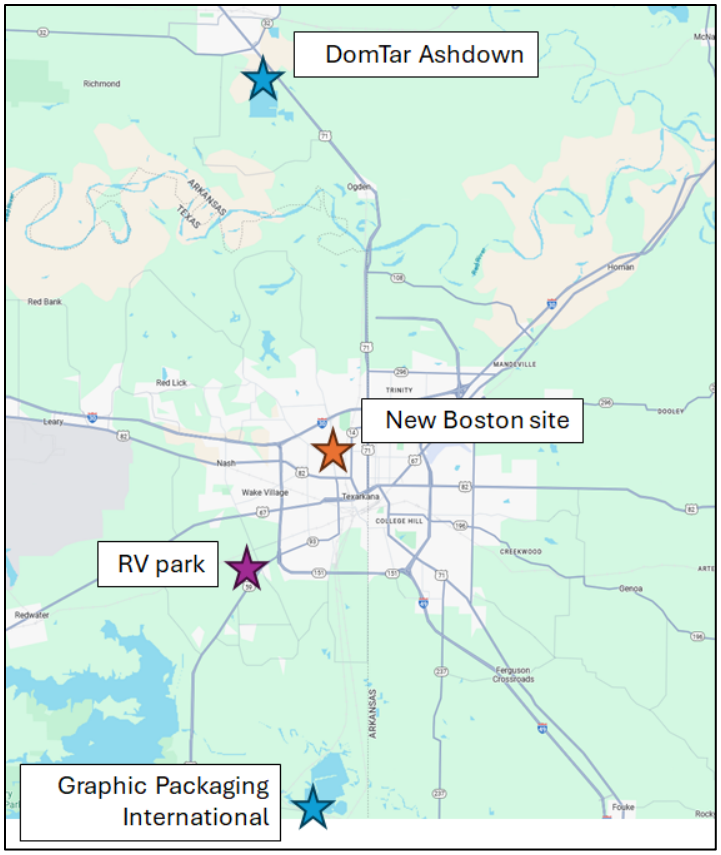

Figure 27. *Location of RV park, C1031 monitoring site and GPI and Domtar facilities.*

The stationary measurements yielded plentiful data and showed that a variety of pollutant levels increased significantly in the latter portion of the field campaign. These pollutants included $PM_{2.5}$, NO_y, CO, SO_2, and HCHO, with maximums often occurring overnight or in the very early morning, as shown in **Figure 28** where overnight (6 p.m.–6 a.m.) periods are shown as shaded regions.

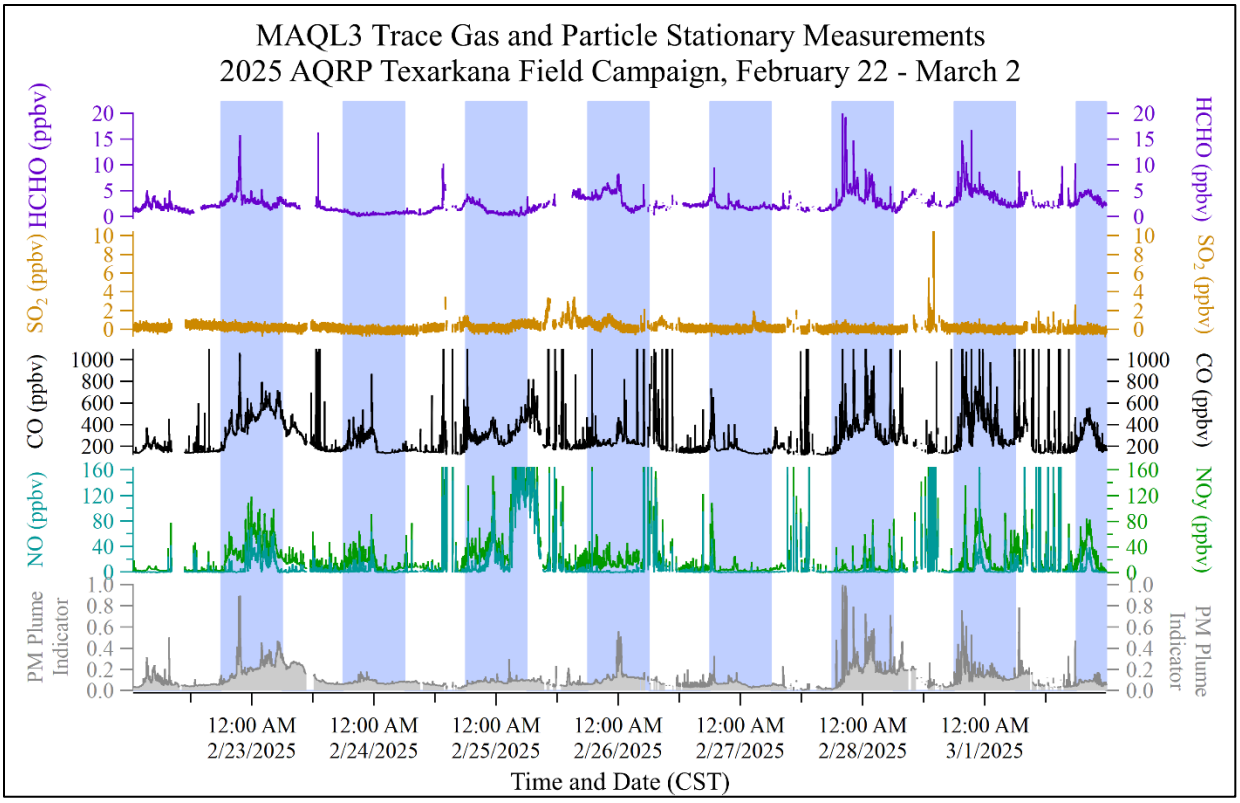

Figure 28. *Several of the MAQL3 UH measurements made while stationary during the later portion of the AQRP Texarkana campaign. Ten-second averages for NO, NO_y, SO_2, CO, HCHO, and the particulate matter relative plume strength indicator (with a maximum of 1, calculated from POPS instrument measurements) are plotted against Central Standard Time. Nighttime (6 p.m. to 6 a.m.) periods are indicated by the shaded regions.*

Enhanced particulate and $C_{10}H_{17}^+$ monoterpene were detected at the RV park on multiple occasions, and their relative correlations can be examined alongside plume intercepts done at different times when the mobile labs were conducting transects closer to the paper mills. **Figure 30** depicts transects done during the day on February 26 downwind of GPI which are compared to measurements the night before at the RV park when winds were coming from the GPI area.

Plumes were also observed at the monitoring site C1031 on at least one occasion coming from the Domtar facility. The comparison of the time series of the POPS on the minAML and the $C_{10}H_{17}^+$ monoterpene ion are shown in **Figure 29** both immediately downwind of Domtar and later that day at the C1031 site.

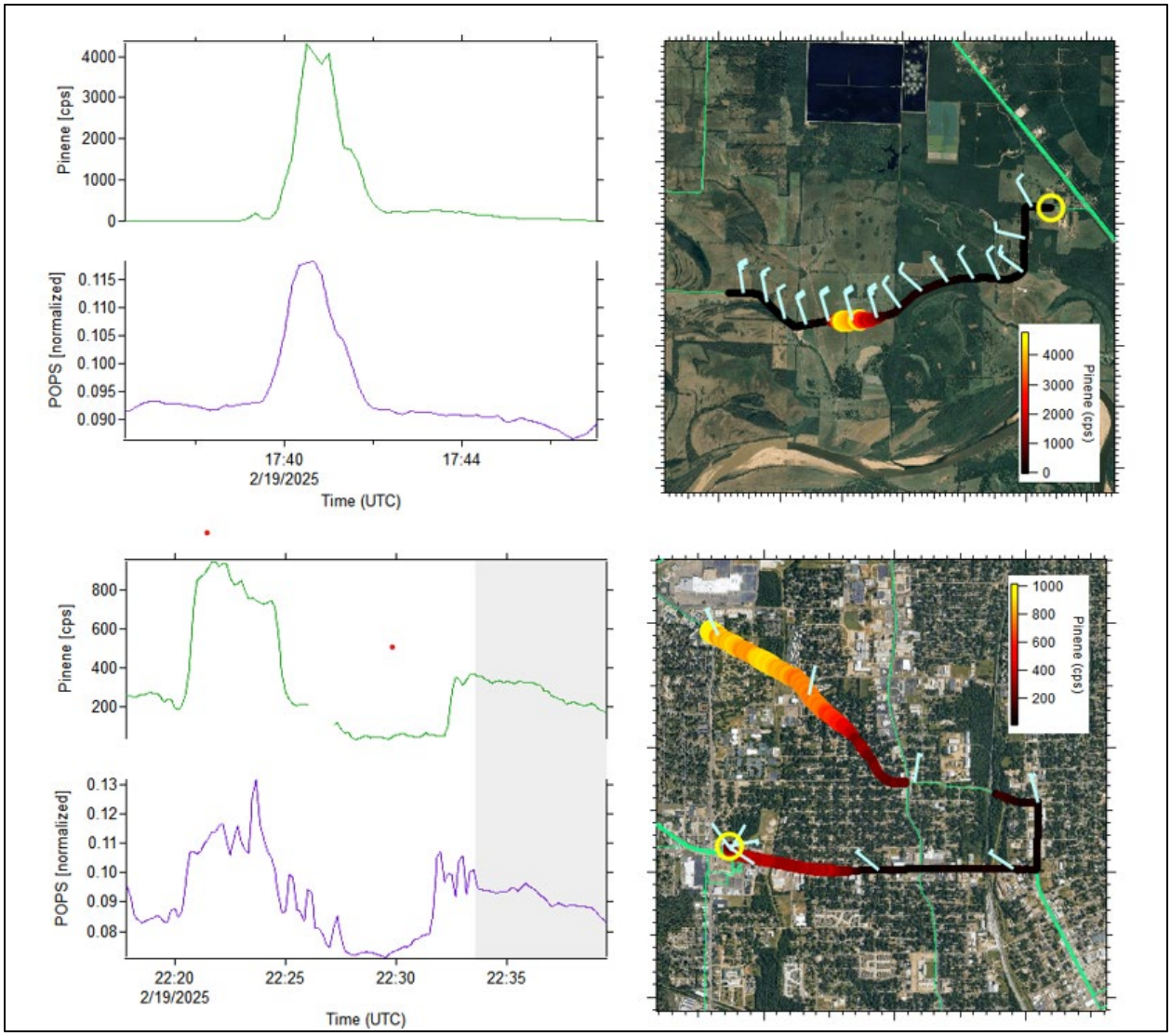

Figure 29. *Time series (left panels) of pinene ions (counts-per-second, $C_{10}H_{17}$) via Vocus PTR-MS and $PM_{2.5}$ via POPS (normalized to 1) during transects near Domtar Ashdown Mill (top) and C1031 (bottom). A yellow circle indicates the position of the minAML at the end of the transect, which implies the direction of travel. A grey shaded section of the bottom left panel indicates a period of time when the minAML was parked near the C1031 monitoring station. Concentration heatmaps (right panels) are colored and sized by the magnitude of pinene values during the transect. Wind barbs (blue staffs) point into the wind and indicate wind speed via flags.*

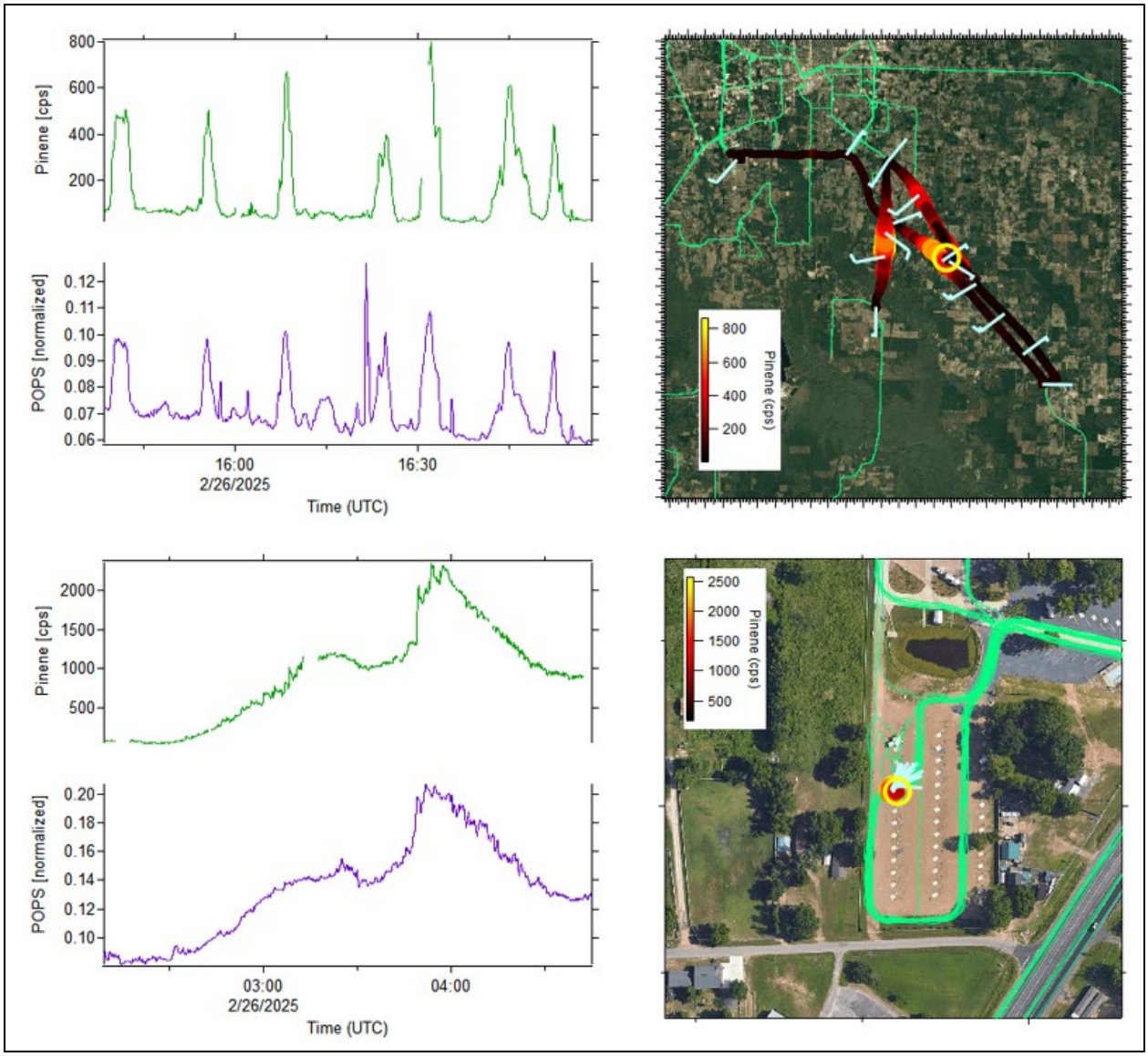

Figure 30. *Time series (left panels) of pinene ions (counts-per-second, $C_{10}H_{17}$) via Vocus PTR-MS and $PM_{2.5}$ via POPS (normalized to 1) during transects near the Graphic Packaging International mill (top) and RV park (bottom). A yellow circle indicates the position of the minAML at the end of the transect, which implies the direction of travel. Concentration heatmaps (right panels) are colored and sized by the magnitude of pinene values during the transect. Wind barbs (blue staffs) point into the wind and indicate wind speed via flags.*

Occasional enhancements of the monoterpene signal were observed at the RV park, as noted above. The plumes to emission sources were correlated by comparing the relative intensity of the mixture of monoterpenes observed in each GC-PTRMS sample. For example, a representative chromatogram for monoterpenes was captured on February 13 at the Domtar plant north-northwest of Texarkana (**Figure 31**). It was noted that the relative abundance of peaks 2, 3, and 4 in this sample was typical of the monoterpene mix observed from the paper plants. Overnight, from February 19 to February 20, an enhancement of monoterpenes was observed at the RV park

through the night. During the evening period with a lower signal, the mixture of monoterpenes at the RV park was markedly different than those observed at the Domtar plant. However, as the signal increased overnight, the mixture of monoterpenes became similar to the Domtar signature, indicating that the paper plant was the likely source of the enhancement. This analysis can be extended by creating a time series that compares the linear correlation of the individual monoterpenes with the average ratio of monoterpenes observed at each paper plant.

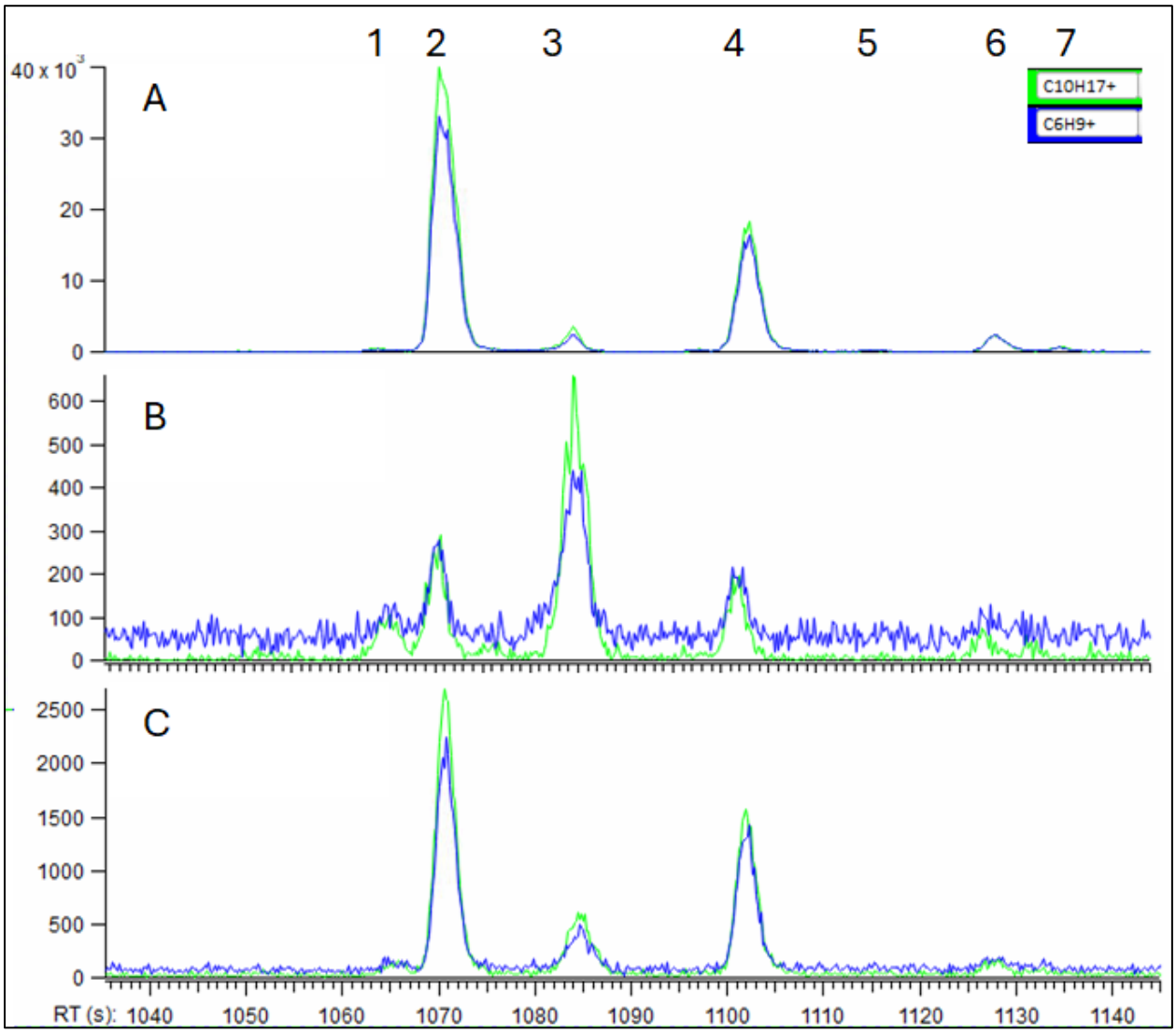

Figure 31. *Chromatograms showing monoterpene parent ion (C10H17+) and fragment ion (C6H9+) for three sample times: February 13 at the DomTar plant, February 19 at 21:45 at the RV park, February 20 at 2:45 at the RV park. The peaks numbered 1-7 correspond to different monoterpenes. Currently, only a known compound (α-Pinene) is assigned to peak 2.*

The $PM_{2.5}$ particle rate measured by the MAQL3 POPS was highest during overnight measurements at the RV park on February 22, 27, and 28 between the hours of 6:00 p.m. to 11:00 p.m. These high-pollution periods were isolated for further analysis, with **Figure 32** showing polar plots for these events. On February 22 and 28, a pronounced hotspot a few miles to the NW, assuming the source is local. Conversely, on February 27, the hotspot appears within a few miles to the SW and NW. The region may also experience pollution being carried in from farther away, potentially from outside the Texarkana area.

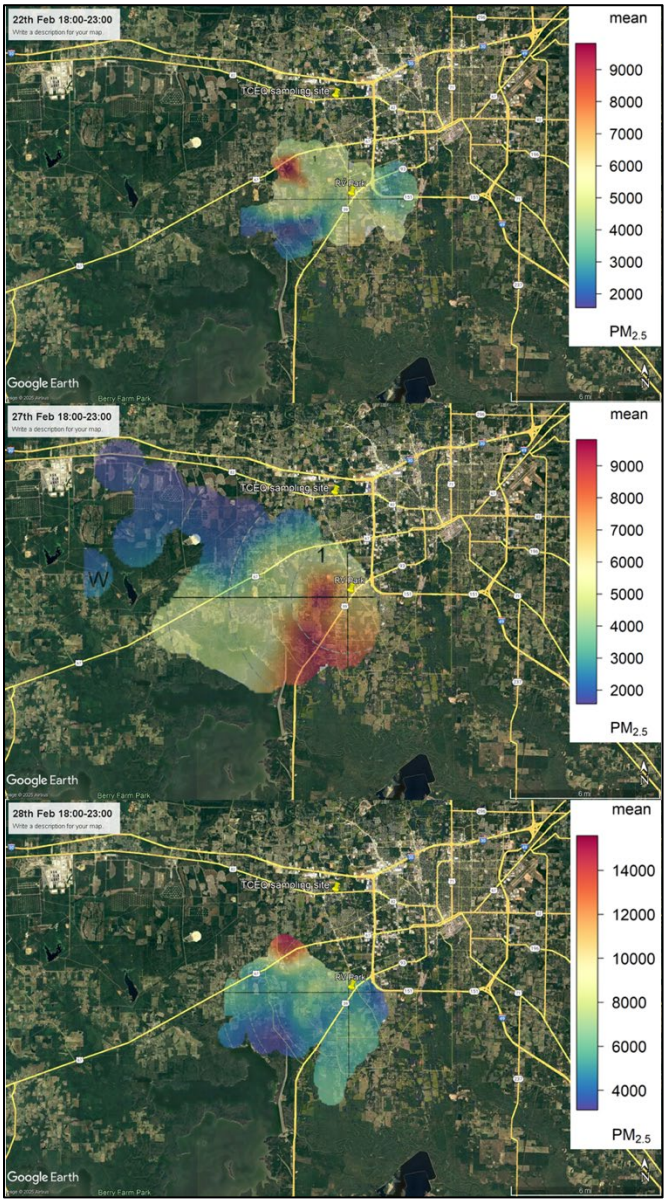

Figure 32. *Bivariate polar plot of MAQL3 $PM_{2.5}$ data on February 22 (upper), 27 (middle), and 28 (bottom) 2025 from 6:00 p.m. to midnight at the RV park ($PM_{2.5}$ in counts per second)*

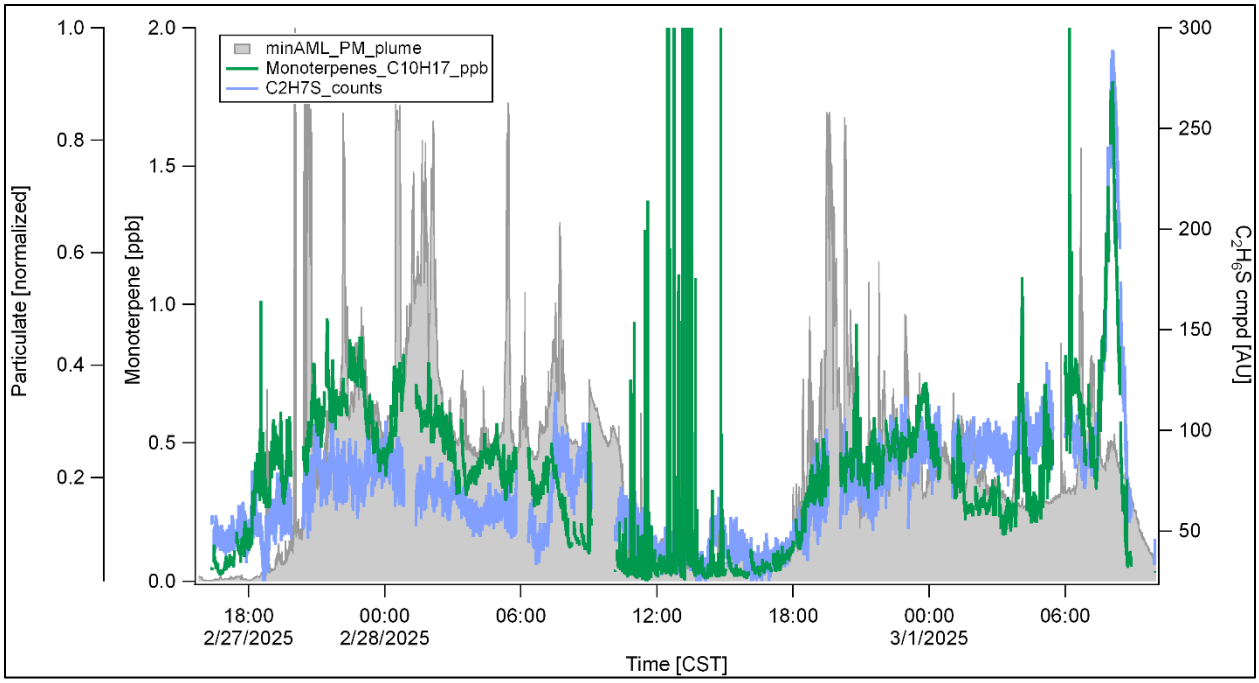

Figure 33. *Timeseries of monoterpene parent ion (C10H17+) and C_2H_6S+ compound via Vocus PTR-MS, and the minAML particulate matter via POPS (normalized to 1) measured overnight February 27, 2025–March 1, 2025 at the RV park.*

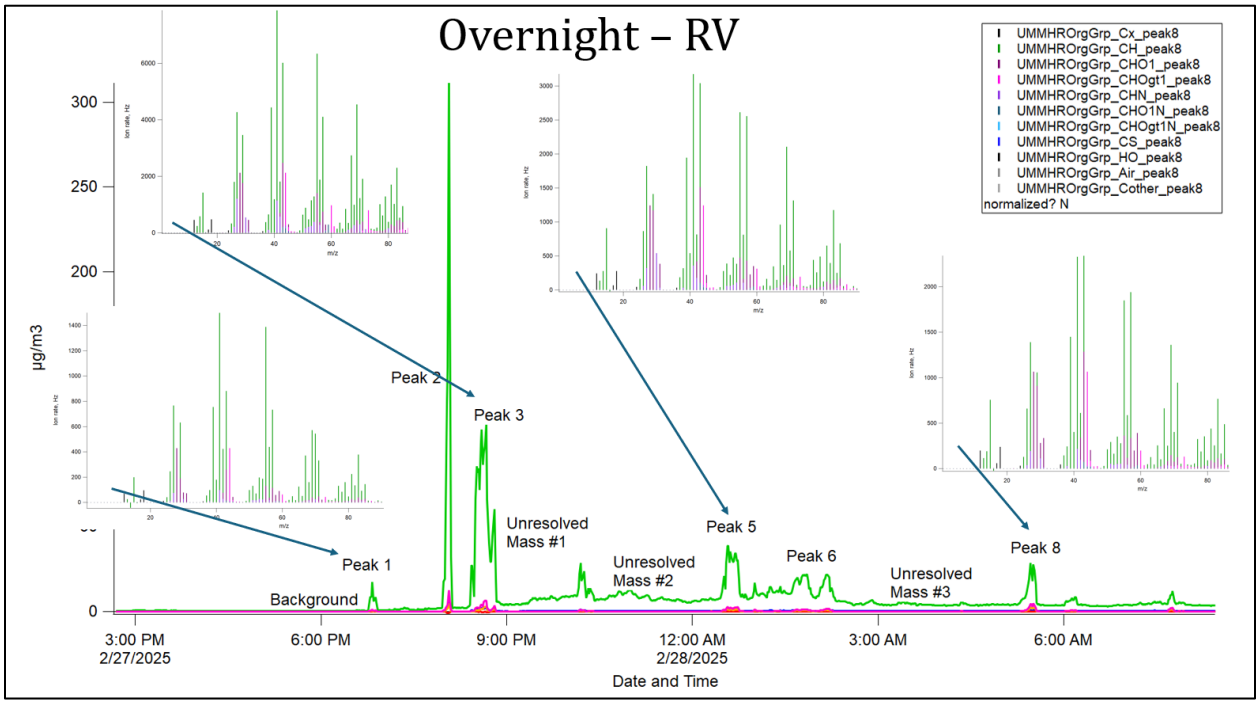

Figure 34. *HR-ToF-AMS time-series of overnight periods at the RV site on February 27 to 28, 2025, with unit mass resolution of Org, NO_3, SO_4, NH_4, and Chl species. HR Org mass spectrum of select peaks observed (four inlays). The mass spectrum of the four peaks (inlays) is dominated by green, suggesting the presence of hydrocarbon-like organic aerosols.*

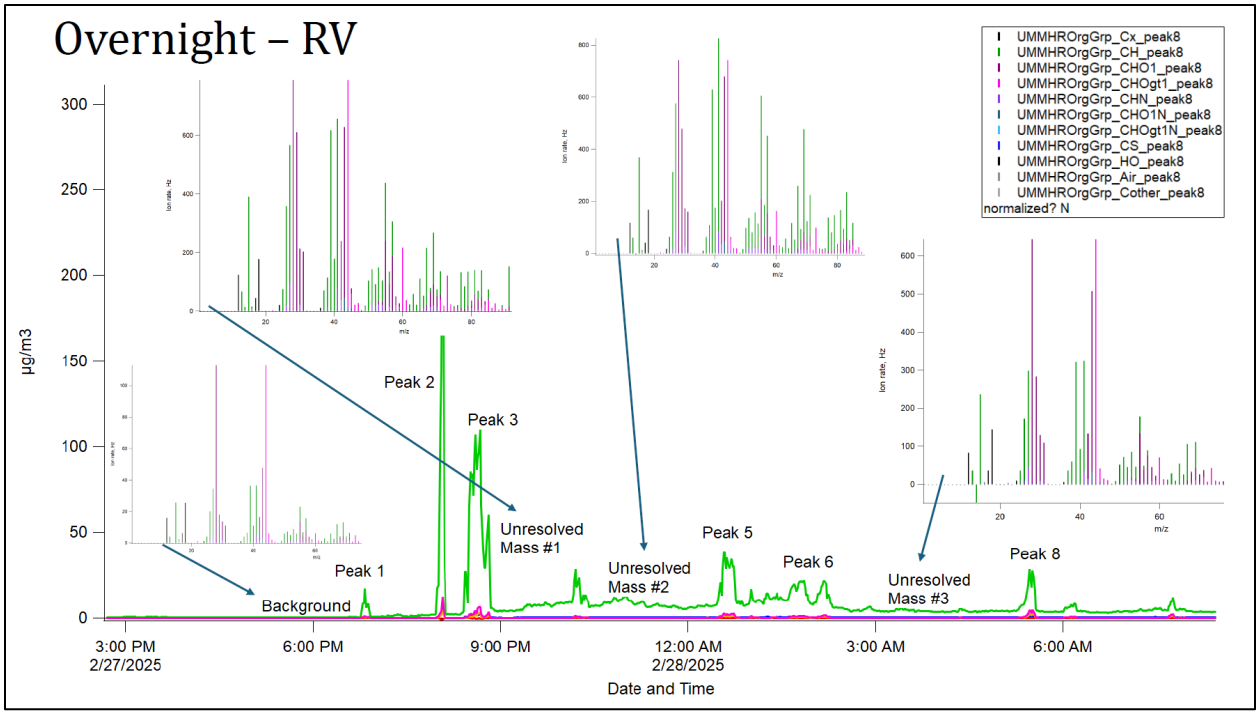

Figure 35. *HR-ToF-AMS time-series of overnight periods at the RV site on February 27 to 28, 2025, with unit mass resolution of Org, NO_3, SO_4, NH_4, and Chl species. HR Org mass spectrum of select periods of unresolved masses (four inlays). The mass spectrum of the underlying plume (identified as unresolved mass) is dominated by magenta (inlays), suggesting the presence of oxygenated organic aerosols.*

During the overnight periods (February 27–28, 2025), the Vocus PTR-MS measured distinct overnight enhancements of monoterpenes and C_2H_6S+ at the RV park, with a temporal timeseries profile that closely resembles the organic aerosol species measured via the HR-ToF-AMS (**Figure 34** and **Figure 35**). The similarity between the VOCs and aerosol measurements suggests that both instruments were characterizing the same plume. Subsequent high-resolution mass spectral analysis of the AMS organic aerosol mass spectra showed that the underlying plume was strongly dominated by oxygenated organic aerosols (OOA), while the more prominent peaks (e.g., peak 1, 3, 5, and 8) were strongly dominated by hydrocarbon-like organic aerosols (see **Figure 34**, **Figure 35** and the Van Krevelen Plot, H:C vs O:C plots in **Figure 36**). This suggests that the prominent peaks were closer to the mobile labs (due to their rapid increase and decrease, peak shape) and resemble primary combustion emissions (e.g., vehicle emissions). The underlying plume overnight plume showed a number of tracers that matched emissions observed during close transects near the pulp and paper plants. Specifically, OOA, monoterpenes, and C_2H_6S+. These observations were supported with NOAA HYSPLIT plume-dispersion modeling for these overnight periods. The model suggests that emissions from the pulp and paper mill (North of Texarkana) were transported southward, impacting both the RV park and C1031 monitoring sites during this period (**Figure 37**). Consistent with these observations, the C1031 site also observed an increase in $PM_{2.5}$ during this period (**Figure 37**).

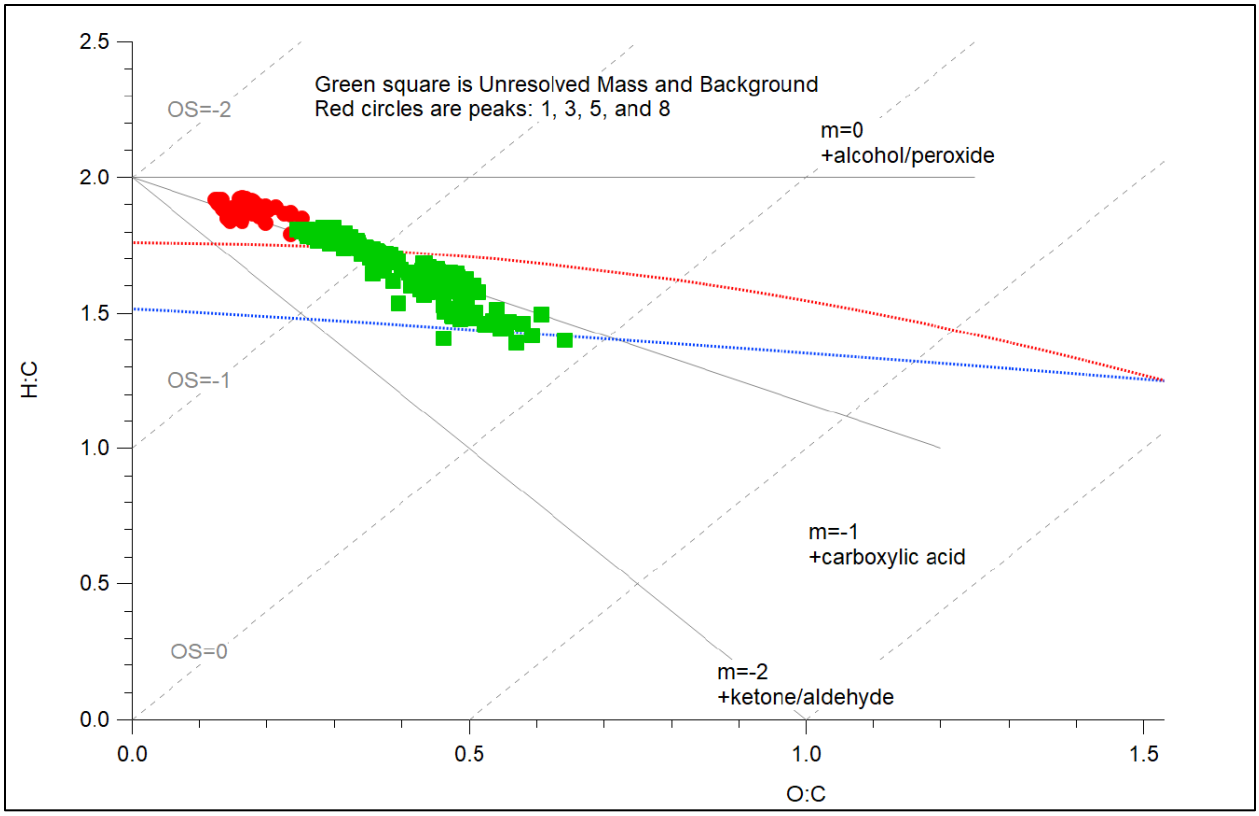

Figure 36. *Van Krevelen plot for the overnight period of February 27 and 28, 2025. Green squares represent periods of unresolved mass and background, and red circles are peaks of 1, 3, 5, and 8.*

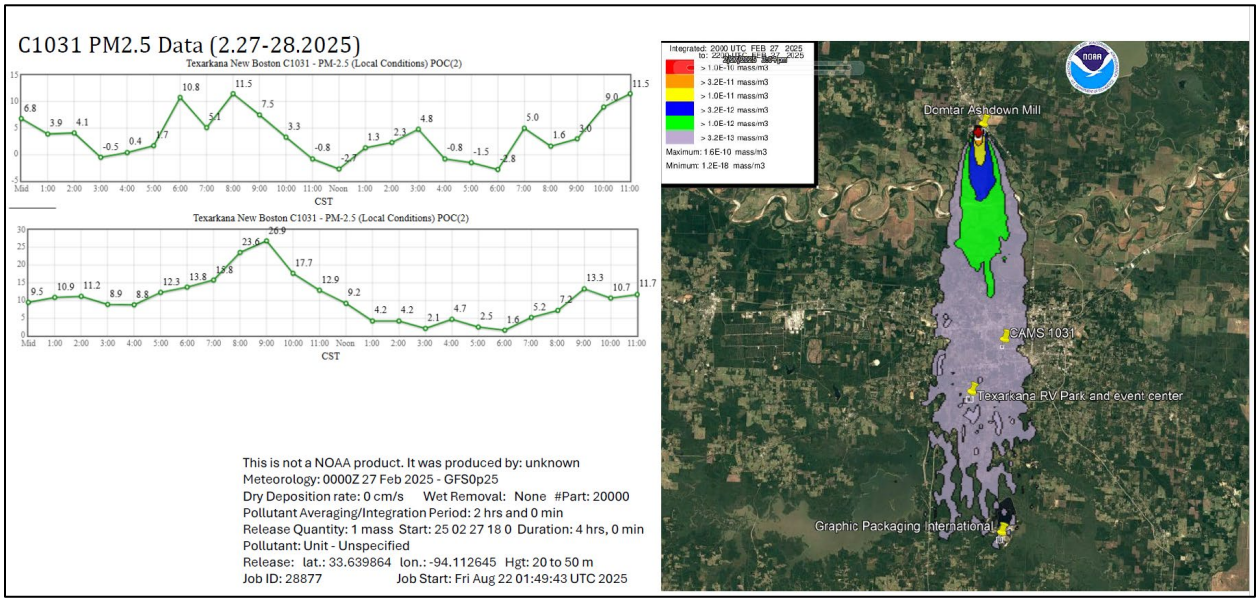

Figure 37. *NOAA HYSPLIT Dispersion model for the evening of February 27 and C1031 hourly $PM_{2.5}$ data for February 27 and 28, 2025*

4.6. Ozone Production Associated with GPI Emissions Plume

While this field campaign took place outside of the typical ozone season when the highest levels of ground level O_3 are most often observed, there was a noteworthy ozone enhancement measured during the February 24 outing. After some close-in passes by the GPI complex, MAQL3 and the minAML proceeded east to make some north-south transects downwind.

Figure 38 shows the three downwind passes, where pass one (1) began at the GPI complex and ended in the north. The O_3 plume was observed to the NE of GPI as was expected with the SSW winds. Significant O_3 enhancement was not seen close to the complex because O_3 is not directly emitted, but instead forms in the atmosphere through various VOC, NO_X, and other O_3 precursor reactions.

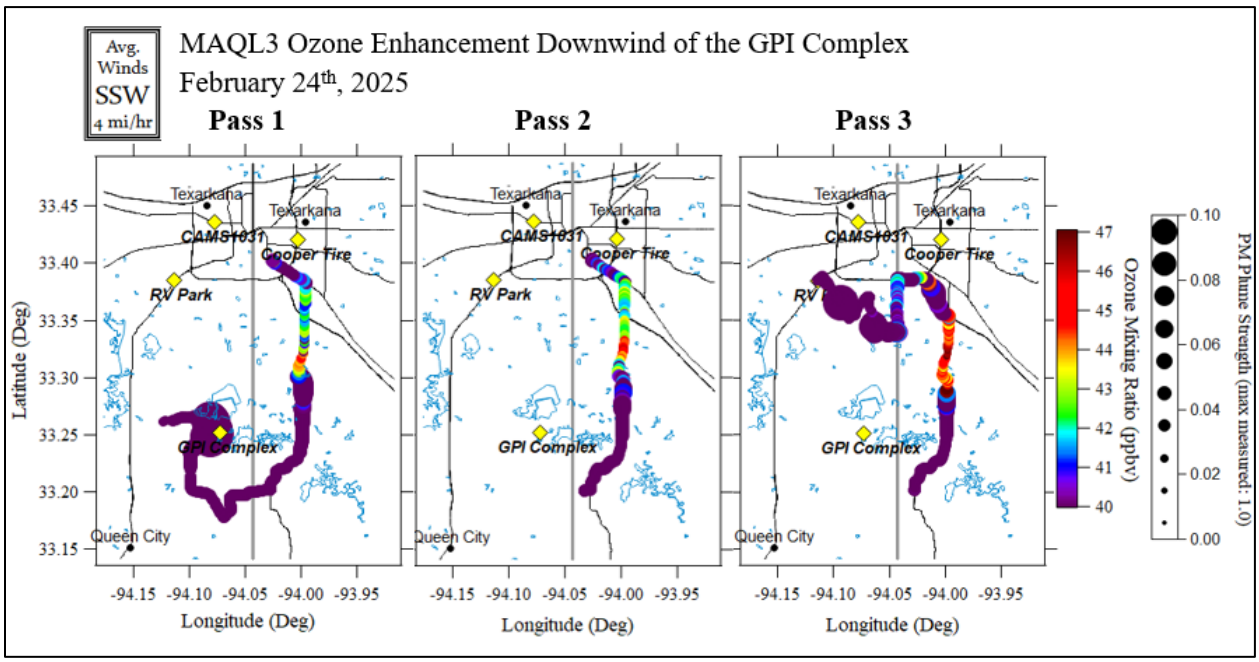

Figure 38. *Three passes downwind of the GPI complex, where an ozone enhancement was measured repeatedly on February 24, 2025 between 2:15 and 4:30 p.m. Each GPS track is colored by ozone and sized by the relative $PM_{2.5}$ plume strength as measured by the POPS.*

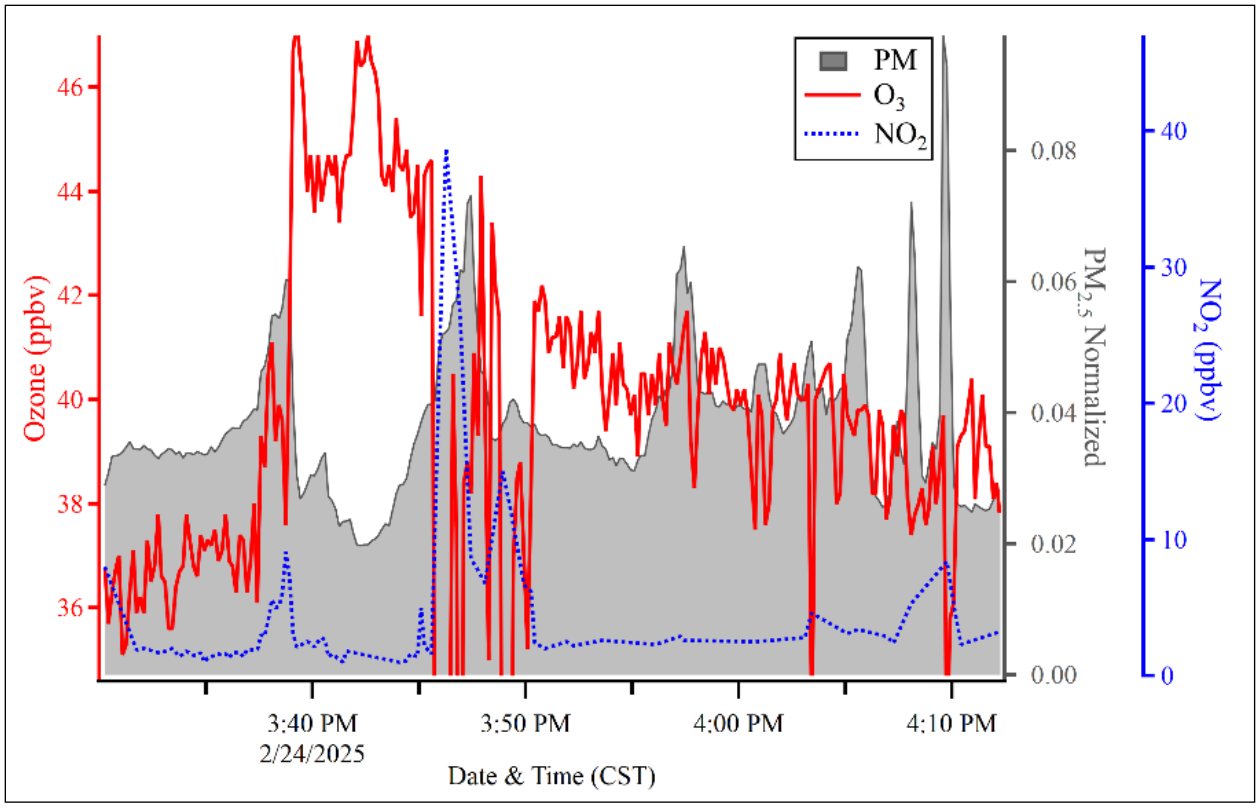

Figure 39. *Time series figure for Pass 3 in* ***Figure 38*** *showing the enhancement in O_3 occurring outside of $PM_{2.5}$ enhanced areas. NO_2 measurements show that the increase in O_3 around 3:40 p.m. is not related to a change in titration and partitioning of O_3 and NO_2.*

The spatial plots in **Figure 38** are colored by O_3, but the markers are sized by the $PM_{2.5}$ measurements from the POPS onboard MAQL3 to show that the O_3 plume was observed repeatedly to the north of the PM enhancement. While other measurements, including monoterpenes, showed evidence that both the PM and O_3 plumes were associated with the GPI complex, the emissions were clearly not uniform, and the part of the plume that resulted in the high ozone may have been from a different part of the facility (**Figure 39**).

This off-season ozone plume shows evidence that the paper mills may be contributing to elevated O_3 pollution in the area, which may be worth further study. In addition to this plume that, through repeated passes in and out of the plume, was shown not to be a simple result of the usual day-night cycle of O_3 formation, MAQL3 also measured the highest ambient O_3 levels of the campaign the following day.

5. CONCLUSION

During the course of this project, UH, Baylor, and Aerodyne successfully deployed two mobile laboratories with unique measurement payloads to sample large or suspected $PM_{2.5}$ point sources in the Texarkana, TX area. These mobile laboratories conducted measurements in tandem as well as separately to characterize plumes near the source and downwind simultaneously. Collocated overnight measurements also measured significant plumes, which were quite strong at times.

Two large-scale paper and packaging facilities, GPI and Domtar, operate near Texarkana and contribute to the region's industrial emissions. These facilities were the primary focus of the study, however, additional potential sources in the area, such as a tire factory, lumber mills, and other point and area sources were also sampled. One challenge the project faced was the atypical weather. During the planning phase, it appeared that the highest PM loadings at the C1031 site were associated with southerly winds. Wind roses from the Texarkana airport showed that southerly winds were the most frequent direction in the month of February. However, during the campaign, south winds were rarely seen at a strength and duration long enough to allow transport to the C1031 site from southern point sources. The one occurrence with moderate, sustained southerly winds occurred early in the morning and the teams deployed at 4:00 a.m. to sample the GPI complex's plume as it moved towards Texarkana. Under southwest winds, this plume was also tracked downwind far enough that had the winds been from the south, the plume would have likely reached Texarkana and the C1031 monitor.

On other days, the plume from the Domtar mill in Arkansas was seen to travel into Texas and the Texarkana area. On one occasion (February 19) the plume was tracked into the C1031 monitor area, although it was highly diluted by that time. Other sources in the area were much less pronounced when compared to the two paper mill operations, even though they too were sampled multiple times in an attempt to detect and characterize their plumes.

While this project was successful in meeting the objectives, there remain potential opportunities to quantify the types and impacts of sources impacting the Texarkana C1031 monitoring site.

Collecting 24-hr filter samples from the C1031 site on a regular basis would provide speciated $PM_{2.5}$ data that can be analyzed to identify and quantify the impacts of sources. Positive Matrix Factorization (PMF) could be applied to identify source contributions, and Conditional Bivariate Probability Function (CBPF) analysis could be used to link wind direction with pollutant levels, providing a clearer understanding of source impacts on air quality.

The BPP results indicate that although the wind conditions occur less frequently, there may be important sources to the southwest. The combination of the existing $PM_{2.5}$ measurement capabilities at C1031 could be combined with filter sampling PMF and CBPF results to further identify likely sources, as well as determine if activities near the monitor are creating a significant impact. There are at least two fast-food hamburger and one BBQ restaurant within approximately 300 m of the site. However, actual wind conditions during the campaign prevented meaningful measurements to identify or rule out these sources. A longer duration study

with speciated filter results complementing the existing site would likely yield valuable results, which could then be verified with additional mobile sampling of targeted areas.

6. REFERENCES

Arkansas Department of Energy and Environment (2022, June 23). *Operating Permit. Arkansas Division of Environmental Quality*. Retrieved July 31, 2025, from https://www.adeq.state.ar.us/downloads/WebDatabases/PermitsOnline/Air/0287-AOP-R24.pdf

Bergstrom, R. W., Pilewskie, P., Russell, P. B., Redemann, J., Bond, T. C., Quinn, P. K., and Sierau, B.: Spectral absorption properties of atmospheric aerosols, Atmospheric Chemistry and Physics, 7, 5937–5943, https://doi.org/10.5194/acp-7-5937-2007, 2007.

Carslaw, N., Creasey, D.J., Harrison, D., Heard, D.E., Hunter, M.C., Jacobs, P.J., Jenkin, M.E., Lee, J.D., Lewis, A.C., Pilling, M.J. and Saunders, S.M., (2001). OH and HO_2 radical chemistry in a forested region of north-western Greece. *Atmospheric Environment*, *35*(27), pp.4725-4737.

DeCarlo, P. F.; Kimmel, J. R.; Trimborn, A.; Northway, M. J.; Jayne, J. T.; Aiken, A. C.; Gonin, M.; Fuhrer, K.; Horvath, T.; Docherty, K. S.; Worsnop, D. R.; Jiménez, J. L. (2006). Field-Deployable, High-Resolution, Time-of-Flight Aerosol Mass Spectrometer. Analytical Chemistry,78 (24), 8281–8289. https://doi.org/10.1021/ac061249n

Dionne, J., & Walker, T. R. (2021). Air pollution impacts from a pulp and paper mill facility located in adjacent communities, Edmundston, New Brunswick, Canada and Madawaska, Maine, United States. *Environmental Challenges*, *5*, 100245.

Dommen, J., Prévôt, A. S. H., Hering, A. M., Staffelbach, T., Kok, G. L., & Schillawski, R. D. (1999). Photochemical production and aging of an urban air mass. *Journal of Geophysical Research: Atmospheres*, *104*(D5), 5493-5506.

Ehhalt, D. H. (1998). Radical ideas. *Science*, *279*(5353), 1002-1003.

Graphic Packaging. (n.d.). Graphic Packaging to create a $6 billion integrated paper-based packaging company by combining with International Paper's North America consumer packaging business. Graphic Packaging Holding Company. Retrieved July 31, 2025, from https://investors.graphicpkg.com/news-events/press-releases/detail/134/graphic-packaging-to-create-a-6-billion-integrated-paper-based-packaging-company-by-combining-with-international-papers-north-america-consumer-packaging-business

Iowa Environmental Mesonet. (n.d.). Dynamic Wind Rose Tool. Retrieved July 30, 2025, from https://mesonet.agron.iastate.edu/sites/dyn_windrose.phtml

Jenkin, M. E., & Clemitshaw K.C. (2000), Ozone and other secondary photochemical pollutants: Chemical processes governing their formation in the planetary boundary layer, *Atmospheric Environment*, 34, 2499–2527.

Kirchstetter, T. W., T. Novakov, and P. V. Hobbs (2004), Evidence that the spectral dependence of light absorption by aerosols is affected by organic carbon, J*ournal of Geophysical Research: Atmospheres*, 109, D21208, doi:10.1029/2004JD004999.

Krechmer J., Lopez-Hilfiker F., Koss A., Hutterli M., Stoermer C., Deming B., Kimmel J., Warneke C., Holzinger R., Jayne J., Worsnop D., Fuhrer K., Gonin M., de Gouw J. Evaluation of a New Reagent-Ion Source and Focusing Ion-Molecule Reactor for Use in Proton-Transfer-Reaction Mass Spectrometry. *Analytical Chemistry*. 90 (20):12011-12018. doi: 10.1021/acs.analchem.8b02641

McKeen, S. A., Hsie, E. Y., and Liu, S. C. (1991). A study of the dependence of rural ozone on ozone precursors in the eastern United States. *Journal of Geophysical Research: Atmospheres*, 96(D8), 15377-15394.

Moosmüller, H. and Chakrabarty, R. K.: Technical Note: Simple analytical relationships between Ångström coefficients of aerosol extinction, scattering, absorption, and single scattering albedo, *Atmospheric Chemistry and Physics*, 11, 10677–10680, https://doi.org/10.5194/acp-11-10677-2011, 2011.

Müller, M., George, C., D'Anna, B. Enhanced spectral analysis of C-TOF Aerosol Mass Spectrometer data: Iterative residual analysis and cumulative peak fitting, *International Journal of Mass Spectrometry*, Volume 306, Issue 1, 2011, Pages 1-8, ISSN 1387-3806, https://doi.org/10.1016/j.ijms.2011.04.007.

Ogren, J. A. (2010) Comment on "Calibration and Intercomparison of Filter-Based Measurements of Visible Light Absorption by Aerosols", *Aerosol Science and Technology*, 44:8, 589-591, DOI: 10.1080/02786826.2010.482111

Ogren, J. A., Wendell, J., Andrews, E., & Sheridan, P. J. (2017). Continuous light absorption photometer for long-term studies. *Atmospheric Measurement Techniques*, **10**(12), 4805–4818. https://doi.org/10.5194/amt-10-4805-2017

Schmeisser, L., Andrews, E., Ogren, J. A., Sheridan, P., Jefferson, A., Sharma, S., Kim, J. E., Sherman, J. P., Sorribas, M., Kalapov, I., Arsov, T., Angelov, C., Mayol-Bracero, O. L., Labuschagne, C., Kim, S.-W., Hoffer, A., Lin, N.-H., Chia, H.-P., Bergin, M., Sun, J., Liu, P., and Wu, H.: Classifying aerosol type using in situ surface spectral aerosol optical properties, *Atmospheric Chemistry and Physics*, 17, 12097–12120, https://doi.org/10.5194/acp-17-12097-2017, 2017.

Schnaiter, M., C. Linke, O. Möhler, K.-H. Naumann, H. Saathoff, R. Wagner, U. Schurath, and B. Wehner (2005), Absorption amplification of black carbon internally mixed with secondary organic aerosol, *Journal of Geophysical Research*, 110, D19204, doi:10.1029/2005JD006046.

Schnaiter, M., M. Gimmler, I. Llamas, C. Linke, C. Jäger, et al. Strong spectral dependence of light absorption by organic carbon particles formed by propane combustion. *Atmospheric Chemistry and Physics Discussions*, 2006, 6 (2), pp.1841-1866. ffhal-00301061f

Seinfeld, J. H., and Pandis S.N. (2006), *Atmospheric Chemistry and Physics: From Air Pollution to Climate Change*, 2nd ed., 1232 pp., Wiley, N. J.

Sillman, S. (1999). The relation between ozone, NO_x and hydrocarbons in urban and polluted rural environments. *Atmospheric Environment*, *33*(12), 1821-1845.

Sillman, S., and He, D. (2002). Some theoretical results concerning O_3-NOx-VOC chemistry and NOx-VOC indicators. *Journal of Geophysical Research: Atmospheres*, 107(D22), ACH 26. https://doi.org/10.1029/2001JD001123

Sillman, S., and West, J. J. (2009). Reactive nitrogen 728 in Mexico City and its relation to ozone precursor sensitivity: results from photochemical models. *Atmospheric Chemistry and Physics*, 9(11), 3477-3489.

Vázquez Santiago, J., Jaimes Palomera, M., Reséndiz Martínez, C., Hernández-Matamoros, A., Hata, H., Inoue, K., & Tonokura, K. (2024). Ozone responses to reduced precursor emissions: A modeling analysis on how attainable goals can improve air quality in the Mexico City Metropolitan Area. *Science of The Total Environment*, *885*, 163925.

World Meteorological Organization, *Global Atmosphere Watch, Aerosols Research*. https://www.nist.gov/system/files/documents/mml/Aerosol-Metrology-Workshop-Report-Final.pdf

7. APPENDIX A – DATA ATLAS (DAILY PLOTS + NOTES)

The following sections provide a summary of activities, timeseries plots and selected spatial plots (**Figure 40**–**Figure 107**), and contemporaneous field notes for the days in which mobile measurements were collected. The stationary days, which are included in the data files associated with this project, tended to be poor weather conditions or days when calibrations and maintenance were occurring.

February 10, 2025

The MAQL3 arrived at the Texarkana RV Resort. Field site and instrument setup and maintenance were completed.

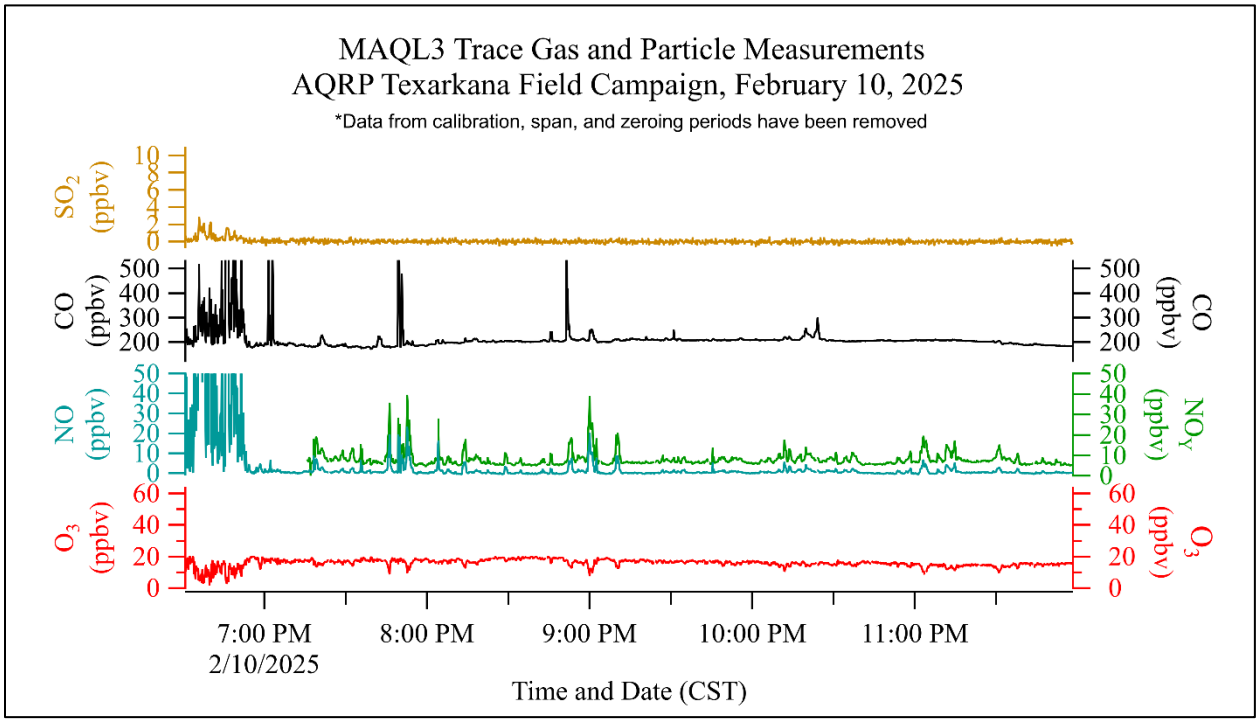

Figure 40. *Data summary of several of the MAQL3 measurements made during the Texarkana campaign. O_3, NO, NO_y, SO_2, and CO are plotted against Central Standard Time. Data was averaged to 10 seconds.*

February 11, 2025

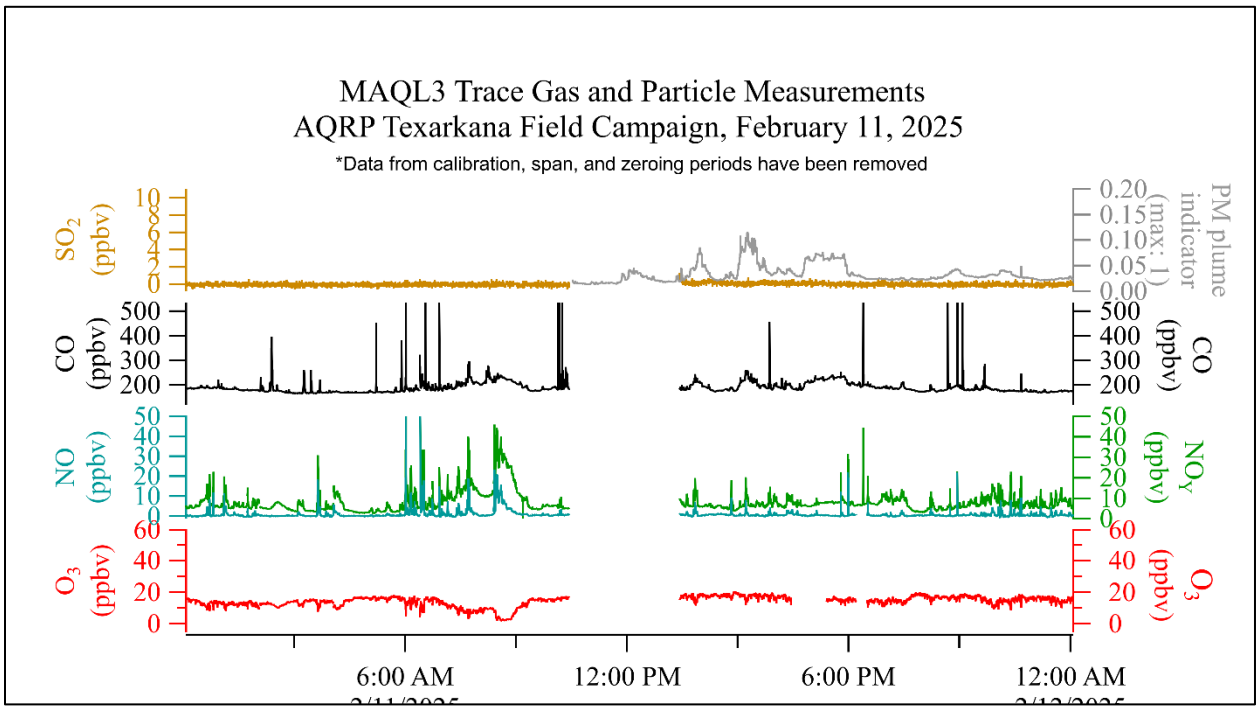

Figure 41. *Data summary of several of the MAQL3 measurements made during the Texarkana campaign. O_3, NO, NO_y, SO_2, CO, HCHO, and the particulate matter (PM) relative plume strength indicator (calculated from POPS instrument measurements) are plotted against Central Standard Time. Data was averaged to 10 seconds.*

February 12, 2025

The route followed for this day involved traveling along US-59 South, then heading east on FM 3129, joining Highway 251, and finally proceeding to AR-237. Along the way, MAQL3 passed through the plume behind the Aerodyne vehicle five times. Elevated signals were detected for sulfate, some nitrates, Persistent Organic Pollutants (POPS) and Condensation Particle Counter (CPC). These signals were especially consistent with increased nephelometer scattering signals, which indicate higher particle concentrations within stronger plume portions. On the southern end of the plume, possible increases in NO_x and CO concentrations were also noted. Since the "canyon effect" from nearby trees may have a substantial impact on plume dispersion, pollutant concentrations, and measurement reliability, it is advised that the sampling distance behind the Aerodyne vehicle be modified in subsequent passes, accounting for both the degree of enclosure produced by roadside vegetation and the current wind conditions.

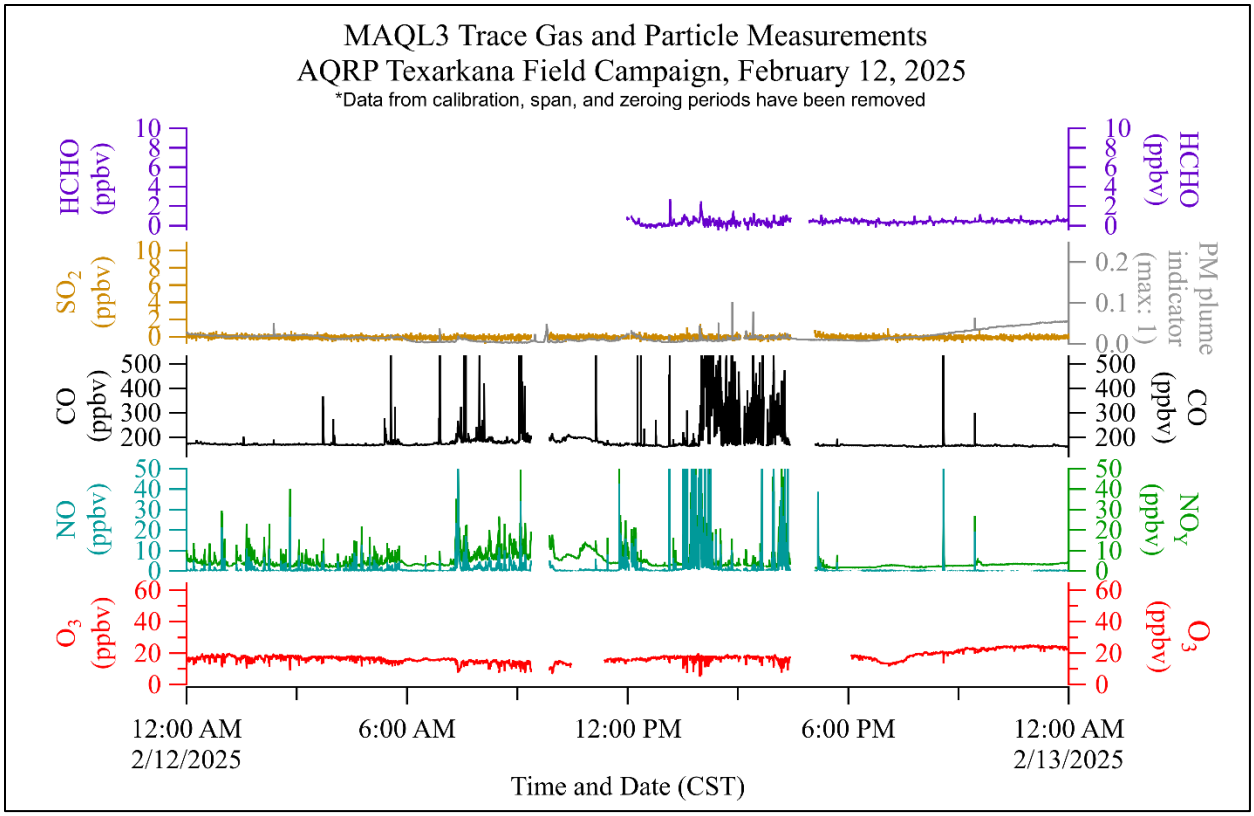

Figure 42. *Data summary of several of the MAQL3 measurements made during the Texarkana campaign. O_3, NO, NO_y, SO_2, CO, HCHO, and PM relative plume strength indicator (calculated from POPS instrument measurements) are plotted against Central Standard Time. Data was averaged to 10 seconds.*

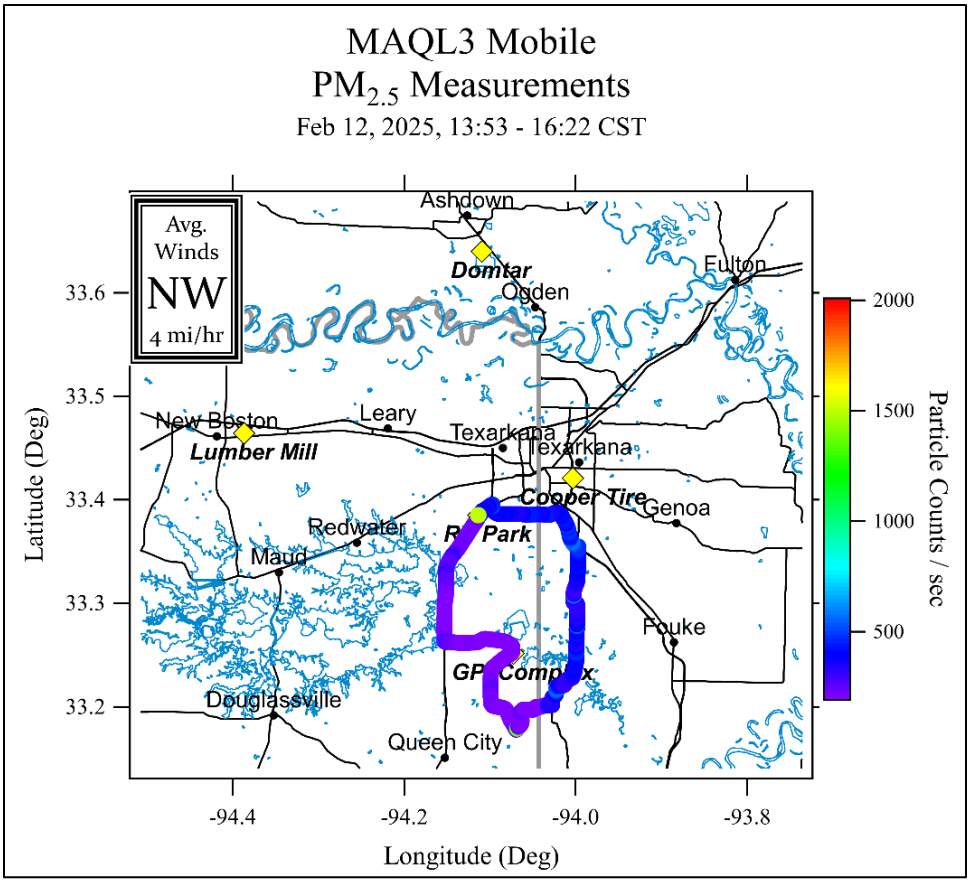

Figure 43. *The UH mobile lab sampling route for February 12, 2025, colored by $PM_{2.5}$ particle count per second measured by the MAQL3 POPS instrument. Average wind conditions (upper left), as reported by CAMS 1031, were calculated for the mobile sampling period (top of graph). The most recent tracks overlay older ones.*

February 13, 2025

A targeted drive was made in the direction of Ashdown, Arkansas, where the Aerodyne had previously located a plume coming from the local paper mill plant. However, access issues emerged since direct sampling close to the source was not possible due to a number of nearby roads being either unpaved or limited to truck traffic. Instead, MAQL3 moved south of the Red River and moved further downwind to find the plume. In this region, the plume was indicated by increased signals in POPS and CPC, as well as slight increases in nephelometer scattering. However, there were no notable changes in the chemical signal detected by the Aerosol Mass Spectrometer. After finishing their on-site sampling near the paper mill, the Aerodyne team rejoined our platform south of the Red River, where both teams successfully observed the plume again north of I-30 but south of the Red River, confirming plume transport into the broader region.

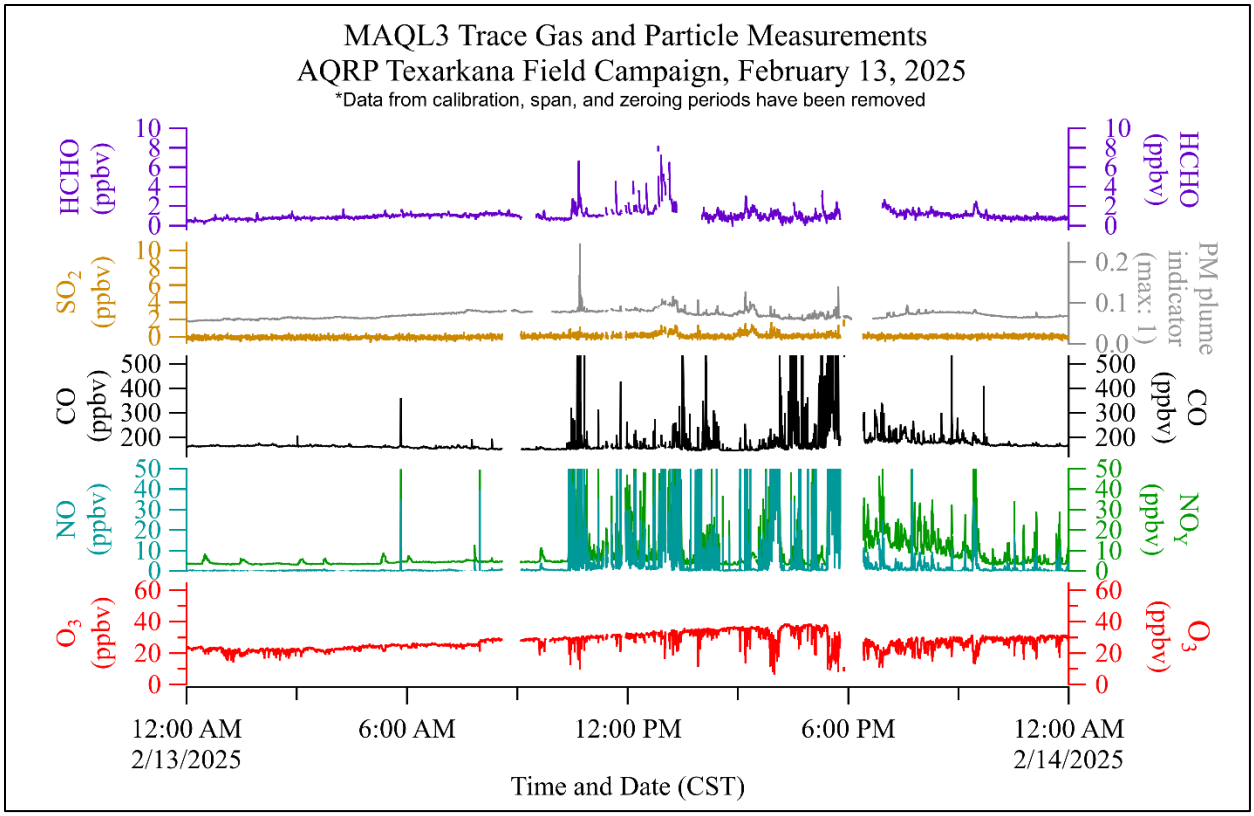

Figure 44. *Data summary of several of the MAQL3 measurements made during the Texarkana campaign. O_3, NO, NO_y, SO_2, CO, HCHO, and the particulate matter (PM) relative plume strength indicator (calculated from POPS instrument measurements) are plotted against Central Standard Time. Data was averaged to 10 seconds.*

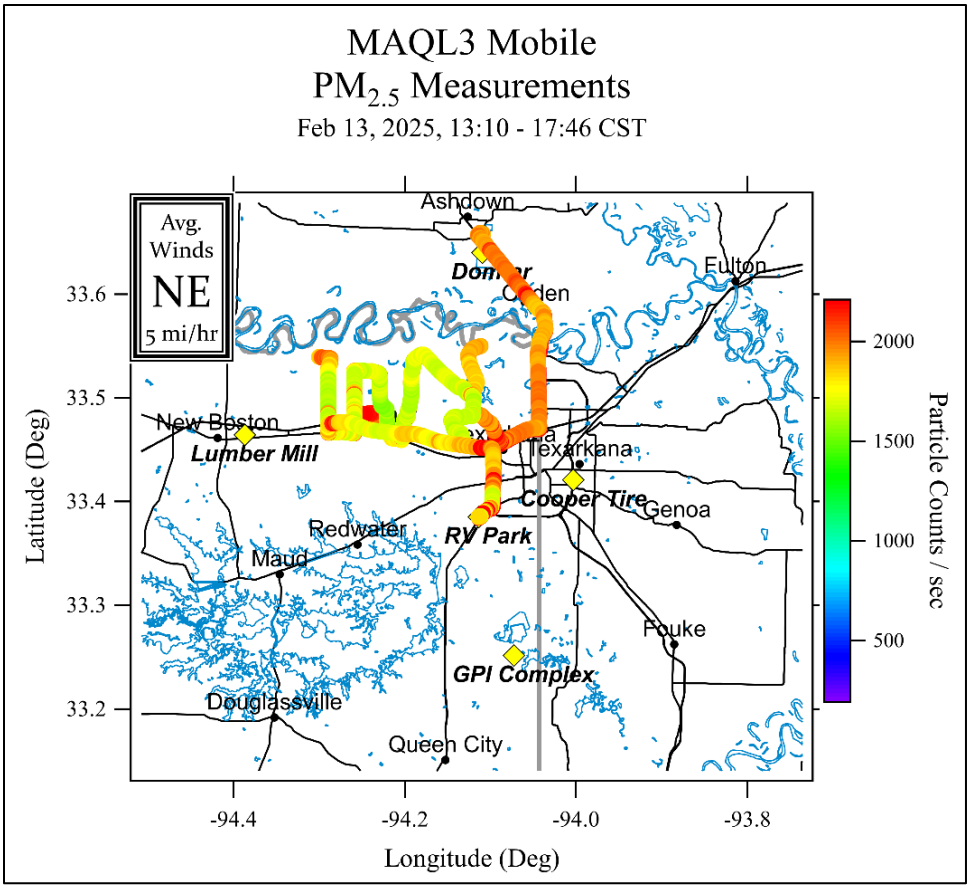

Figure 45. *The UH mobile lab sampling route for February 13, 2025, colored by $PM_{2.5}$ particle count per second measured by the MAQL3 POPS instrument. Average wind conditions (upper left), as reported by CAMS 1031, were calculated for the mobile sampling period (top of graph). The most recent tracks overlay older ones.*

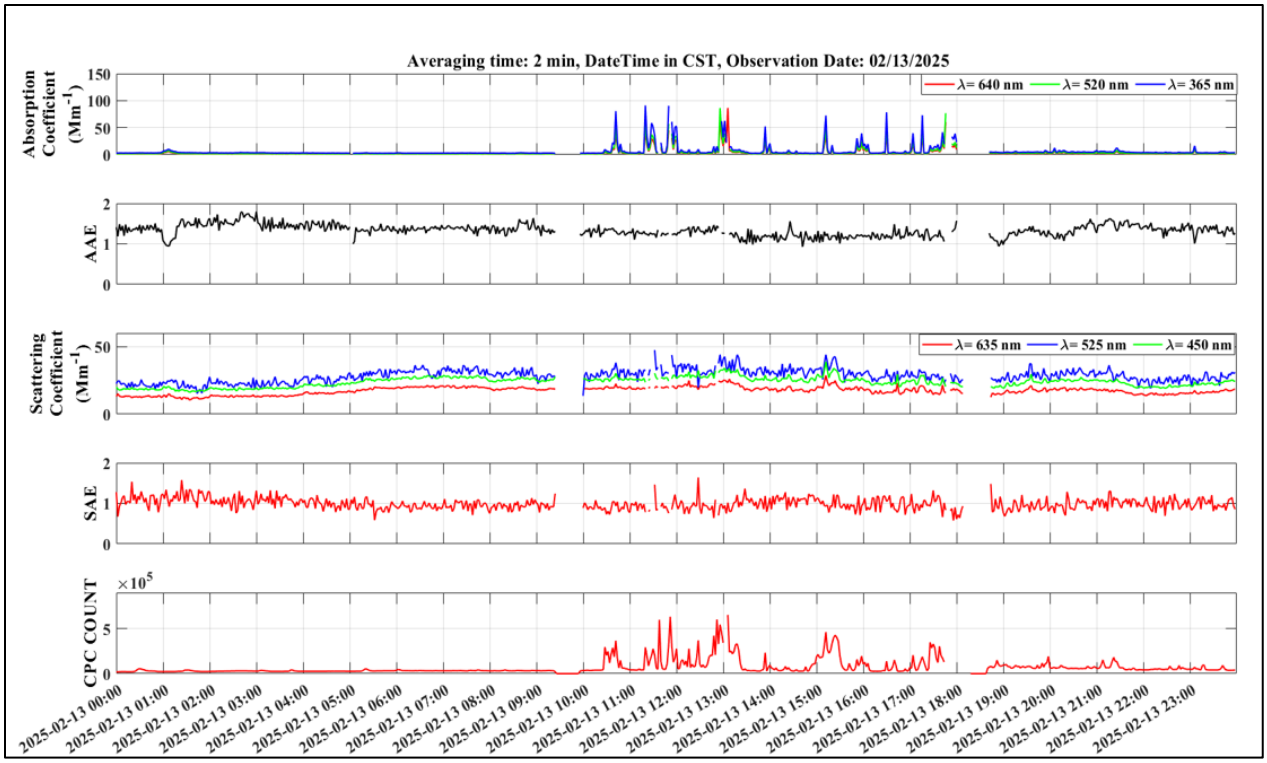

Figure 46. *Time-series data of select MAQL3 aerosol measurements made during the Texarkana campaign for February 13, 2025. Absorption and scattering coefficients, AAE and SAE (calculated values) and particle counts averaged over 120 seconds.*

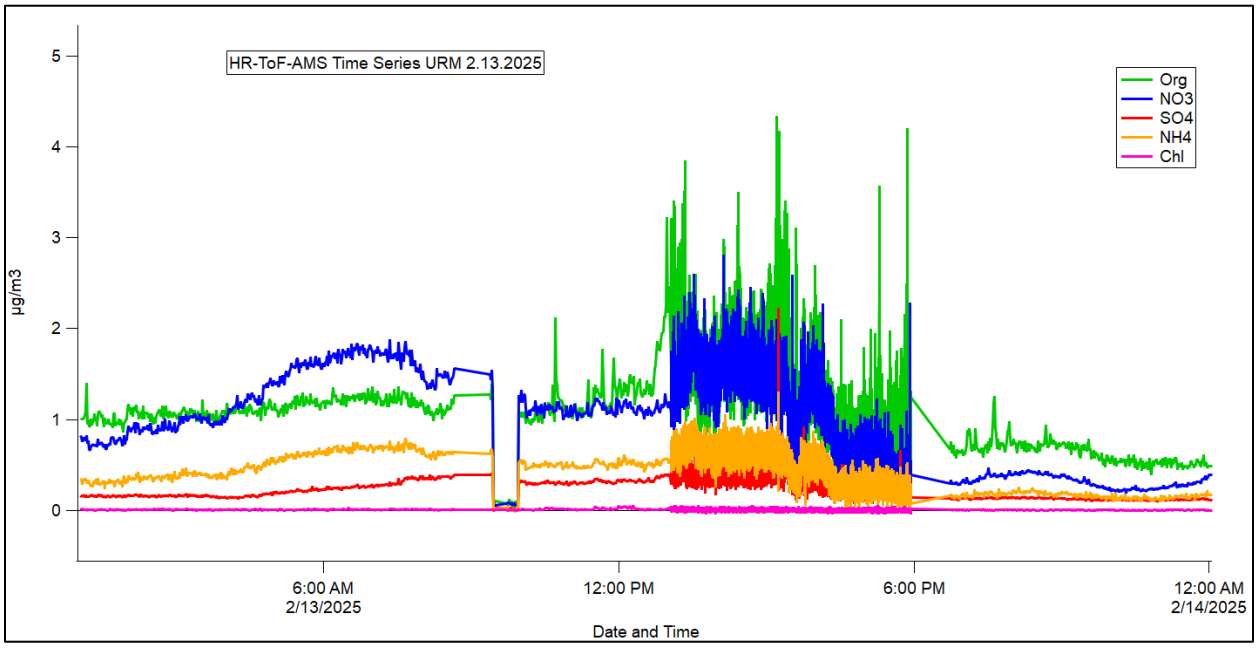

Figure 47. *Time-series data of select HR-ToF-AMS species (Organics, Nitrate, Sulfate, Ammonium, Chloride) made during the Texarkana campaign for February 13, 2025.*

February 14, 2025

MAQL3 did close-range sampling near the GPI paper mill in the morning, followed by plume tracking along US-59 after noon, and along US-67 later in the day. Elevated signals were observed in CPC, POPS, and NO_X, with occasional SO_2 enhancements, particularly during close-range passes near the facility. Observations suggest the possibility of multiple distinct plumes originating from the paper mill area.

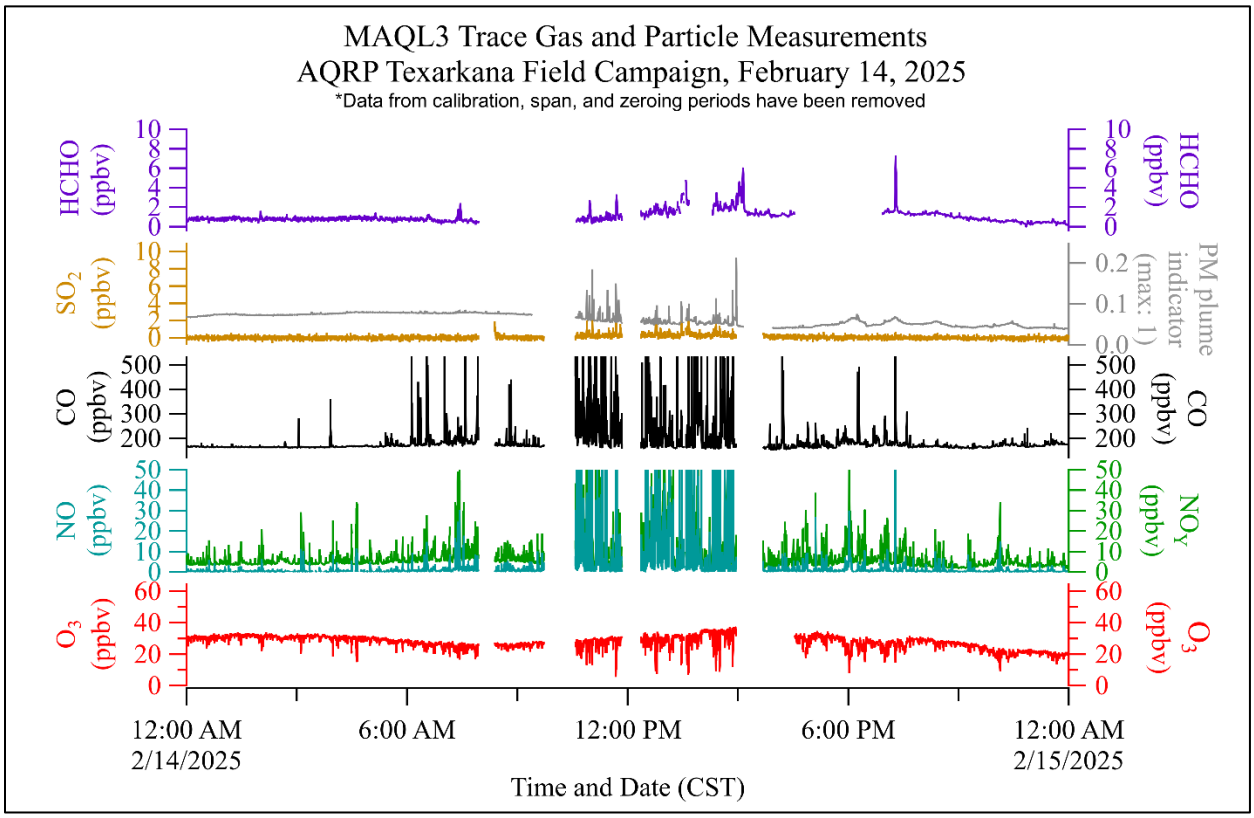

Figure 48 . *Data summary of several of the MAQL3 measurements made during the Texarkana campaign. O_3, NO, NO_y, SO_2, CO, HCHO, and the particulate matter relative plume strength indicator (calculated from POPS instrument measurements) are plotted against Central Standard Time. Data was averaged to 10 seconds.*

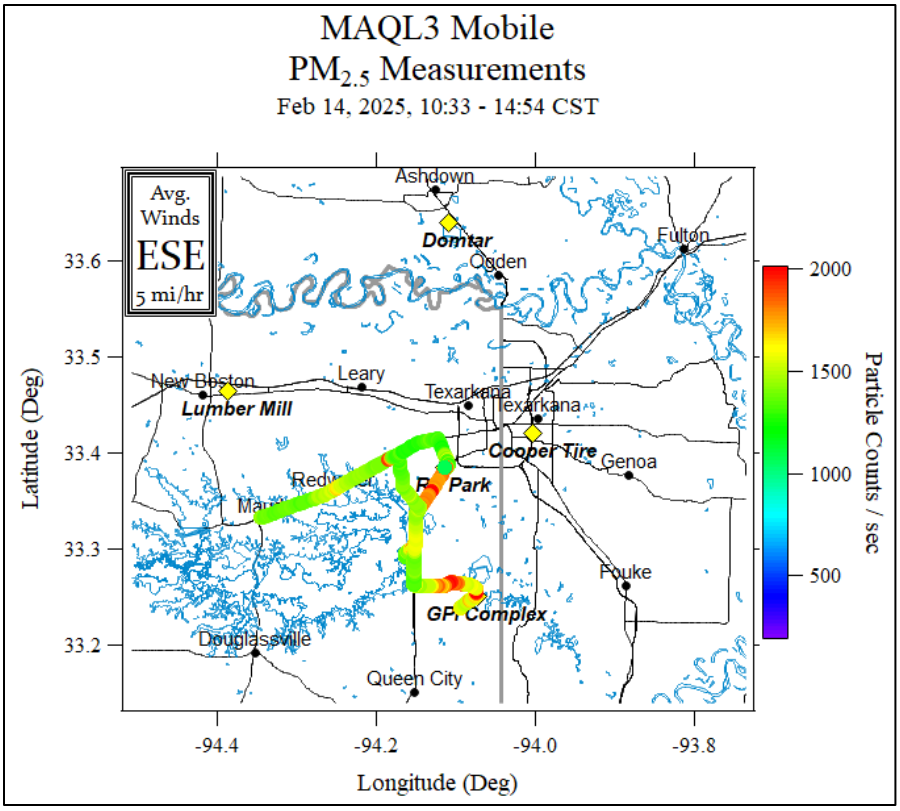

Figure 49. *The UH mobile lab sampling route for February 14, 2025, colored by $PM_{2.5}$ particle count per second measured by the MAQL3 POPS instrument. Average wind conditions (upper left), as reported by CAMS 1031, were calculated for the mobile sampling period (top of graph). The most recent tracks overlay older ones.*

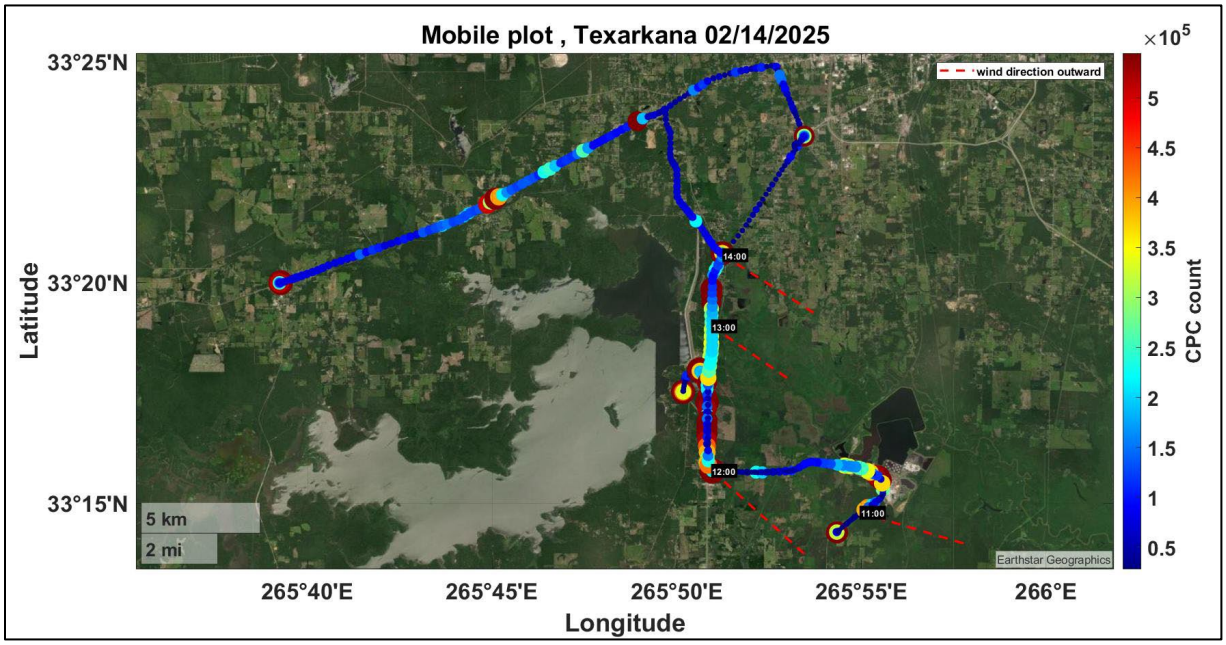

Figure 50. *The MAQL3 sampling route for February 14, 2025, colored by CPC particle count. Average hourly wind direction indicated by dash red lines, as reported by CAMS 1031, were calculated for the mobile sampling period. The most recent tracks overlay older ones.*

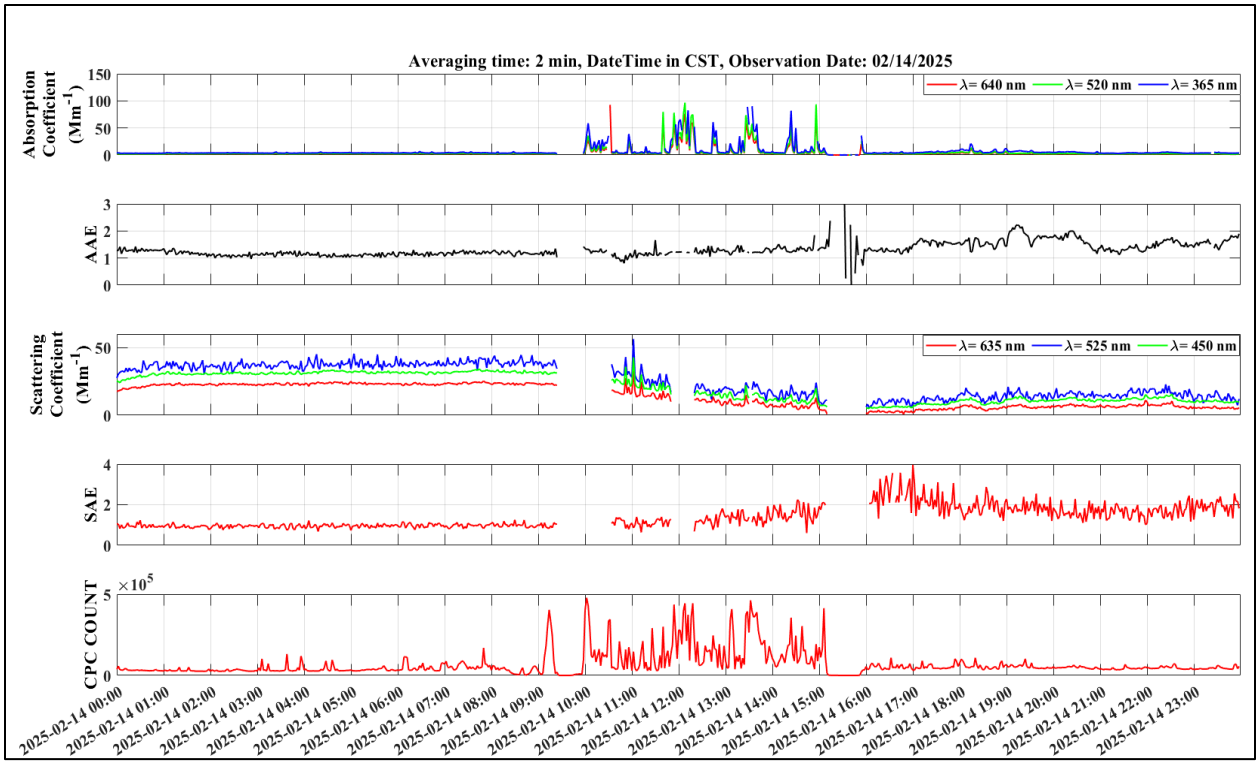

Figure 51. *Time-series data of select MAQL3 aerosol measurements made during the Texarkana campaign for February 14, 2025. Absorption and scattering coefficients, AAE and SAE (calculated values) and particle counts averaged over 120 seconds.*

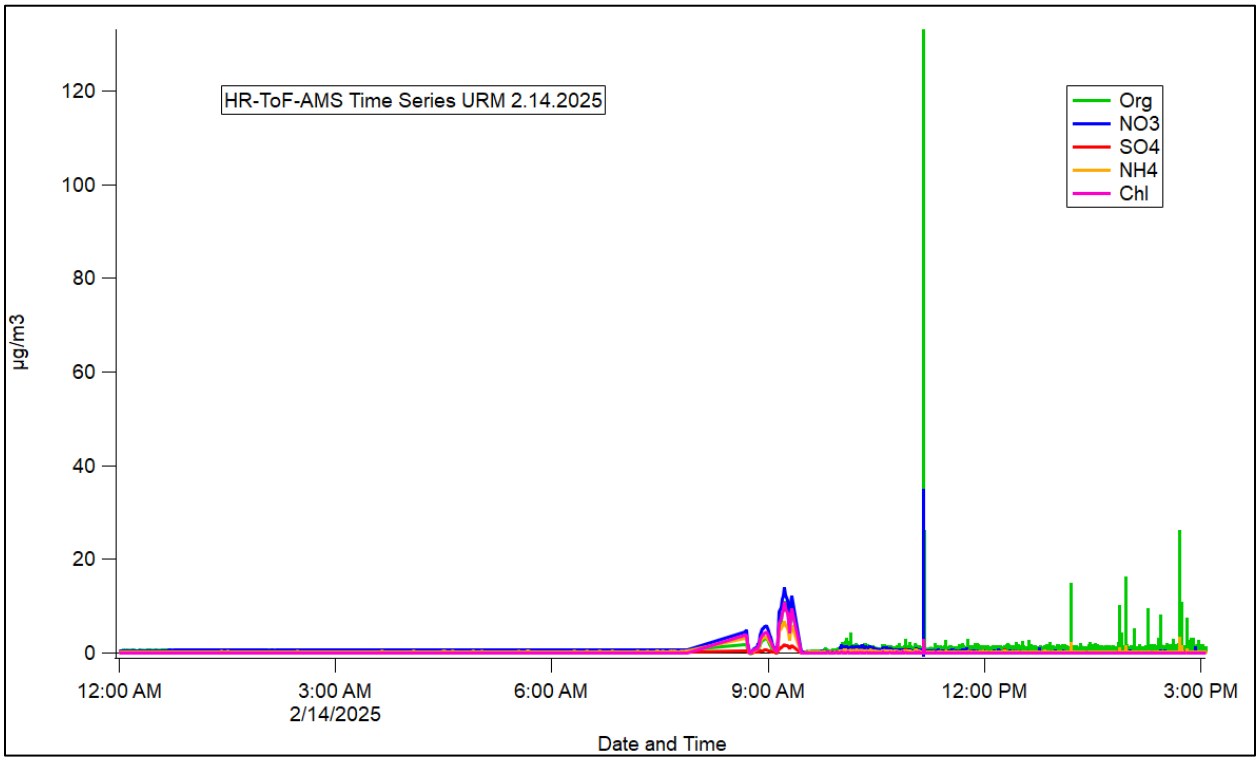

Figure 52. *Time-series data of select HR-ToF-AMS species (Organics, Nitrate, Sulfate, Ammonium, Chloride) made during the Texarkana campaign for February 14, 2025.*

February 15, 2025

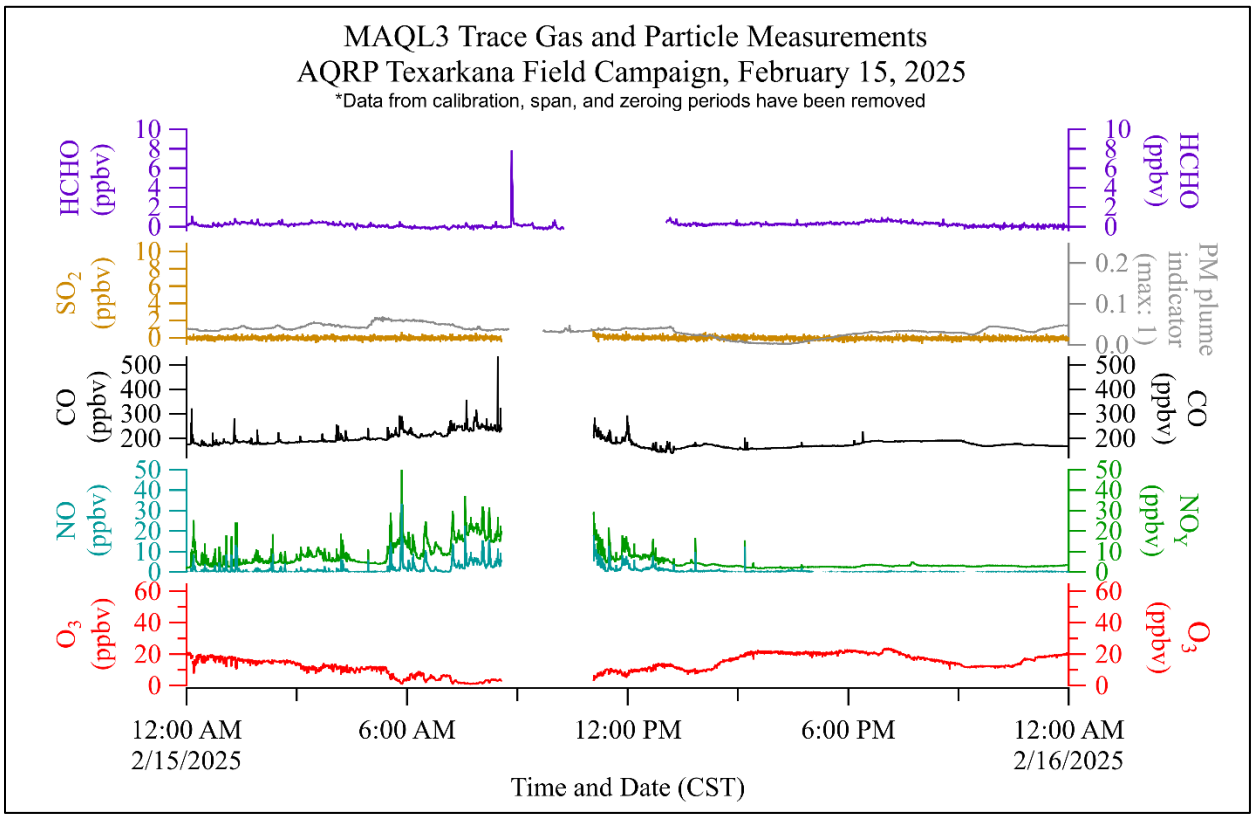

Figure 53. *Data summary of several of the MAQL3 measurements made during the Texarkana campaign. O_3, NO, NO_y, SO_2, CO, HCHO, and the particulate matter (PM) relative plume strength indicator (calculated from POPS instrument measurements) are plotted against Central Standard Time. Data was averaged to 10 seconds.*

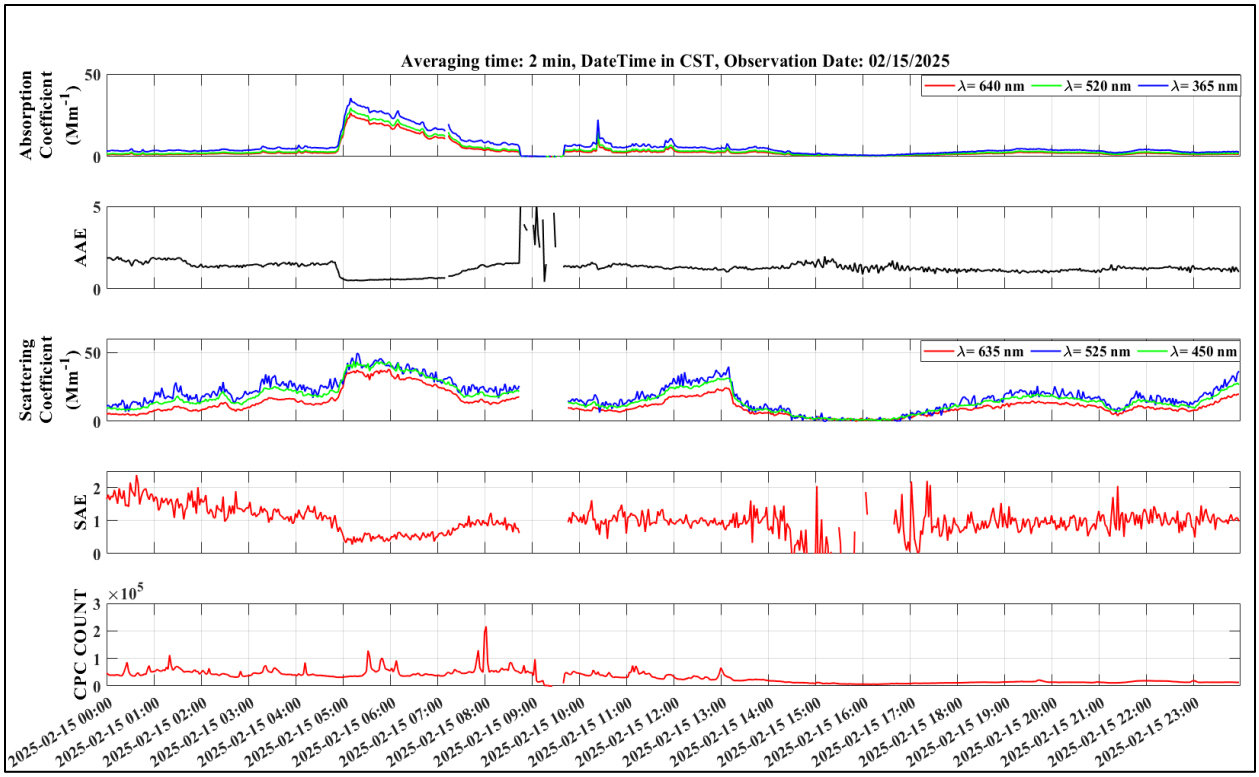

Figure 54*. Time-series data of select MAQL3 aerosol measurements made during the Texarkana campaign for February 15, 2025. Absorption and scattering coefficients, AAE and SAE (calculated values) and particle counts averaged over 120 seconds.*

February 16, 2025

MAQL3 drove to Ashdown, AR to sample the paper mill emissions. Two upwind passes were completed, followed by repeated loops south on US-59 to Hwy 108 to I-30. While MAQL3 mapped the plume extent, Aerodyne collected a GC sample in Ogden. The route continued along US-67 to I-30, then north to Ashdown via US-49. Attempts to work further south of I-30 were limited by road clearance and weight restrictions. Four passes along Hwy 82 confirmed plume presence in CPC and POPS.

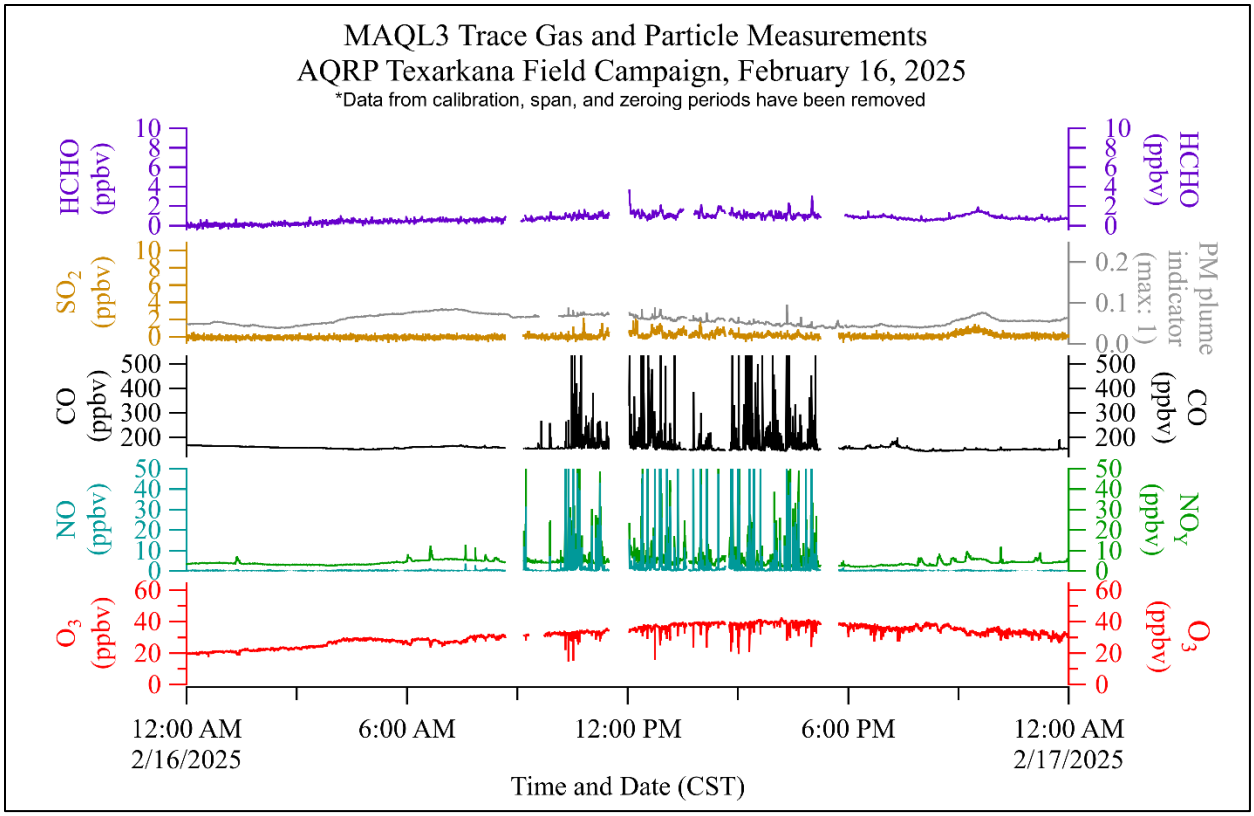

Figure 55. *Data summary of several of the MAQL3 measurements made during the Texarkana campaign. O_3, NO, NO_y, SO_2, CO, HCHO, and the particulate matter (PM) relative plume strength indicator (calculated from POPS instrument measurements) are plotted against Central Standard Time. Data was averaged to 10 seconds.*

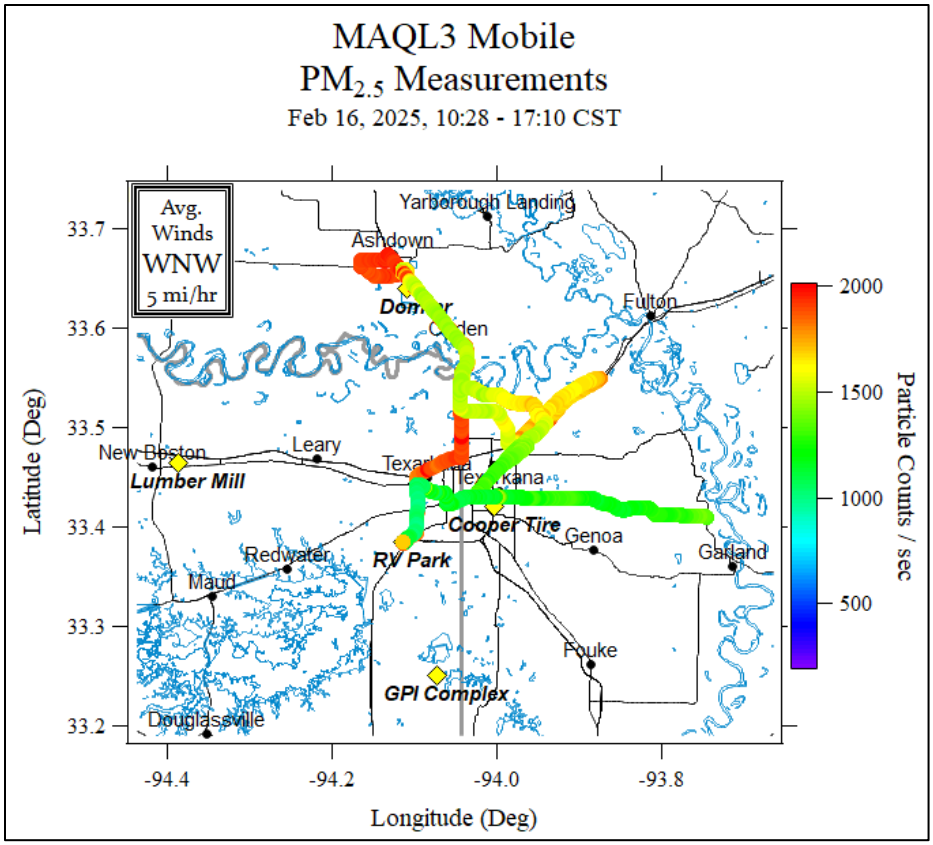

Figure 56. *The UH mobile lab sampling route for February 16, 2025, colored by $PM_{2.5}$ particle count per second measured by the MAQL3 POPS instrument. Average wind conditions (upper left), as reported by CAMS 1031, were calculated for the mobile sampling period (top of graph). The most recent tracks overlay older ones.*

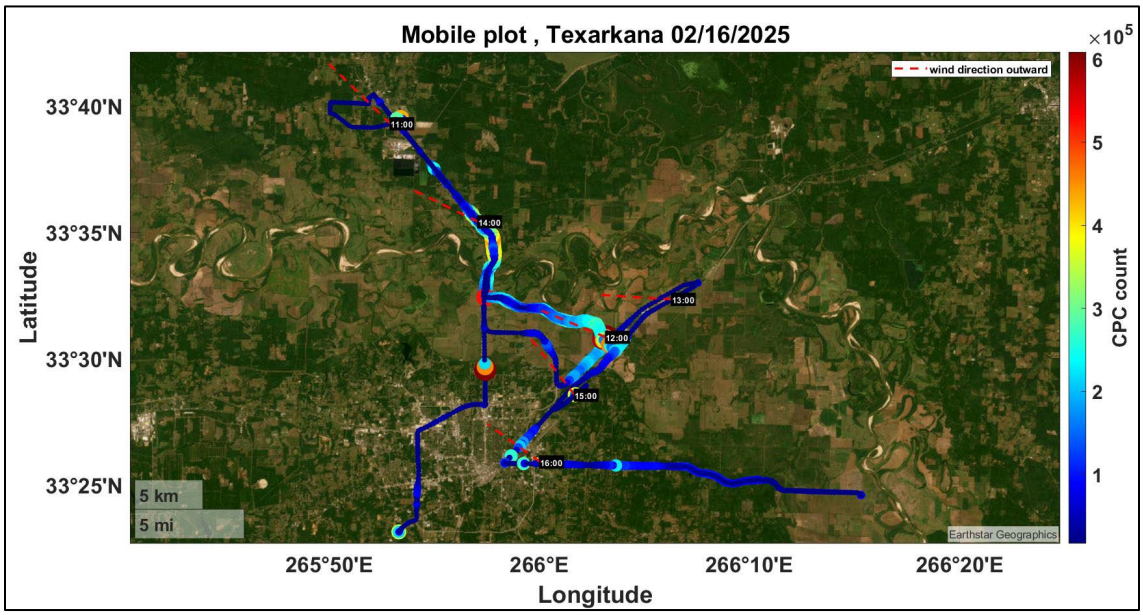

Figure 57*. The MAQL3 sampling route for February 16, 2025, colored by CPC particle count. Average hourly wind direction indicated by dash red lines, as reported by CAMS 1031, were calculated for the mobile sampling period. The most recent tracks overlay older ones.*

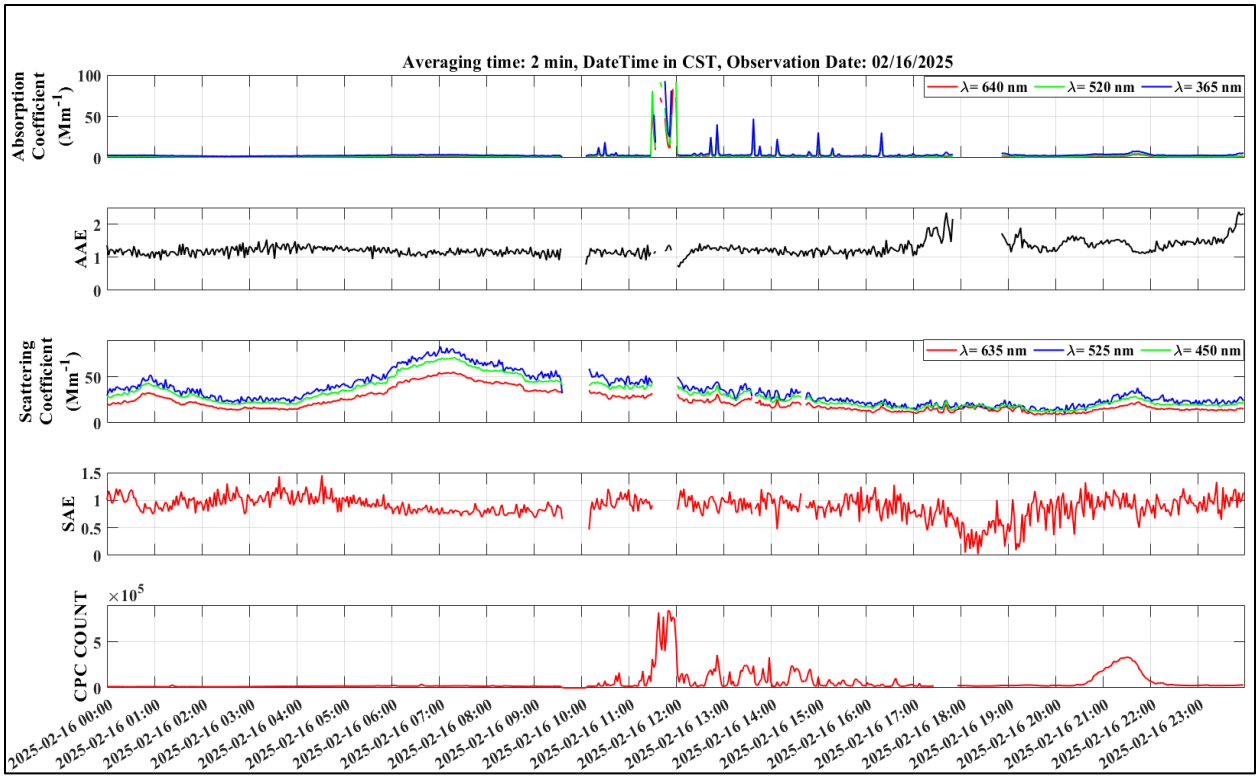

Figure 58. *Time-series data of select MAQL3 aerosol measurements made during the Texarkana campaign for February 16, 2025. Absorption and scattering coefficients, AAE and SAE (calculated values) and particle counts averaged over 120 seconds.*

February 17, 2025

MAQL3 traveled east to the Cooper Tire facility; no detectable plumes observed. Continued to the GPI and tracked the plume past Maud toward Corley and the New Boston area. No significant emissions were observed from the New Boston Lumber Mill, though Aerodyne reported potential monoterpene signals in that area.

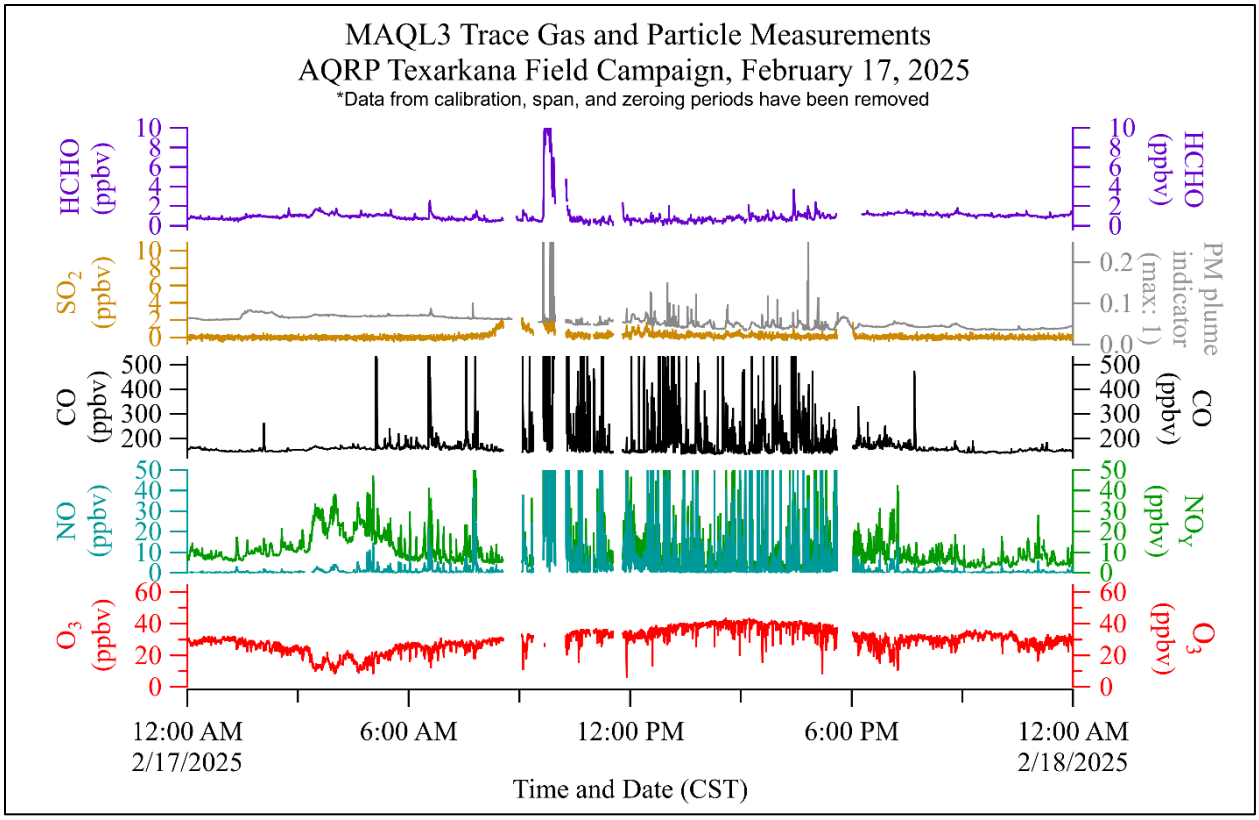

Figure 59. *Data summary of several of the MAQL3 measurements made during the Texarkana campaign. O_3, NO, NO_y, SO_2, CO, HCHO, and the PM relative plume strength indicator (calculated from POPS instrument measurements) are plotted against Central Standard Time. Data was averaged to 10 seconds.*

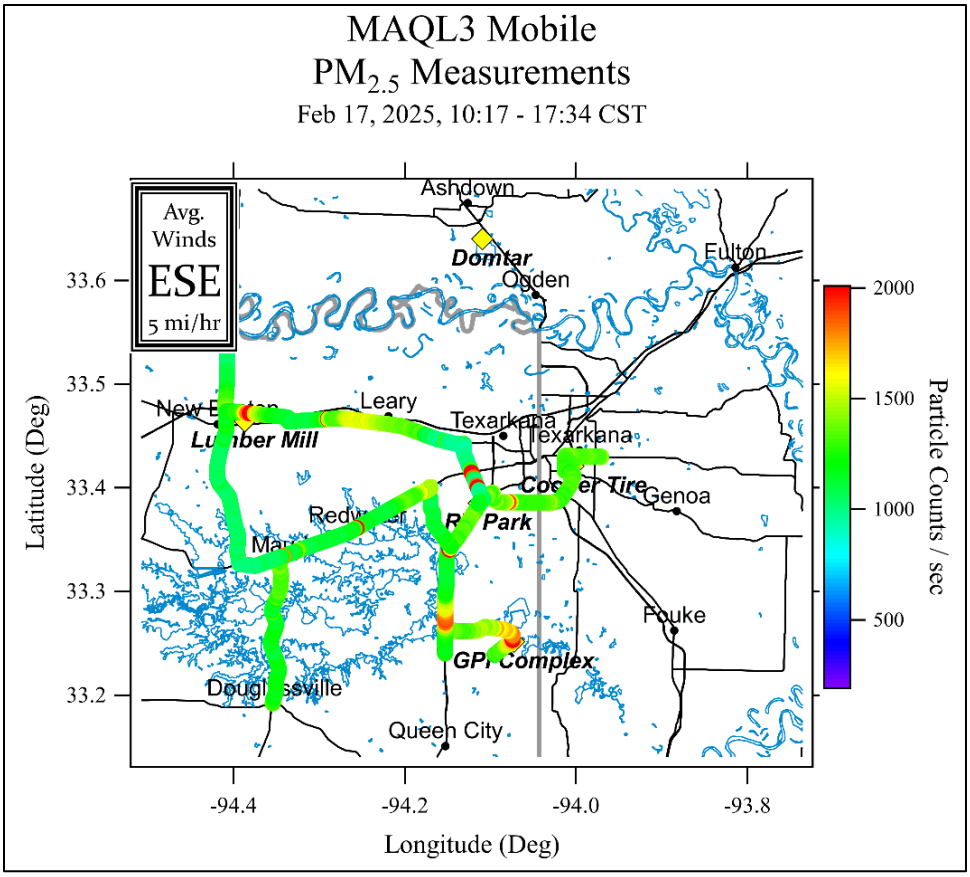

Figure 60. *The UH mobile lab sampling route for February 14, 2025, colored by $PM_{2.5}$ particle count per second measured by the MAQL3 POPS instrument. Average wind conditions (upper left), as reported by CAMS 1031, were calculated for the mobile sampling period (top of graph). The most recent tracks overlay older ones.*

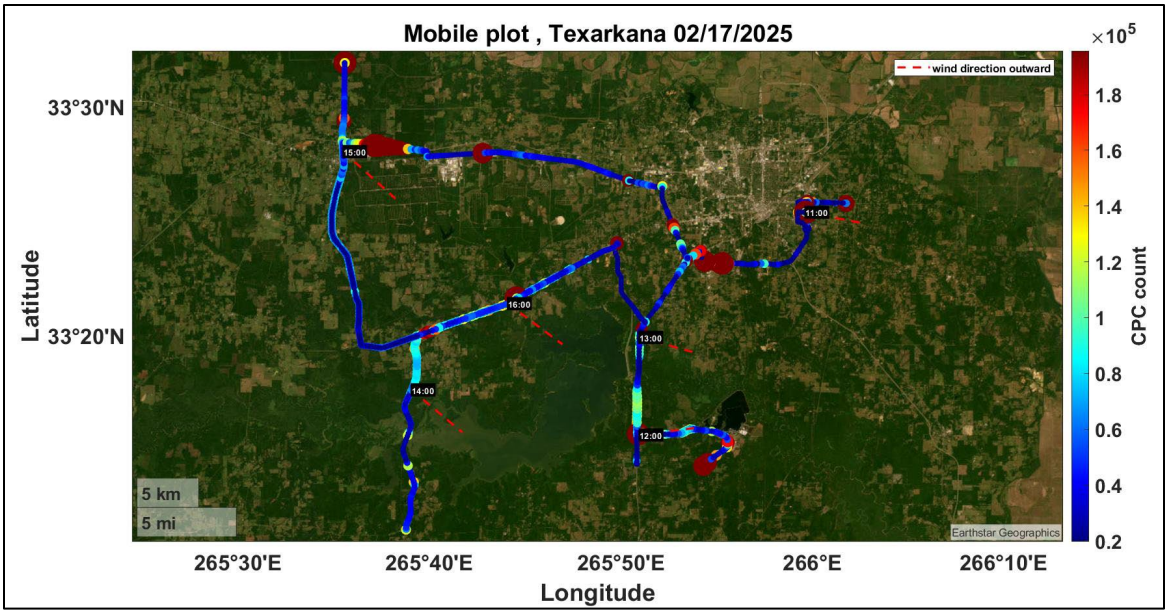

Figure 61. *The MAQL3 sampling route for February 17, 2025, colored by CPC particle count. Average hourly wind direction indicated by dash red lines, as reported by CAMS 1031, were calculated for the mobile sampling period. The most recent tracks overlay older ones.*

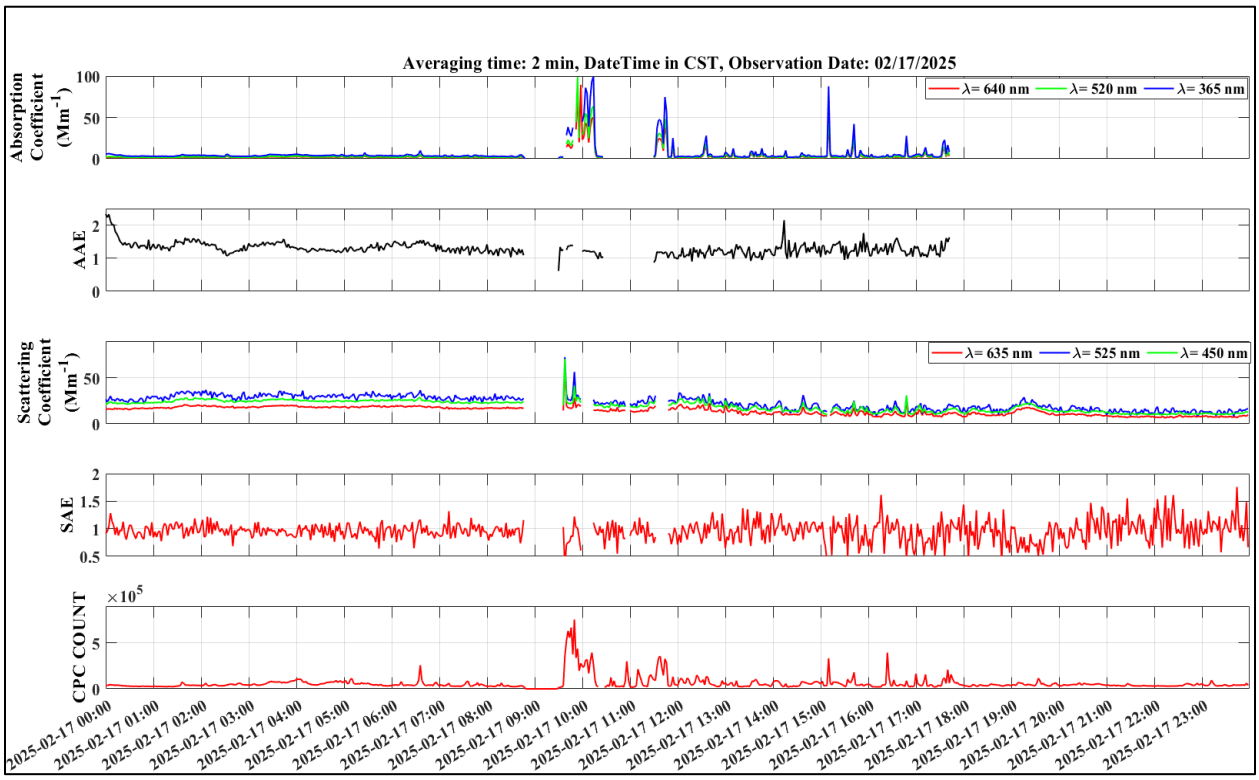

Figure 62. *Time-series data of select MAQL3 aerosol measurements made during the Texarkana campaign for February 17, 2025. Absorption and scattering coefficients, AAE and SAE (calculated values) and particle counts averaged over 120 seconds.*

February 18, 2025

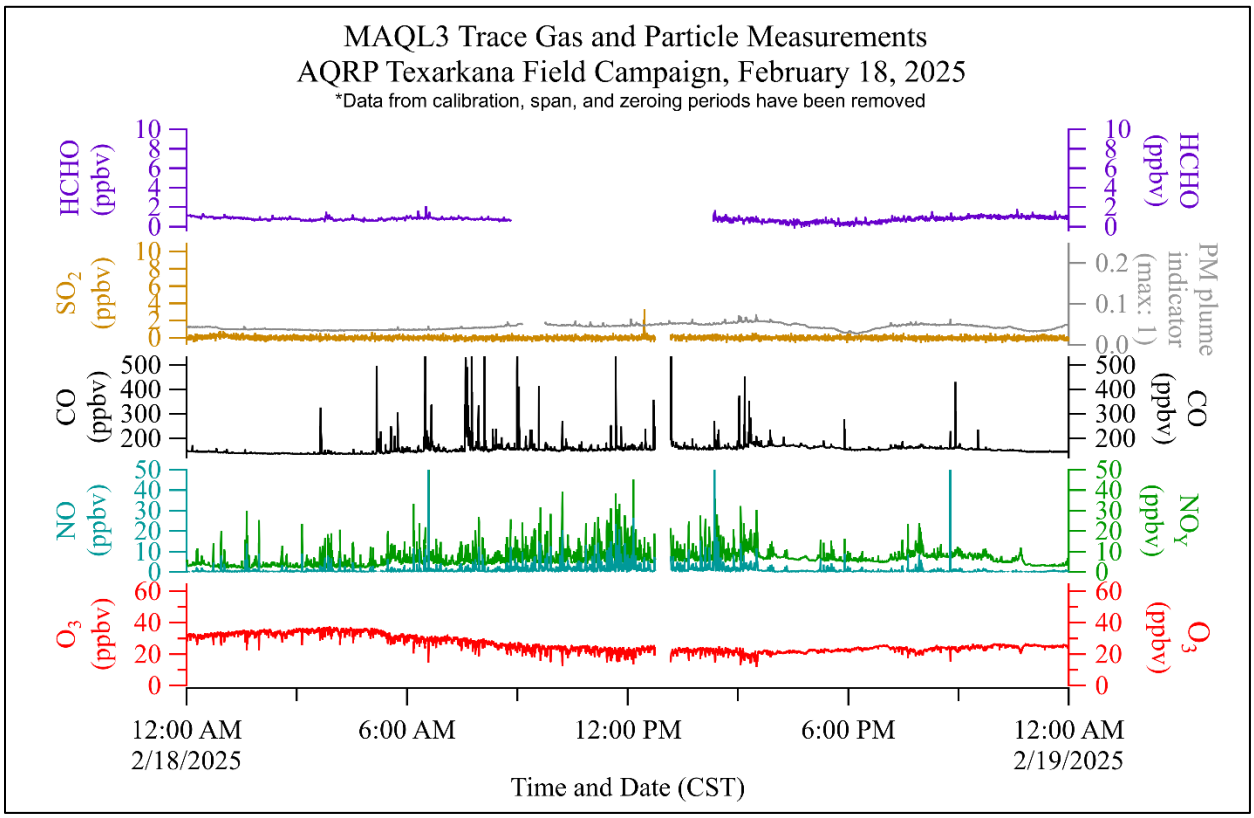

Figure 63. *Data summary of several of the MAQL3 measurements made during the Texarkana campaign. O_3, NO, NO_y, SO_2, CO, HCHO, and the particulate matter (PM) relative plume strength indicator (calculated from POPS instrument measurements) are plotted against Central Standard Time. Data was averaged to 10 seconds.*

February 19, 2025

MAQL3 drove to the Domtar plume entering the Texarkana area and tracked it multiple times upwind along Springhill Road. The plume was followed closer to Texarkana and was eventually detected at the TCEQ monitoring station, confirming its transport into the local monitoring network.

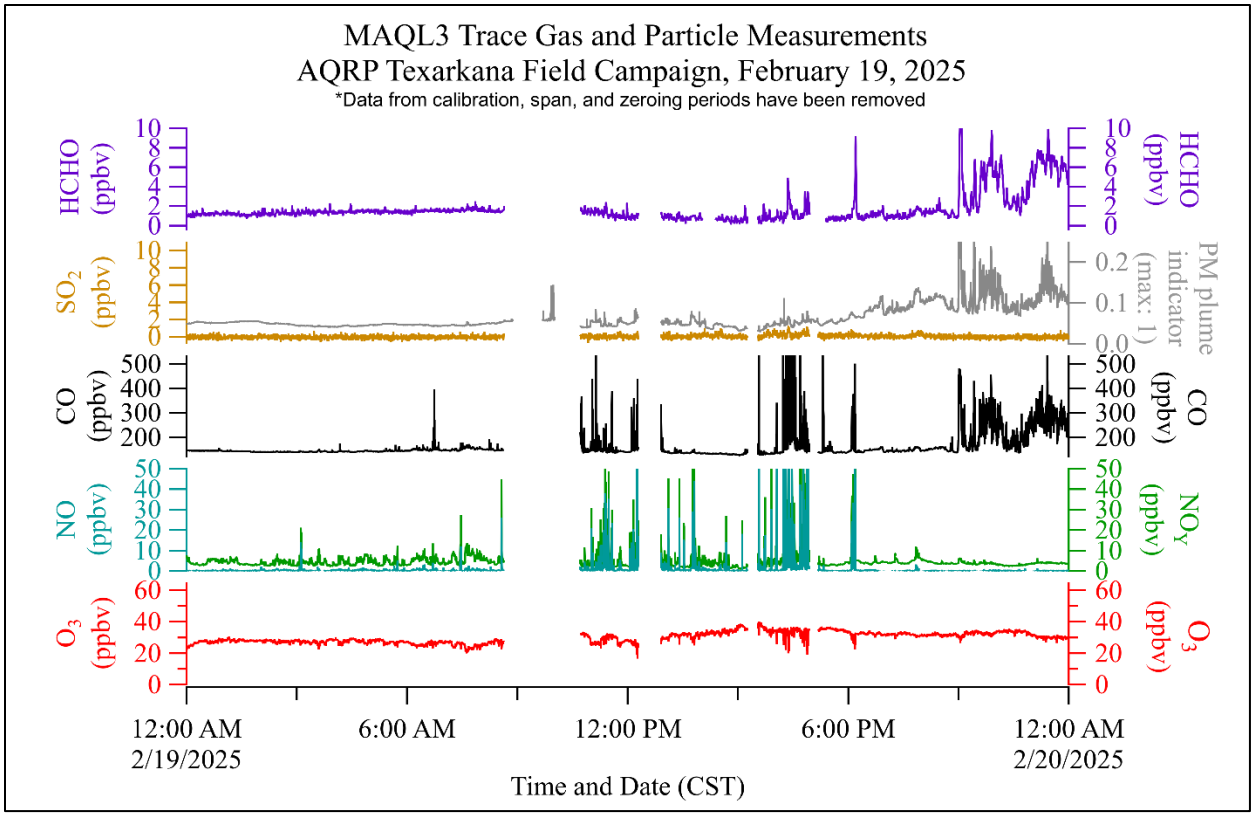

Figure 64. *Data summary of several of the MAQL3 measurements made during the Texarkana campaign. O_3, NO, NO_y, SO_2, CO, HCHO, and the PM relative plume strength indicator (calculated from POPS instrument measurements) are plotted against Central Standard Time. Data was averaged to 10 seconds.*

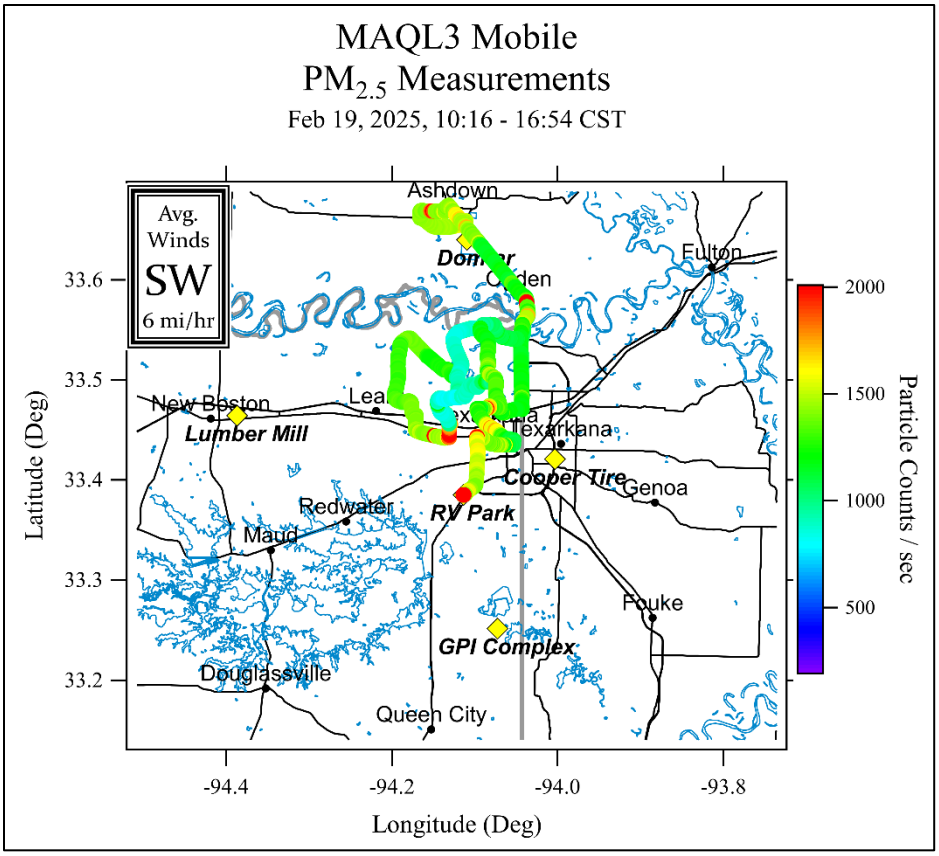

Figure 65. *The UH mobile lab sampling route for February 19, 2025, colored by $PM_{2.5}$ particle count per second measured by the MAQL3 POPS instrument. Average wind conditions (upper left), as reported by CAMS 1031, were calculated for the mobile sampling period (top of graph). The most recent tracks overlay older ones.*

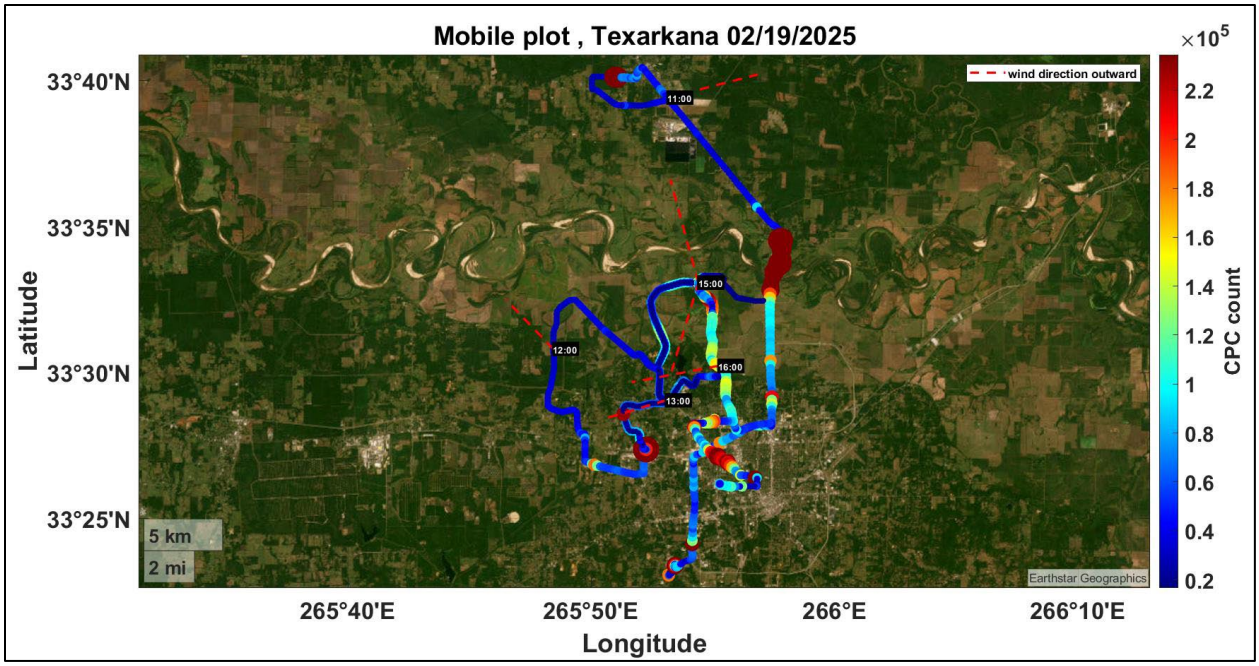

Figure 66. *The MAQL3 sampling route for February 19, 2025, colored by CPC particle count. Average hourly wind direction indicated by dashed red lines, as reported by CAMS 1031, was calculated for the mobile sampling period. The most recent tracks overlay older ones.*

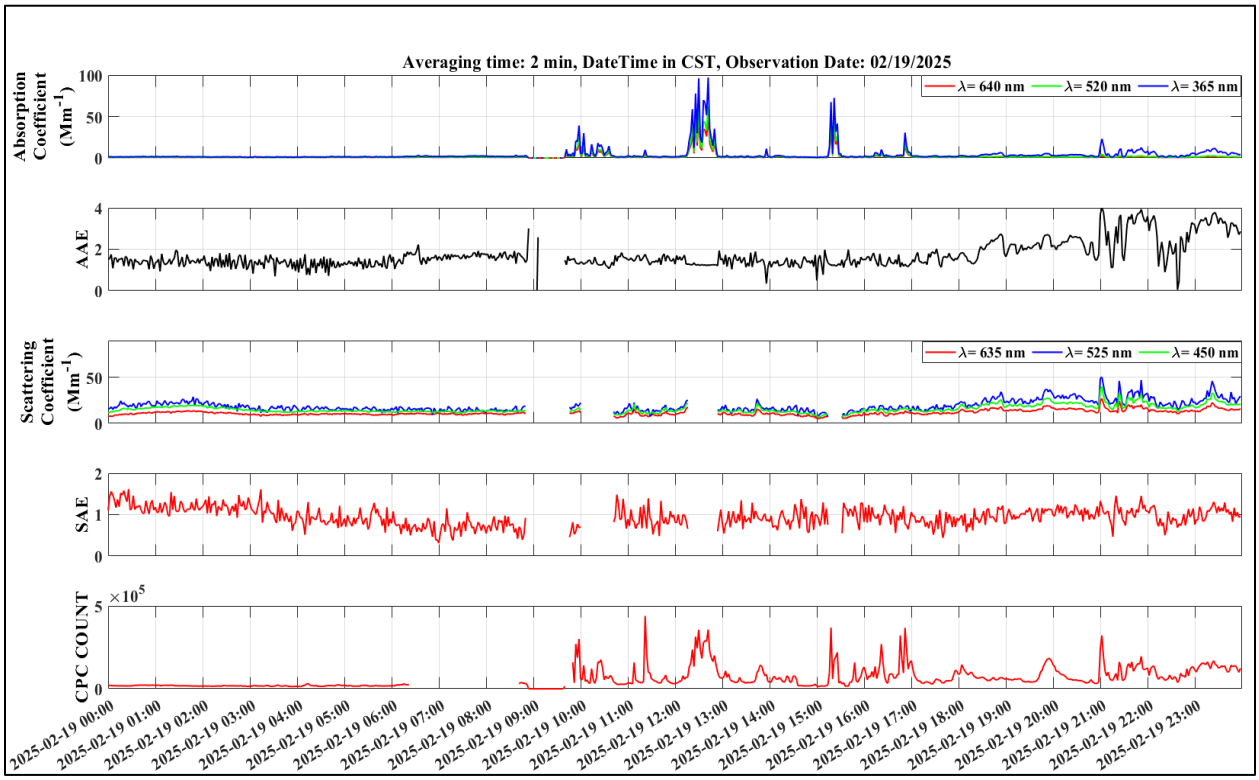

Figure 67. *Time-series data of select MAQL3 aerosol measurements made during the Texarkana campaign for February 19, 2025. Absorption and scattering coefficients, AAE and SAE (calculated values), and particle counts averaged over 120 seconds.*

February 20, 2025

Two passes were made on Highway 108 upwind of Texarkana, followed by travel along the I-49 loop east around the city to Highway 93 and then east to Ann Street. To record plume impacts, three hours of sampling were done at a fixed position downwind of Texarkana.

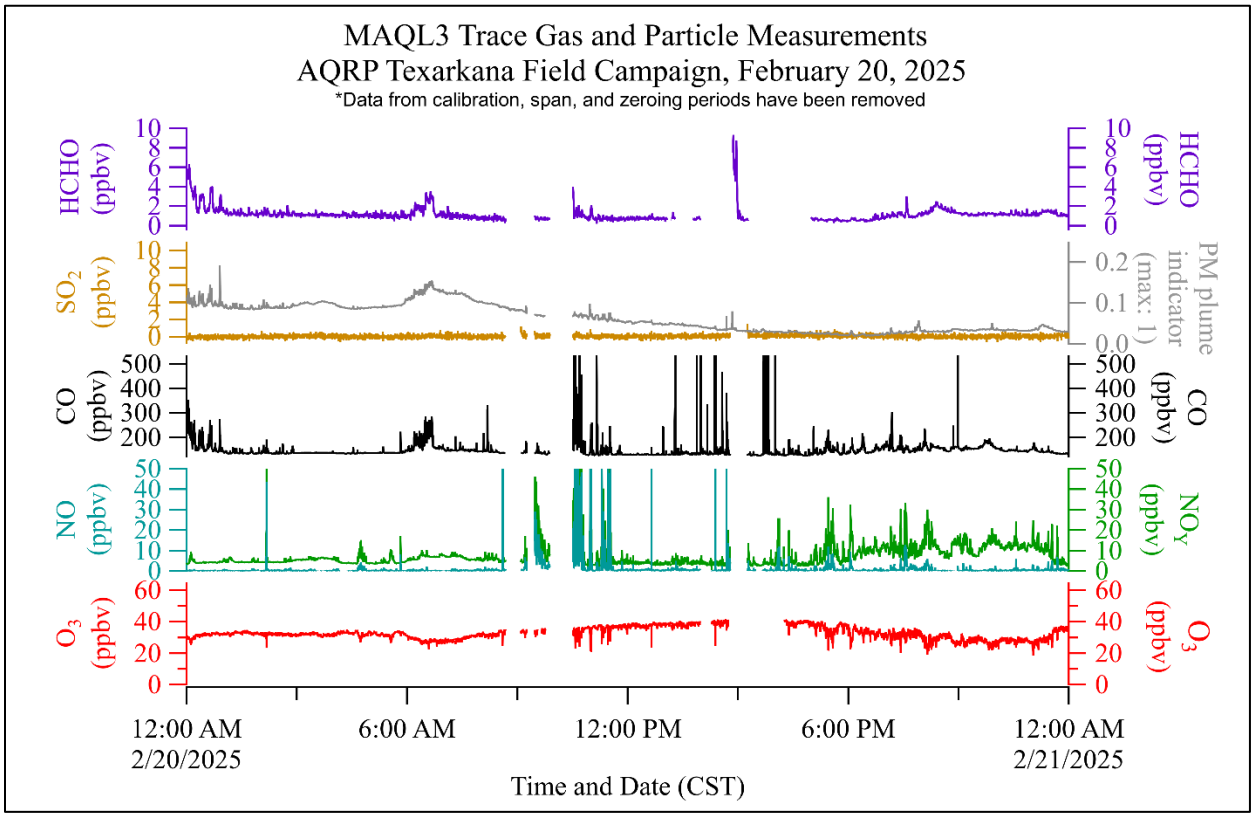

Figure 68. *Data summary of several of the MAQL3 measurements made during the Texarkana campaign. O_3, NO, NO_y, SO_2, CO, HCHO, and the PM relative plume strength indicator (calculated from POPS instrument measurements) are plotted against Central Standard Time. Data was averaged to 10 seconds.*

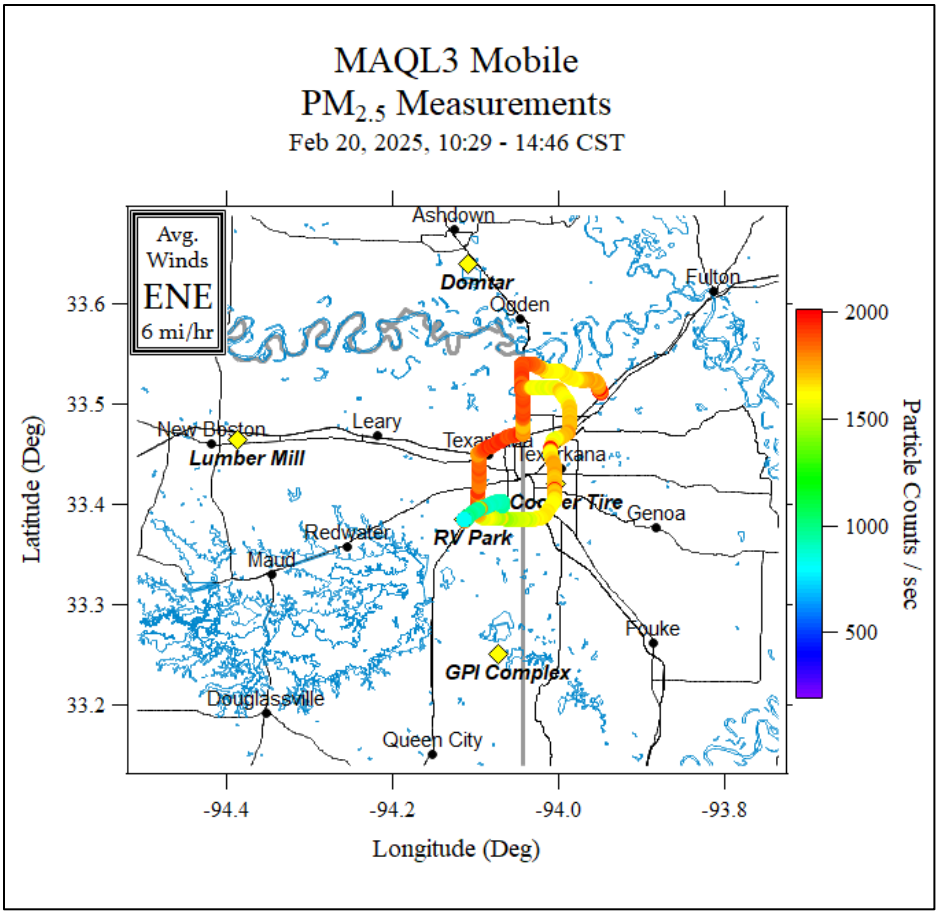

Figure 69. *The UH mobile lab sampling route for February 20, 2025, colored by $PM_{2.5}$ particle count per second measured by the MAQL3 POPS instrument. Average wind conditions (upper left), as reported by CAMS 1031, were calculated for the mobile sampling period (top of graph). The most recent tracks overlay older ones.*

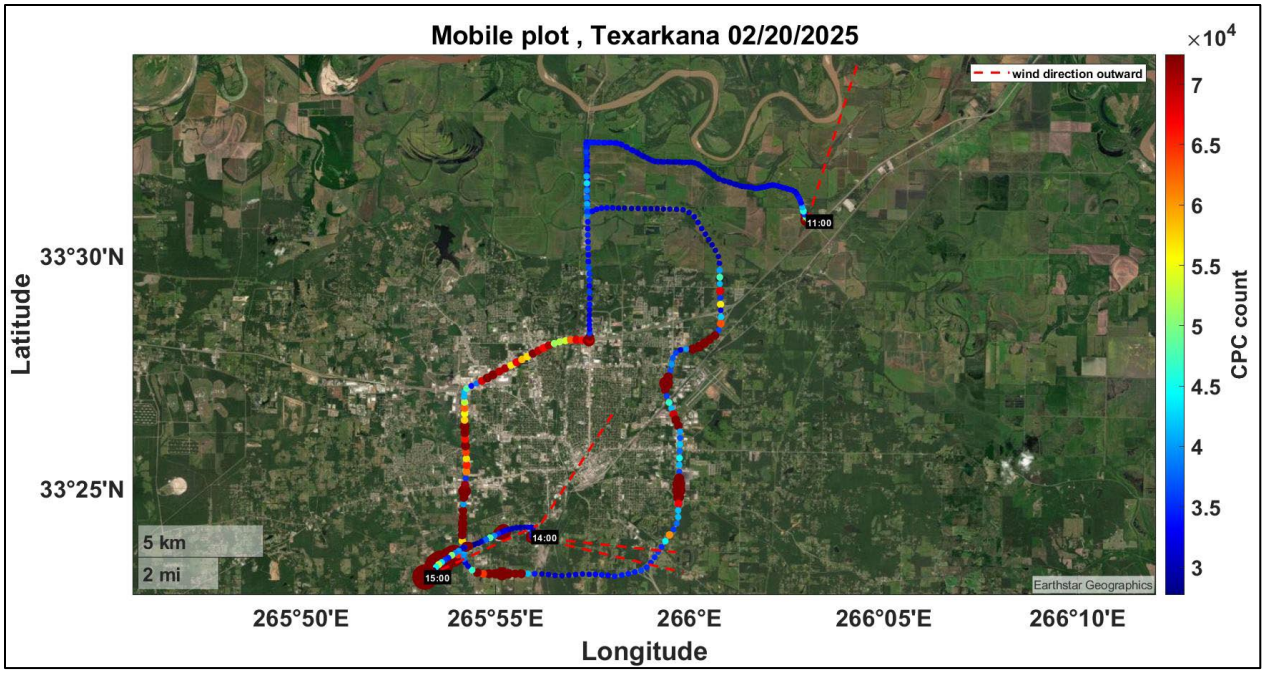

Figure 70. *The MAQL3 sampling route for February 20, 2025, colored by CPC particle count. Average hourly wind direction indicated by dashed red lines, as reported by CAMS 1031, was calculated for the mobile sampling period. The most recent tracks overlay older ones.*

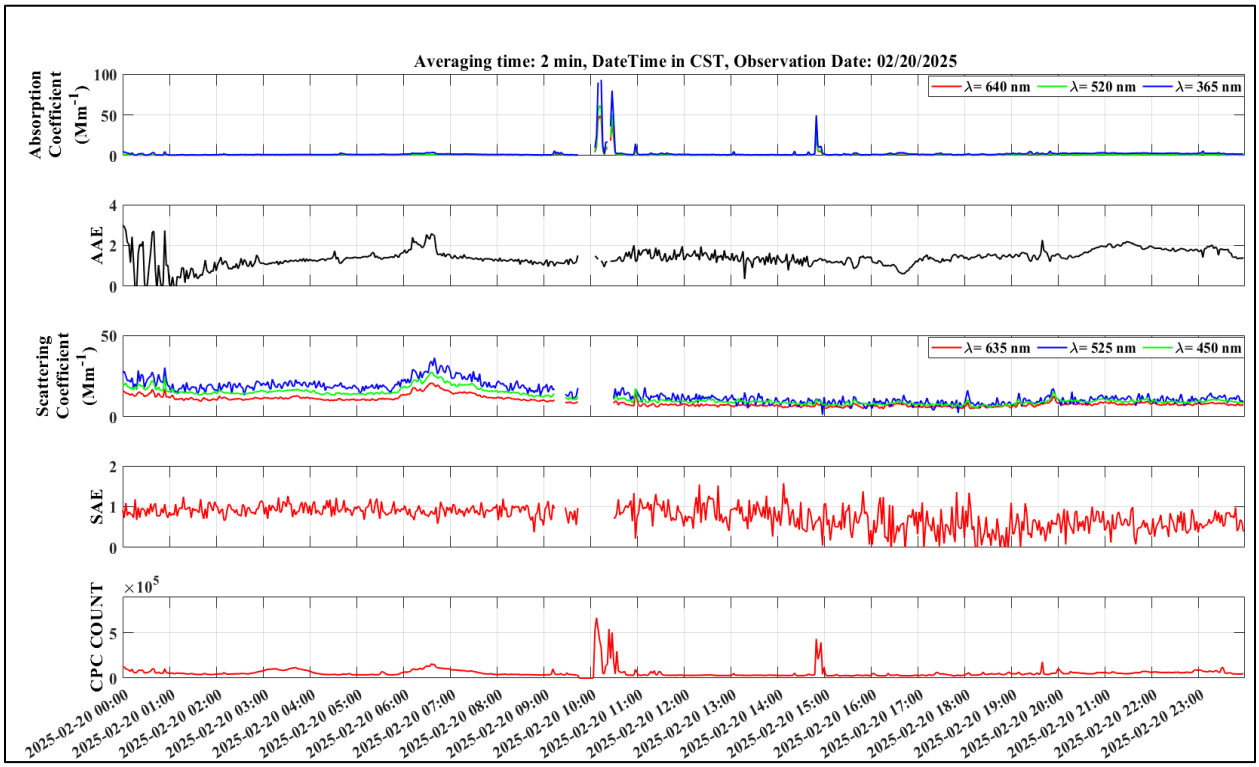

Figure 71. *Time-series data of select MAQL3 aerosol measurements made during the Texarkana campaign for February 20, 2025. Absorption and scattering coefficients, AAE and SAE (calculated values), and particle counts averaged over 120 seconds.*

February 21, 2025

Both MAQL3 and minAML conducted mobile sampling around the coal power plant in Fulton, however, winds were not strong enough to blow the plume down far enough to reach the MAQL3 or minAML sampling height. Since no notable emissions were sampled, the mobile labs drove south to sample near Cooper Tire and then over to the TCEQ monitoring site. However, the winds were too calm and variable for meaningful data collection near the monitor, so the team returned to the RV park for stationary sampling on shore power.

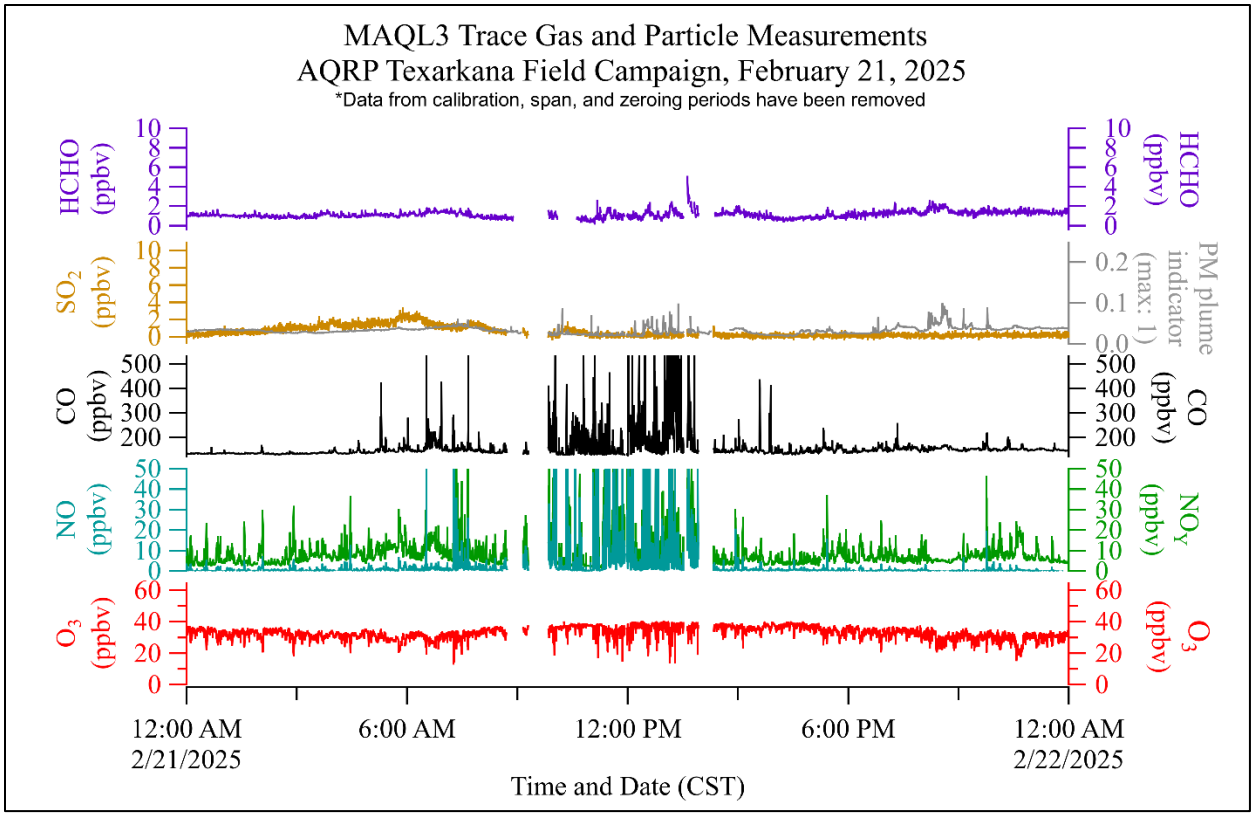

Figure 72. *Data summary of several of the MAQL3 measurements made during the Texarkana campaign. O_3, NO, NO_y, SO_2, CO, HCHO, and the PM relative plume strength indicator (calculated from POPS instrument measurements) are plotted against Central Standard Time. Data was averaged to 10 seconds.*

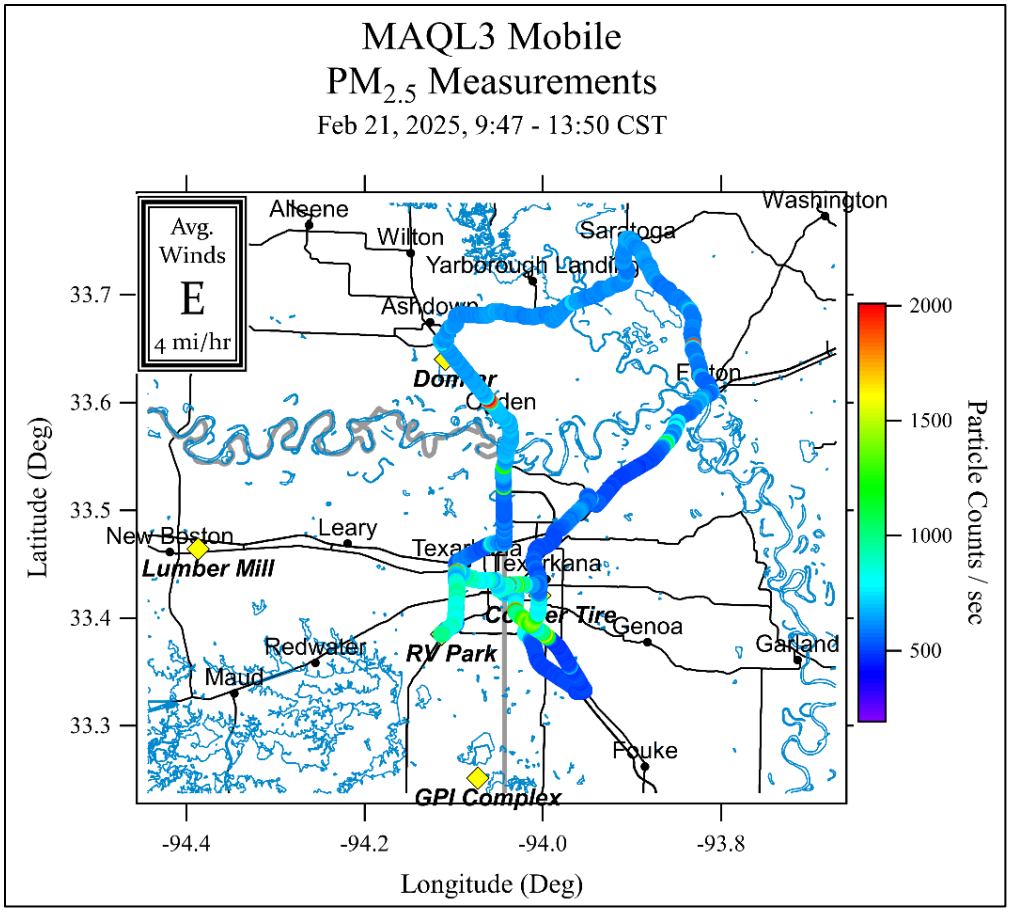

Figure 73. *The UH mobile lab sampling route for February 21, 2025, colored by $PM_{2.5}$ particle count per second measured by the MAQL3 POPS instrument. Average wind conditions (upper left), as reported by CAMS 1031, were calculated for the mobile sampling period (top of graph). The most recent tracks overlay older ones.*

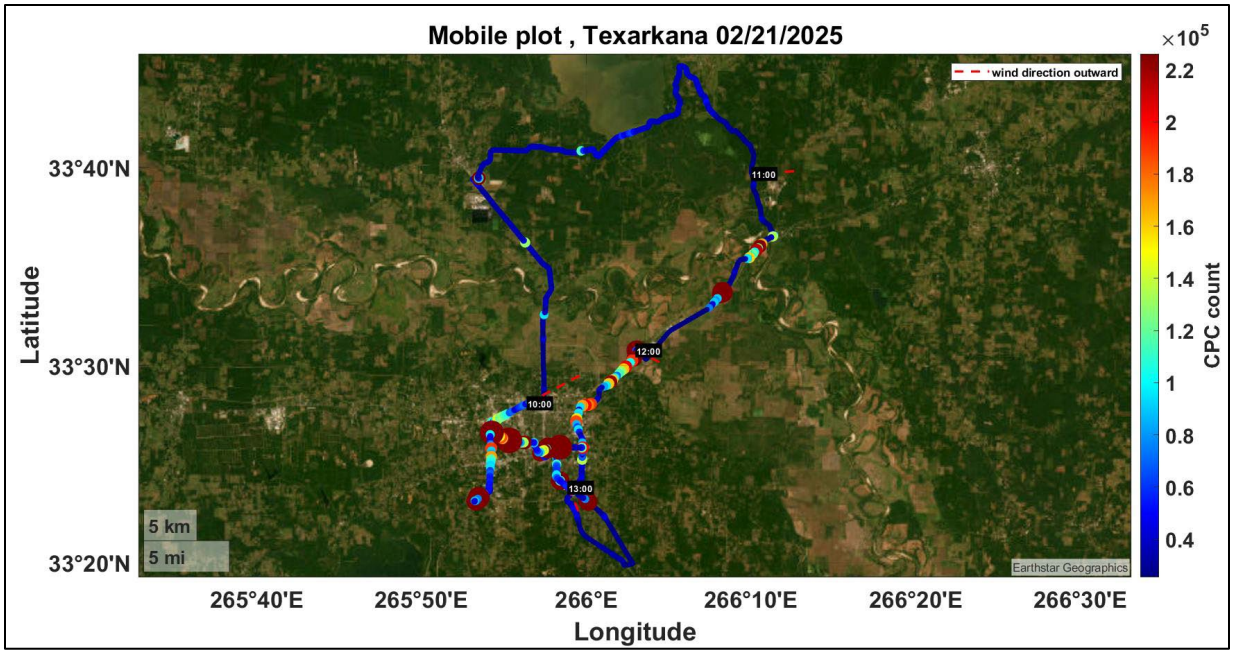

Figure 74. *The MAQL3 sampling route for February 21, 2025, colored by CPC particle count. Average hourly wind direction indicated by dashed red lines, as reported by CAMS 1031, was calculated for the mobile sampling period. The most recent tracks overlay older ones.*

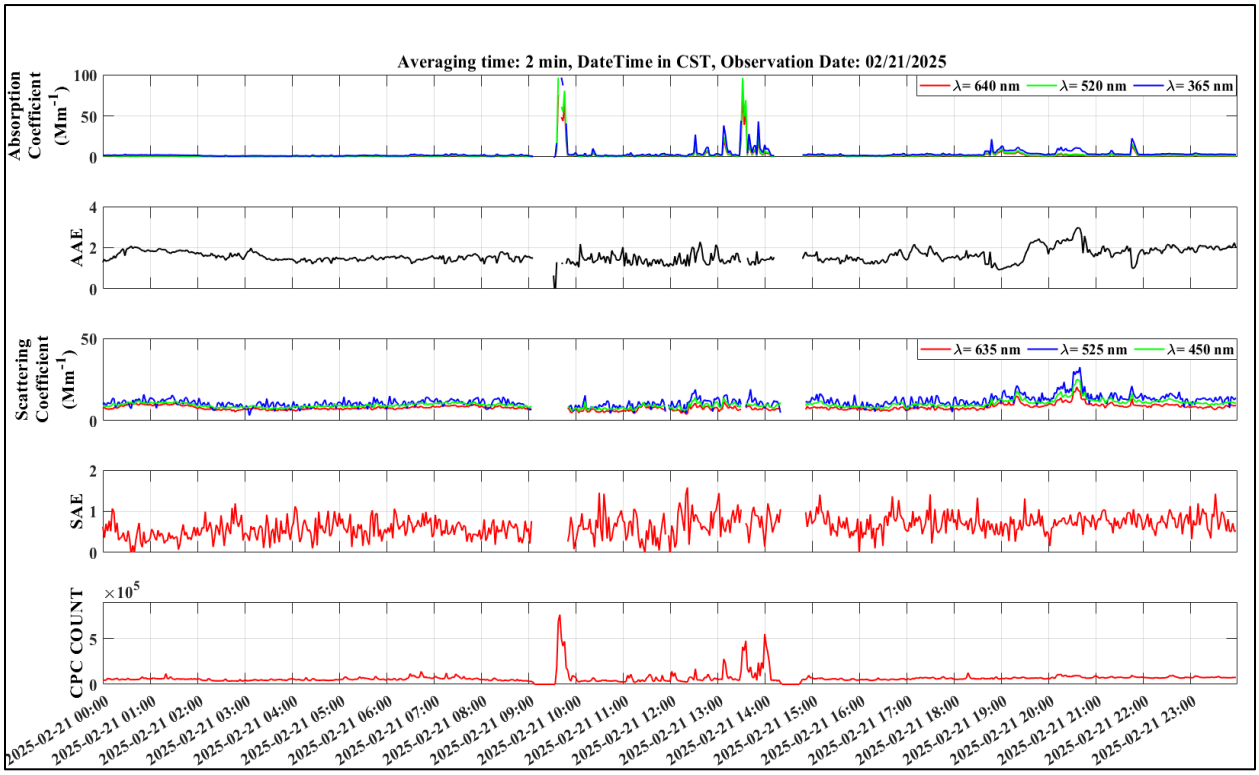

Figure 75. *Time-series data of select MAQL3 aerosol measurements made during the Texarkana campaign for February 21, 2025. Absorption and scattering coefficients, AAE and SAE (calculated values), and particle counts averaged over 120 seconds.*

February 22, 2025

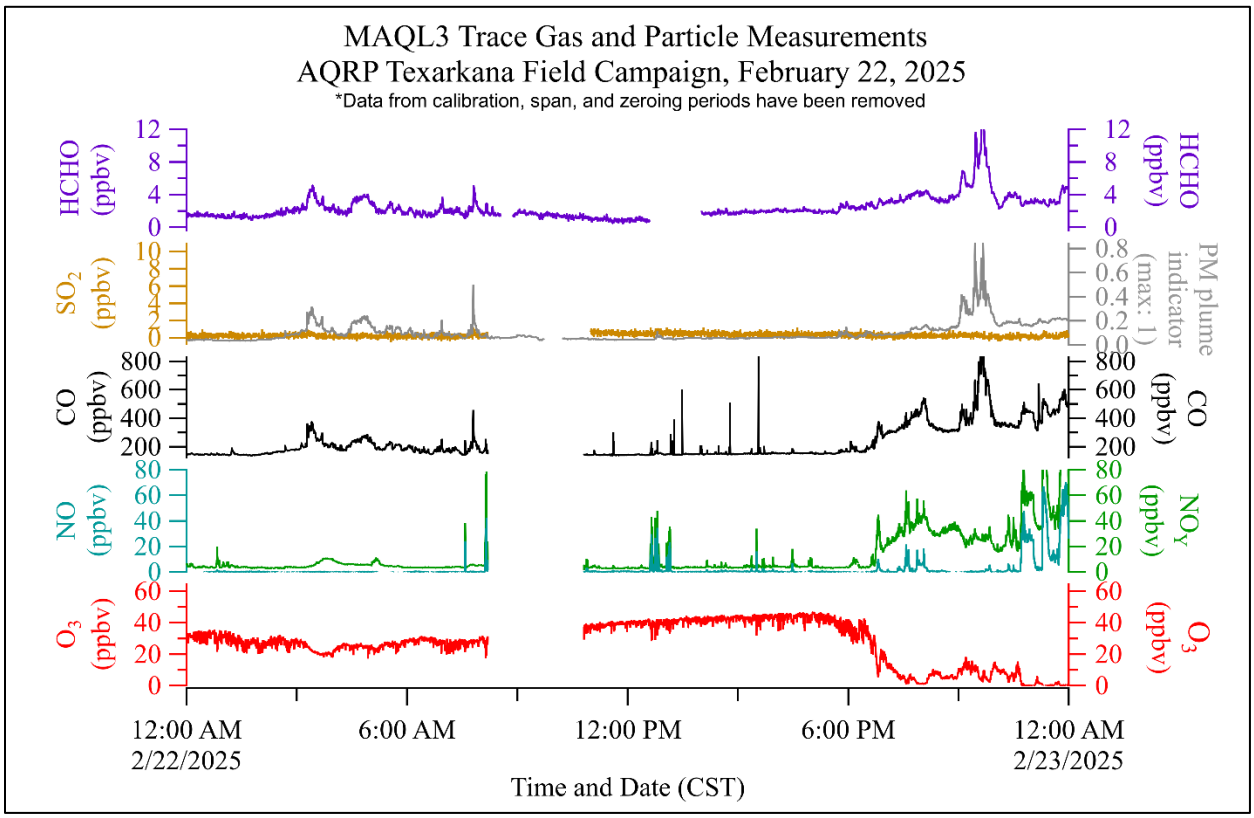

Figure 76. *Data summary of several of the MAQL3 measurements made during the Texarkana campaign. O_3, NO, NO_y, SO_2, CO, HCHO, and the PM relative plume strength indicator (calculated from POPS instrument measurements) are plotted against Central Standard Time. Data was averaged to 10 seconds.*

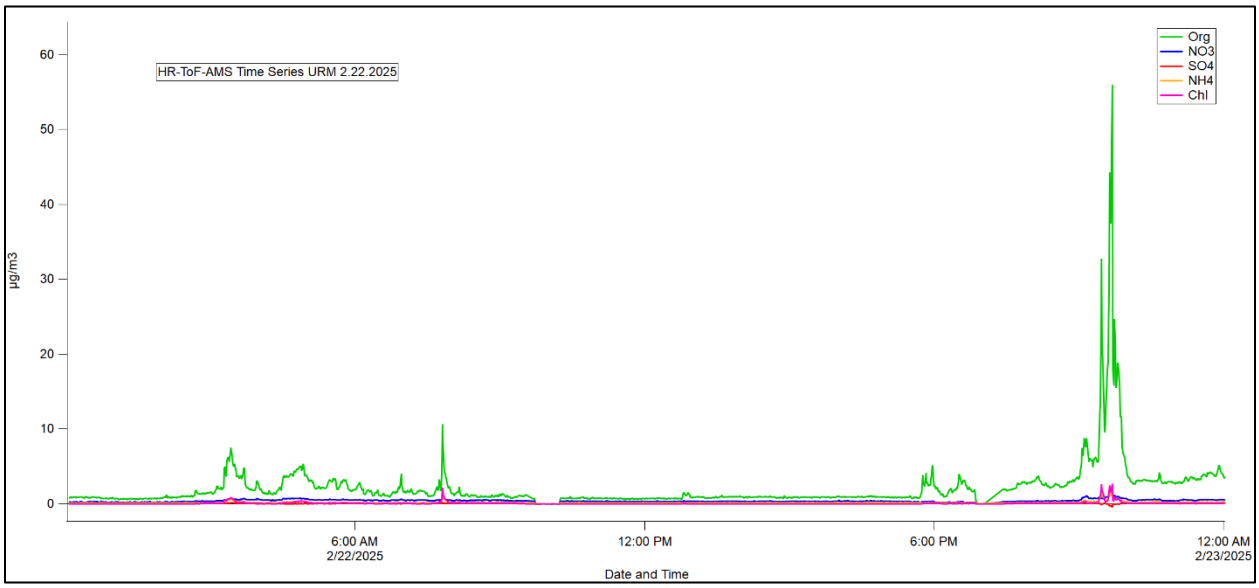

Figure 77. *Time-series data of select HR-ToF-AMS species (Organics, Nitrate, Sulfate, Ammonium, Chloride) made during the Texarkana campaign for February 22, 2025.*

February 23, 2025

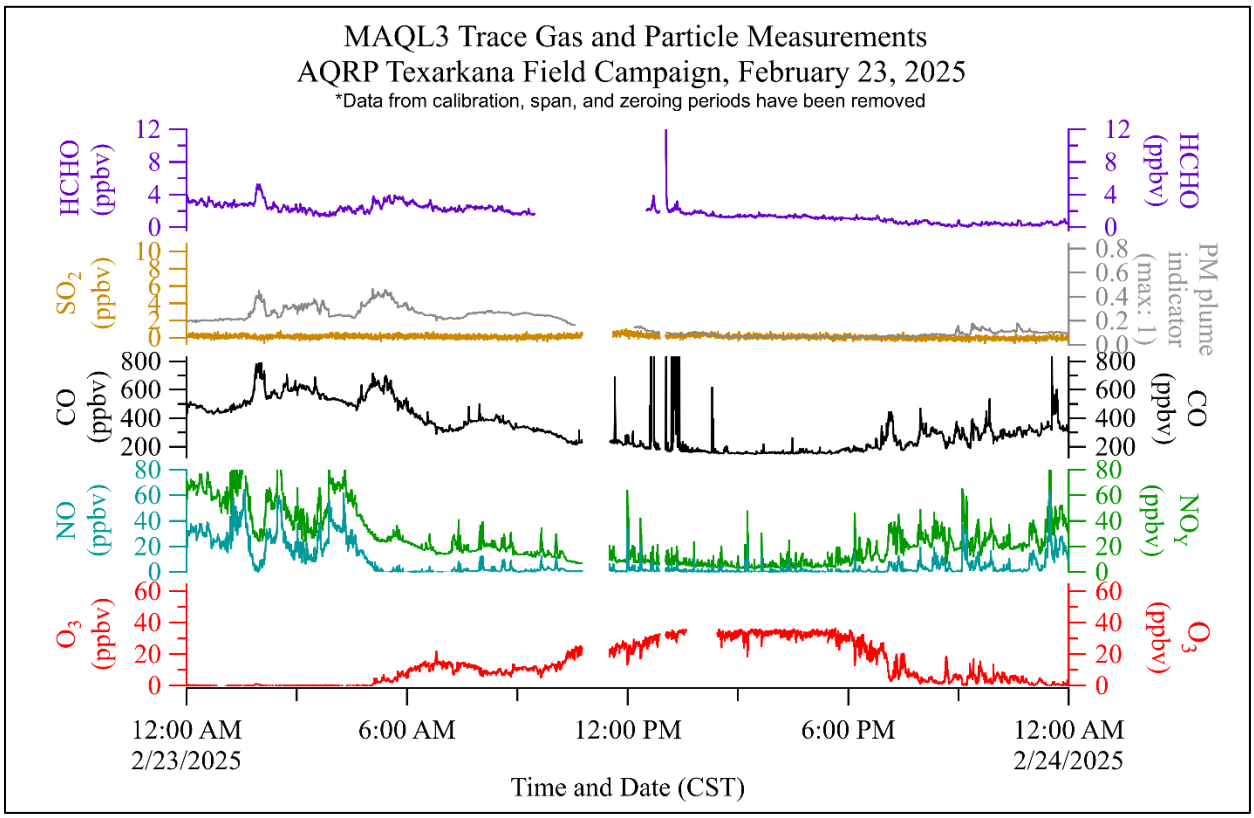

Figure 78. *Data summary of several of the MAQL3 measurements made during the Texarkana campaign. O_3, NO, NO_y, SO_2, CO, HCHO, and the PM relative plume strength indicator (calculated from POPS instrument measurements) are plotted against Central Standard Time. Data was averaged to 10 seconds.*

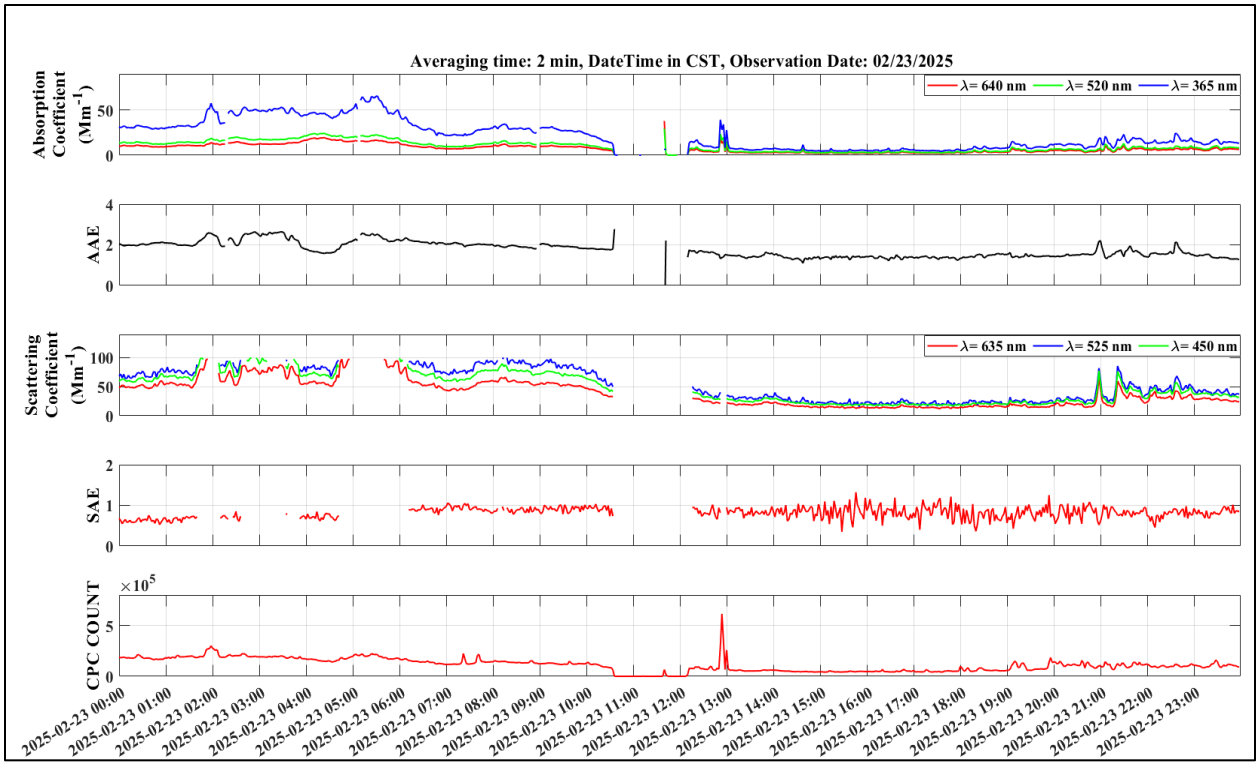

Figure 79. *Time-series data of select MAQL3 aerosol measurements made during the Texarkana campaign for February 23, 2025. Absorption and scattering coefficients, AAE and SAE (calculated values), and particle counts averaged over 120 seconds.*

February 24, 2025

Light southwest winds were pushing the morning Graphic Packaging emission blob around. Three passes were made in front of GPI, where significant emission impacts were observed. Additionally, three passes were completed along AR-237. The first two passes on 237 encountered a large, wide plume (approximately 3–4 minutes in duration), while the third pass revealed a much narrower plume, likely representing more typical emissions after the initial blob moved out of the area. The route continued via Stateline Road and Buchanan Loop to Highway 989, with no significant plume detections. MAQL3 returned to the RV and was on ground power when Aerodyne stopped at the Racetrack for fuel. After refueling, they decided to change plans and resume mobile sampling instead of returning to the RV park.

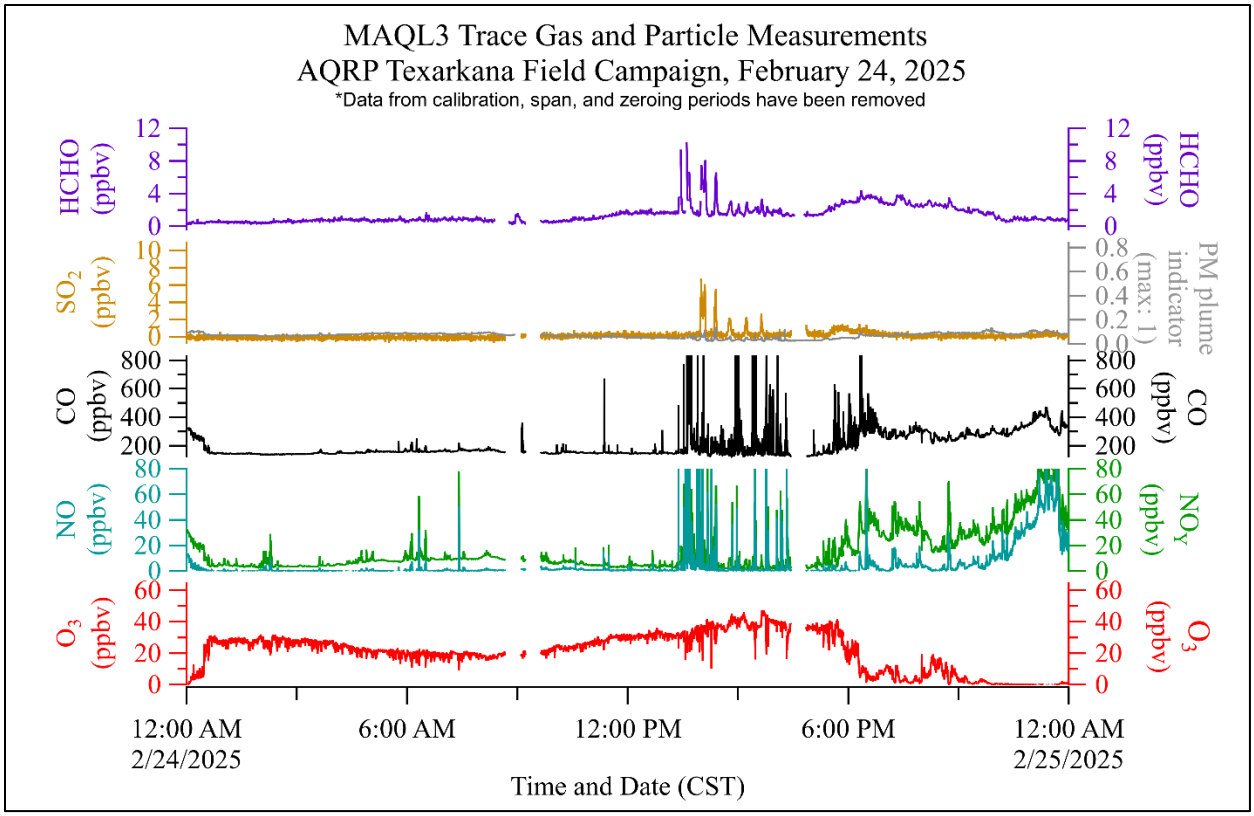

Figure 80. *Data summary of several of the MAQL3 measurements made during the Texarkana campaign. O_3, NO, NO_y, SO_2, CO, HCHO, and the PM relative plume strength indicator (calculated from POPS instrument measurements) are plotted against Central Standard Time. Data was averaged to 10 seconds.*

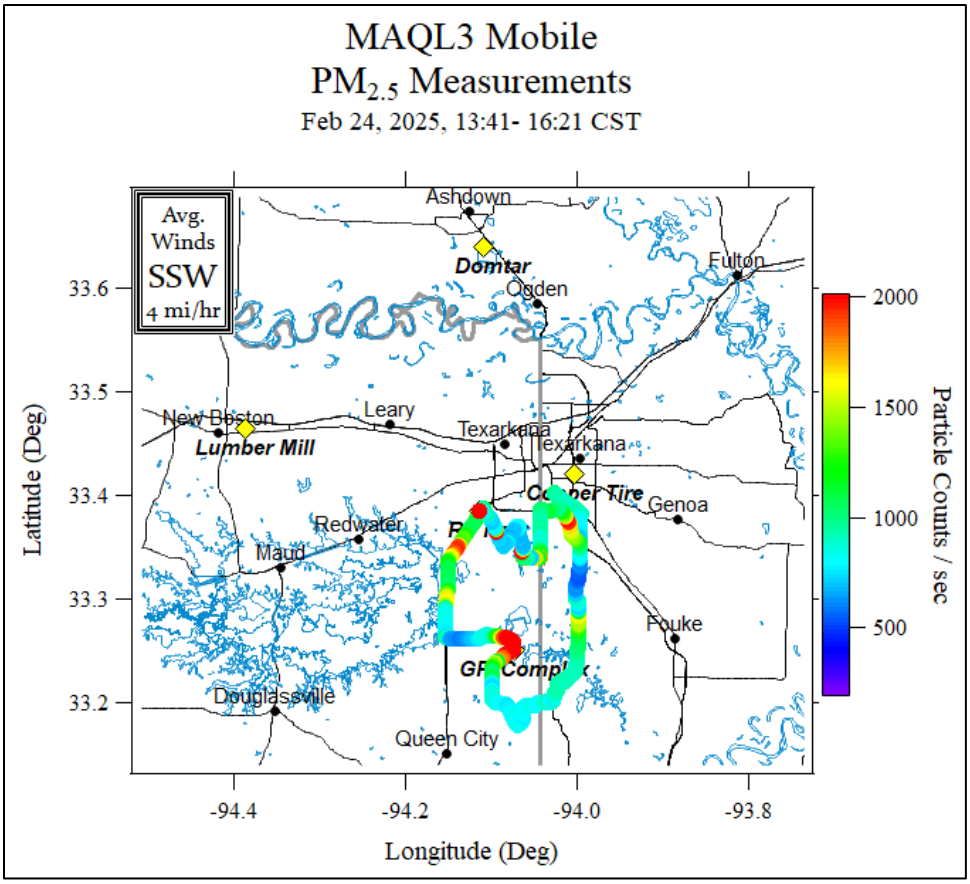

Figure 81. *The UH mobile lab sampling route for February 24, 2025, colored by $PM_{2.5}$ particle count per second measured by the MAQL3 POPS instrument. Average wind conditions (upper left), as reported by CAMS 1031, were calculated for the mobile sampling period (top of graph). The most recent tracks overlay older ones.*

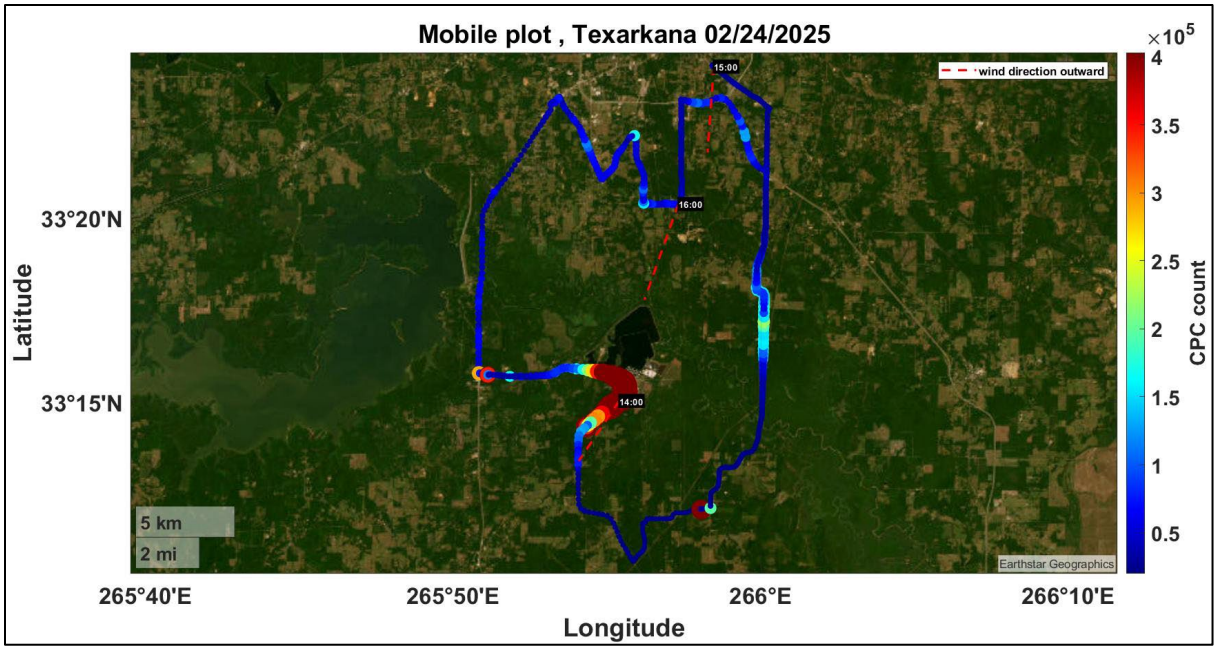

Figure 82. *The MAQL3 sampling route for February 24, 2025, colored by CPC particle count. Average hourly wind direction indicated by dash red lines, as reported by CAMS 1031, were calculated for the mobile sampling period. The most recent tracks overlay older ones.*

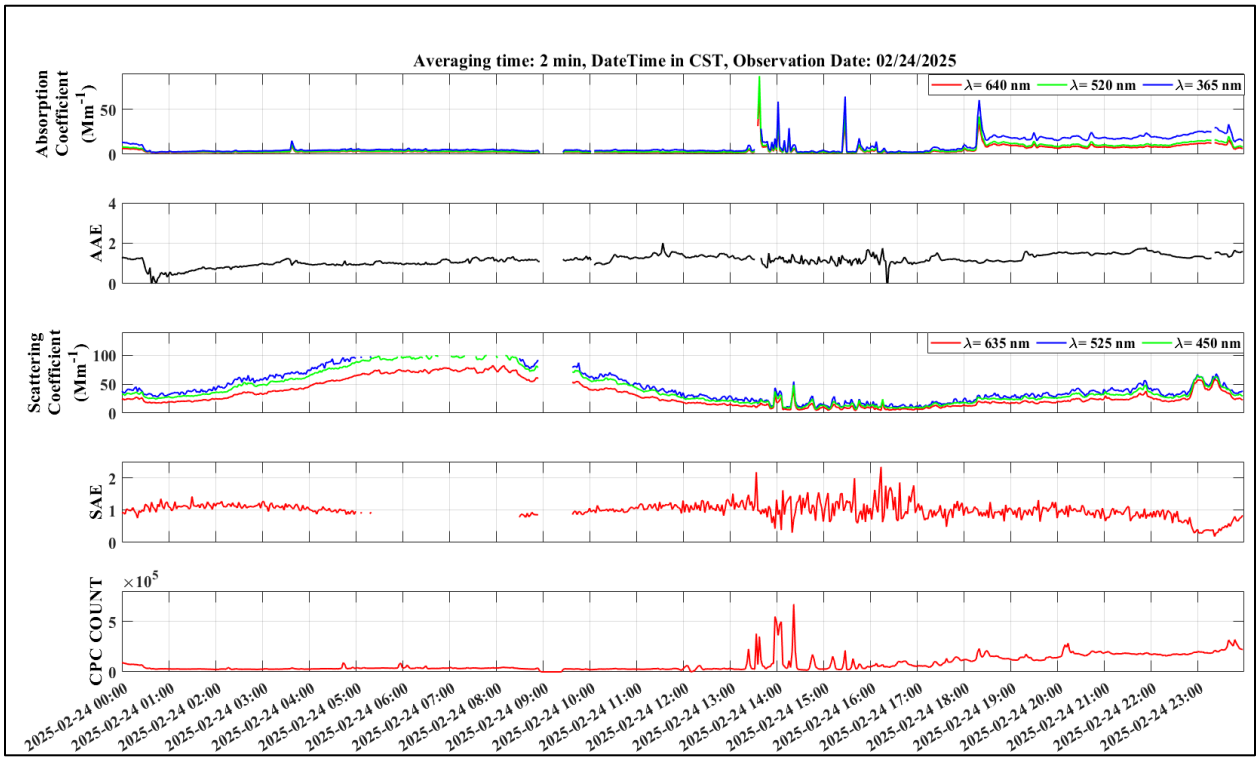

Figure 83*. Time-series data of select MAQL3 aerosol measurements made during the Texarkana campaign for February 24, 2025. Absorption and scattering coefficients, AAE and SAE (calculated values), and particle counts averaged over 120 seconds.*

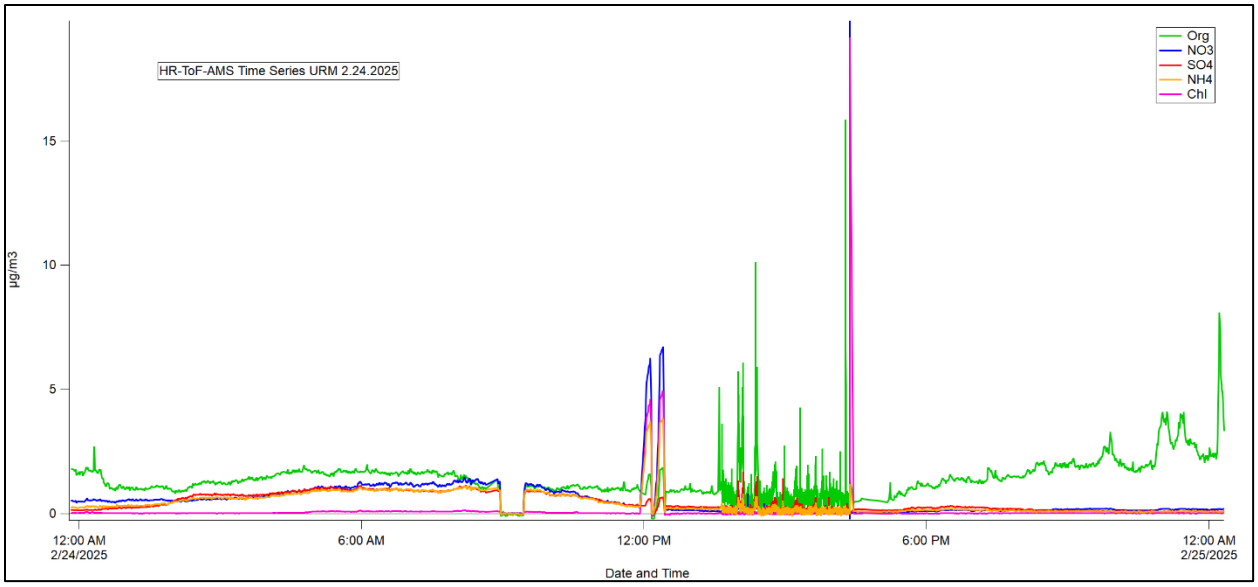

Figure 84. *Time-series data of select HR-ToF-AMS species (Organics, Nitrate, Sulfate, Ammonium, Chloride) made during the Texarkana campaign for February 24, 2025.*

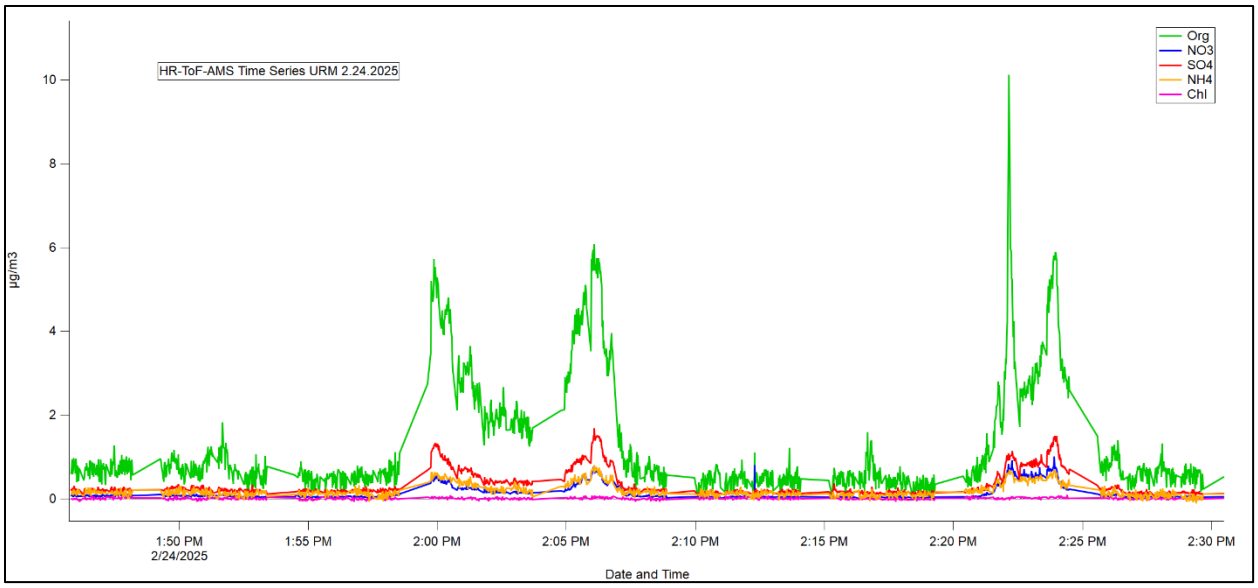

Figure 85. *Time-series data of select HR-ToF-AMS species (Organics, Nitrate, Sulfate, Ammonium, Chloride) made during the Texarkana campaign for February 24, 2025, focusing on the emissions directly downwind of the GPI plant.*

February 25, 2025

MAQL3 drove to Ashdown via the I-49 loop and observed the Domtar plume; however, the plume was not in a favorable position to conduct stationary sampling. On the return, approximately 1.5 laps were completed around the Texarkana loop. Sampling concluded early to prepare for an early morning sampling targeting favorable southerly winds. Coordination with

the Aerodyne van was challenging following the crew change, resulting in communication gaps and poor coordination of plan adjustments, which caused significant separation between vehicles throughout the day.

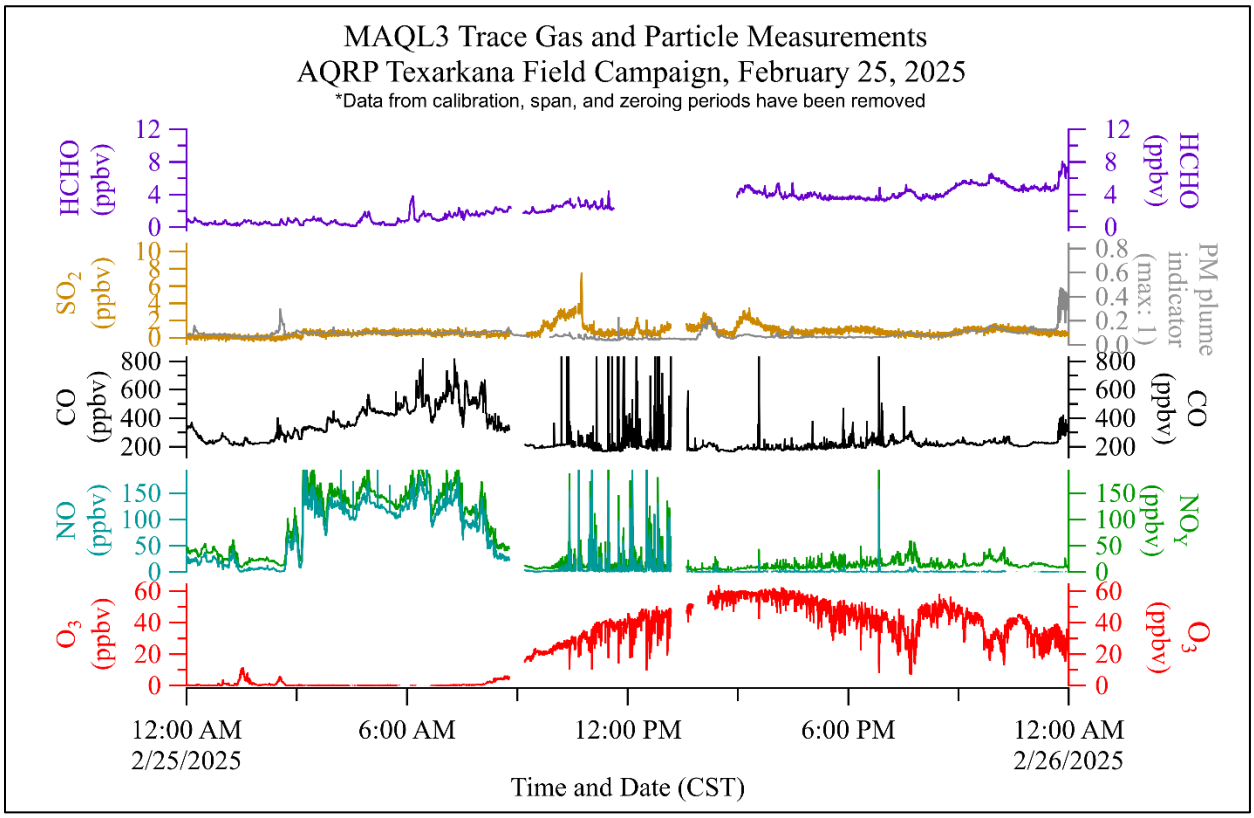

Figure 86. *Data summary of several of the MAQL3 measurements made during the Texarkana campaign. O_3, NO, NO_y, SO_2, CO, HCHO, and the particulate matter (PM) relative plume strength indicator (calculated from POPS instrument measurements) are plotted against Central Standard Time. Data was averaged to 10 seconds.*

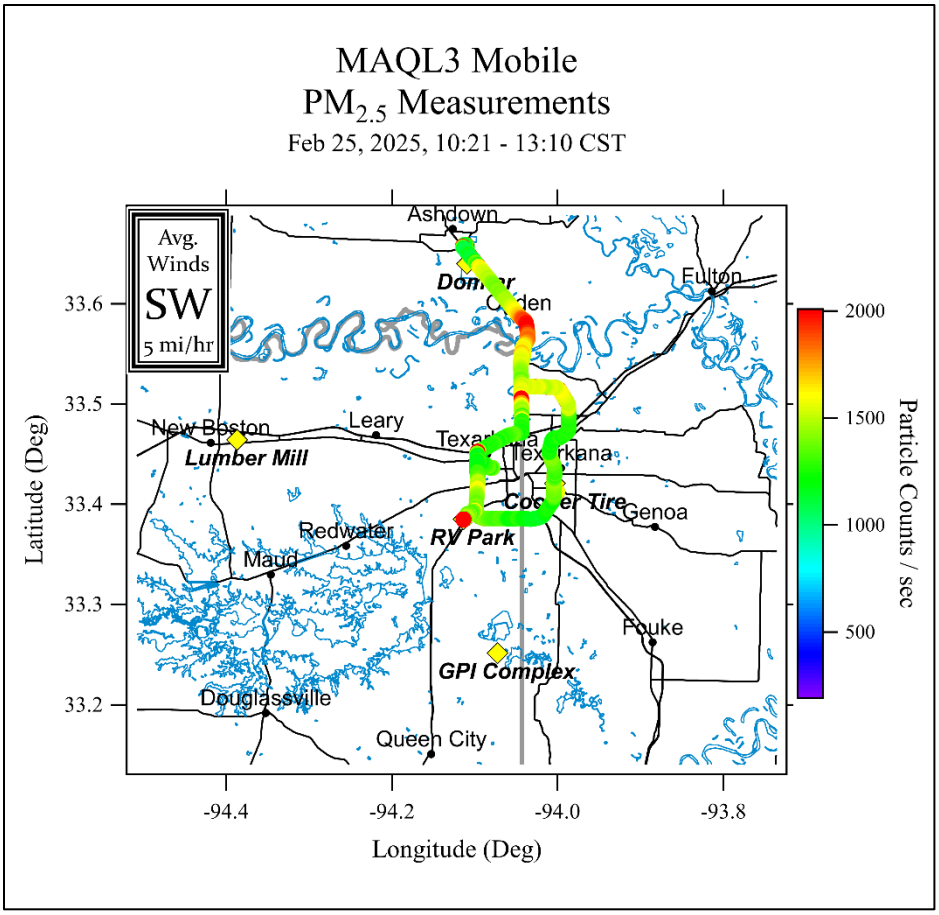

Figure 87. *The UH mobile lab sampling route for February 25, 2025, colored by $PM_{2.5}$ particle count per second measured by the MAQL3 POPS instrument. Average wind conditions (upper left), as reported by CAMS 1031, were calculated for the mobile sampling period (top of graph). The most recent tracks overlay older ones.*

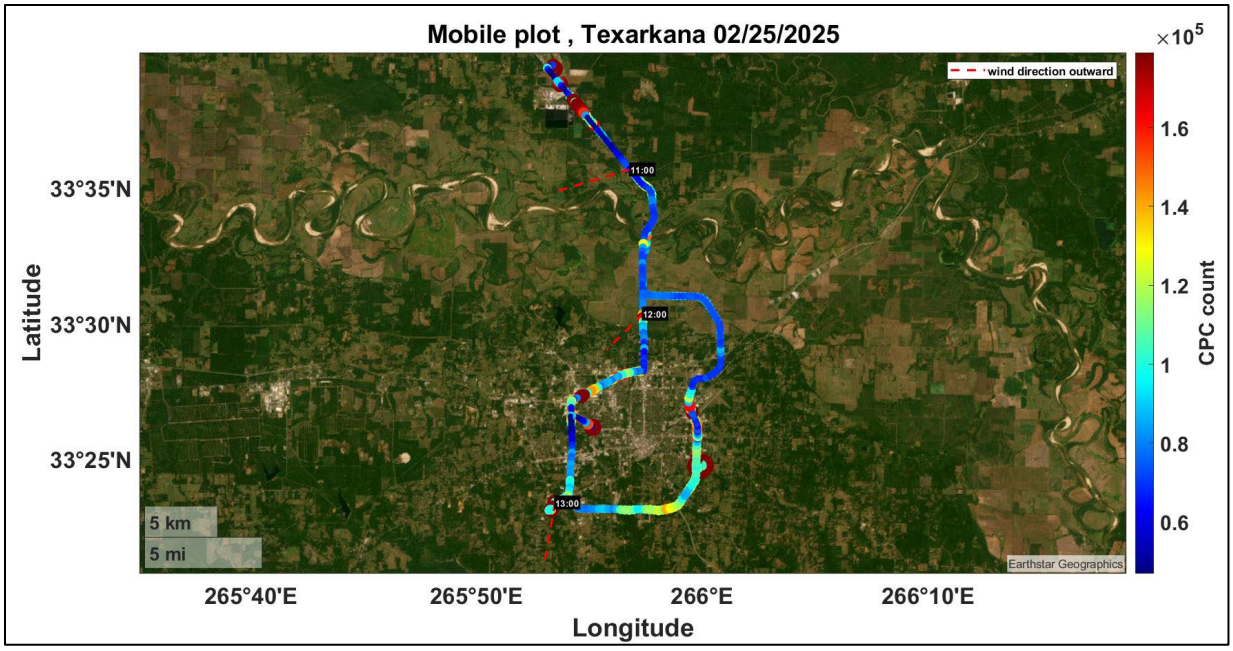

Figure 88. *The MAQL3 sampling route for February 25, 2025, colored by CPC particle count. Average hourly wind direction indicated by dash red lines, as reported by CAMS 1031, were calculated for the mobile sampling period. The most recent tracks overlay older ones.*

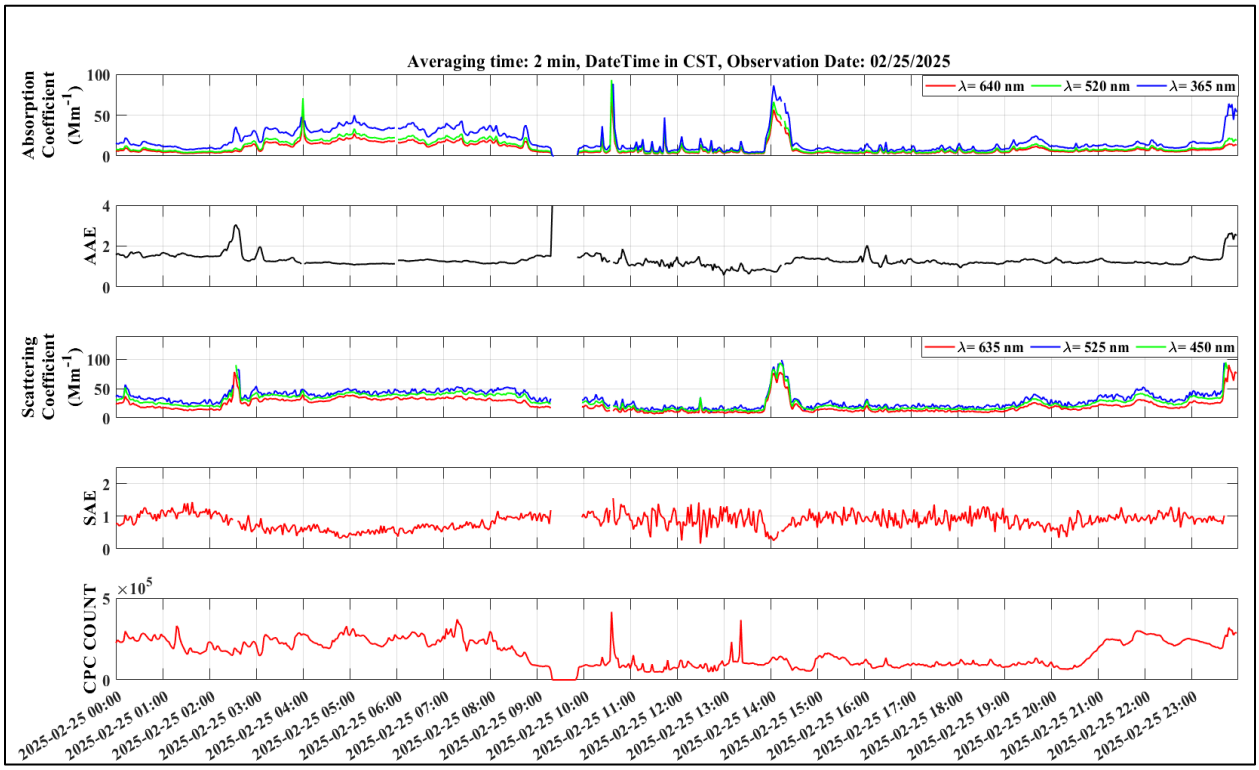

Figure 89. *Time-series data of select MAQL3 aerosol measurements made during the Texarkana campaign for February 25, 2025. Absorption and scattering coefficients, AAE and SAE (calculated values) and particle counts averaged over 120 seconds.*

February 26, 2025

Early morning sampling was conducted to capture the GPI plume under southerly wind conditions. An upwind pass was made near Queen City, followed by a return to the area near the closed road by Domino Mill around sunrise, then north to the Buchanan Loop area, and over to a parking location just south of the 151 loops. Around sunrise, winds became calm, and fog developed over fields. The MAQL3 then drove 93 to 67 to 82, positioning near the monitor. Southerly winds resumed, but the plume remained east of the monitor. The MAQL3 drove east to intercept a moderate GPI plume in Texarkana before heading south. Winds shifted to the southwest, and a strong plume was encountered along AR-237, I-49, and Highway 71. Multiple successful downwind passes were completed at varying distances before returning to the RV park.

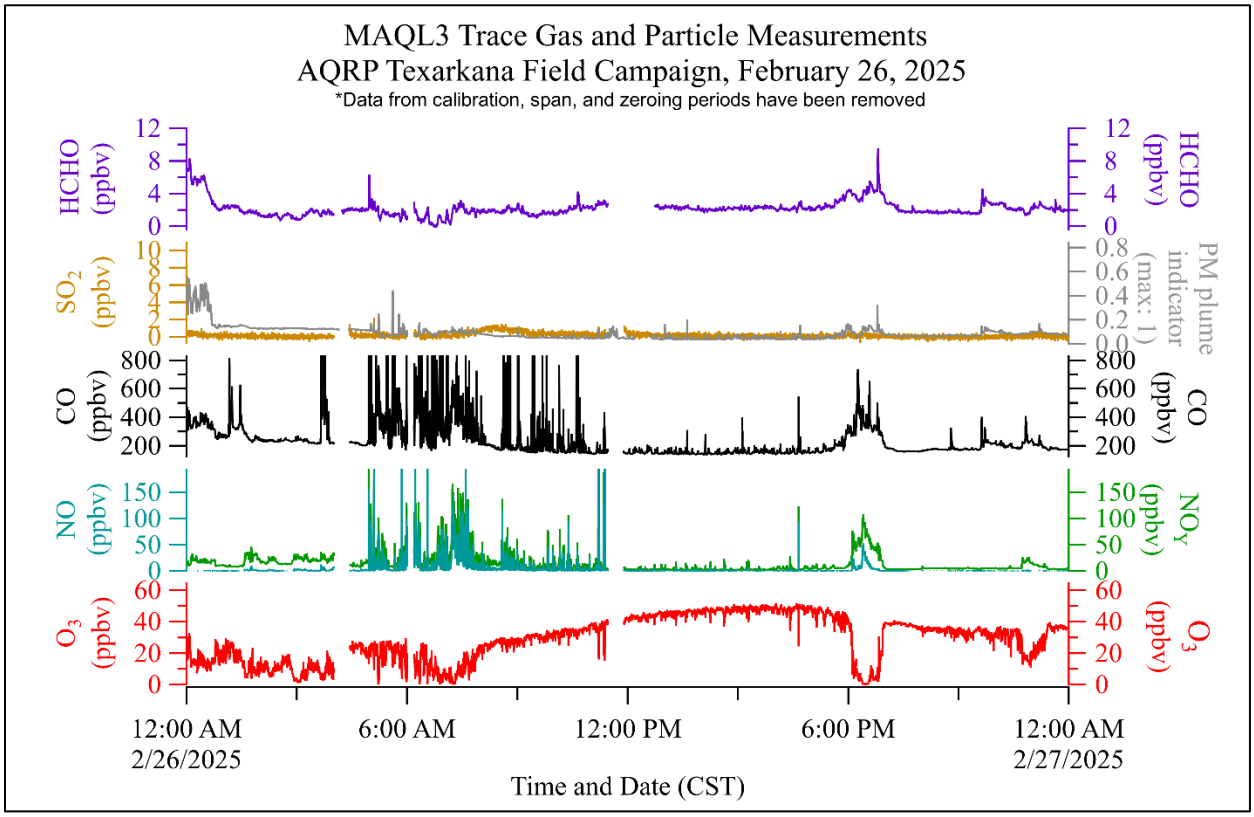

Figure 90. *Data summary of several of the MAQL3 measurements made during the Texarkana campaign. O_3, NO, NO_y, SO_2, CO, HCHO, and the particulate matter (PM) relative plume strength indicator (calculated from POPS instrument measurements) are plotted against Central Standard Time. Data was averaged to 10 seconds.*

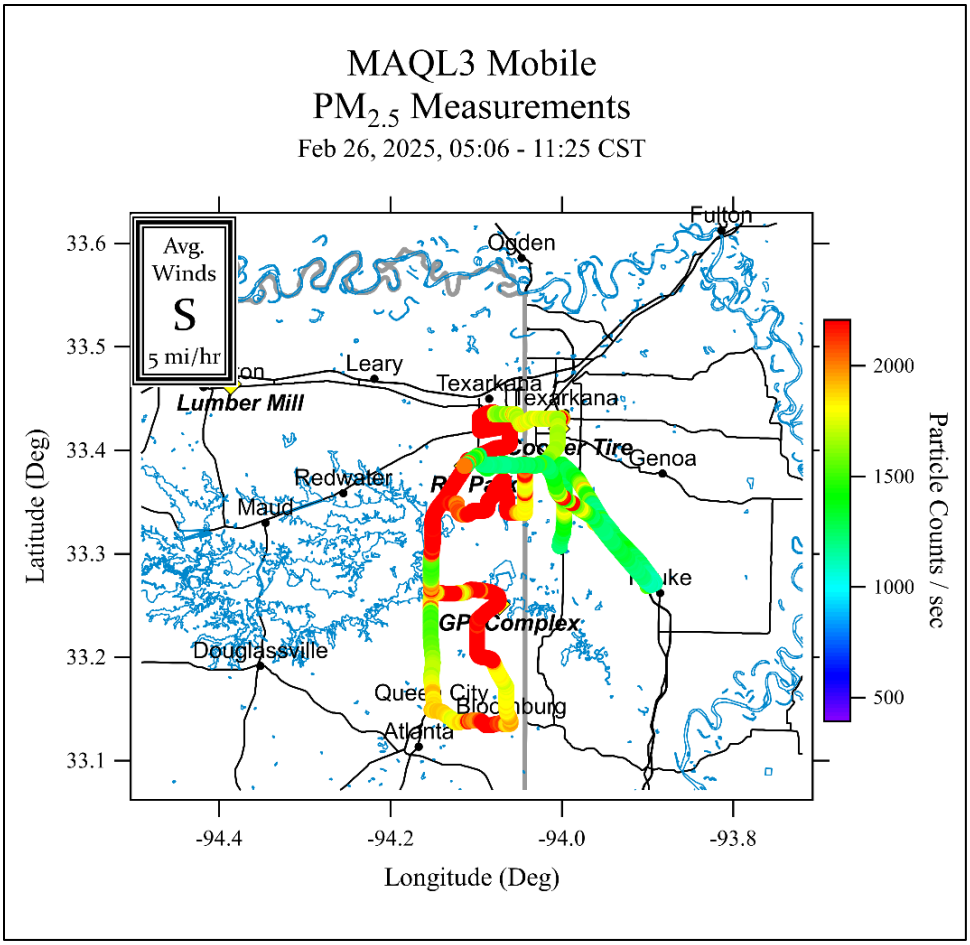

Figure 91. *The UH mobile lab sampling route for February 26, 2025, colored by $PM_{2.5}$ particle count per second measured by the MAQL3 POPS instrument. Average wind conditions (upper left), as reported by CAMS 1031, were calculated for the mobile sampling period (top of graph). The most recent tracks overlay older ones.*

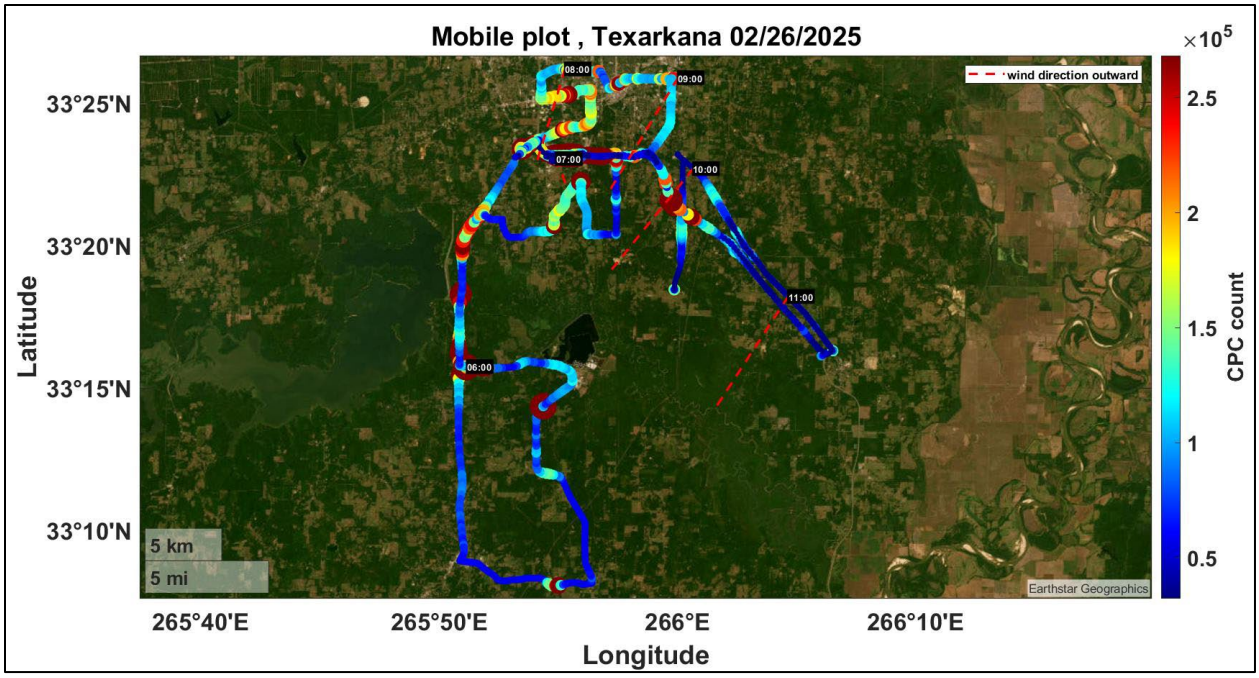

Figure 92. *The MAQL3 sampling route for February 26, 2025, colored by CPC particle count. Average hourly wind direction indicated by dash red lines, as reported by CAMS 1031, were calculated for the mobile sampling period. The most recent tracks overlay older ones.*

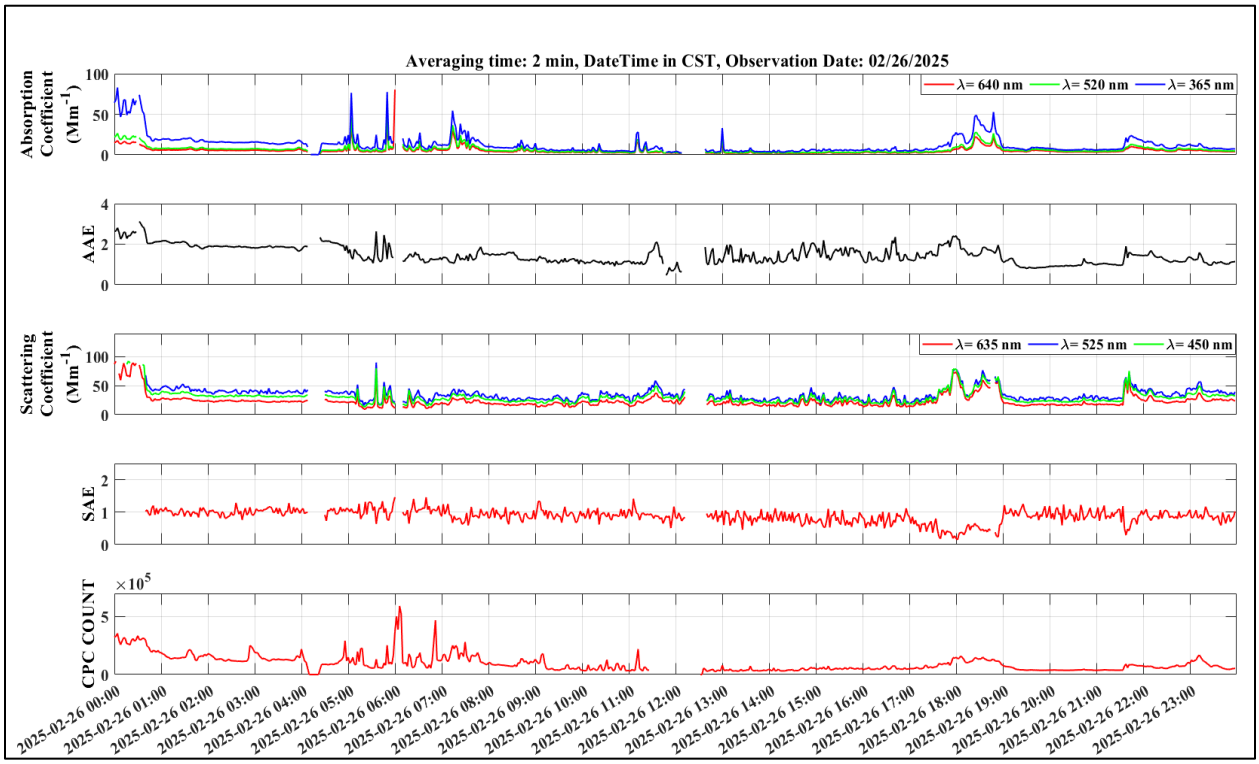

Figure 93. *Time-series data of select MAQL3 aerosol measurements made during the Texarkana campaign for February 26, 2025. Absorption and scattering coefficients, AAE and SAE (calculated values) and particle counts averaged over 120 seconds.*

February 27, 2025

MAQL3 traveled west on I-30 to just before New Boston, then south to Highway 82 and west along 82 to conduct downwind sampling of the lumber mill. The route continued south on Highway 8, then west along a series of FM roads to complete a second downwind pass targeting both the lumber mill and Red River Army Depot (RRAD). No significant plume was observed on the east side of RRAD. The team then followed the previous route north of I-30 to sample the Domtar plume, concluding with a stop at the TCEQ monitor in Texarkana. Afterward, the team investigated the southeast corner of the Texarkana loop for a previously observed mystery PM source but did not detect any significant plume activity during this pass. The day concluded with refueling and a return to the RV park.

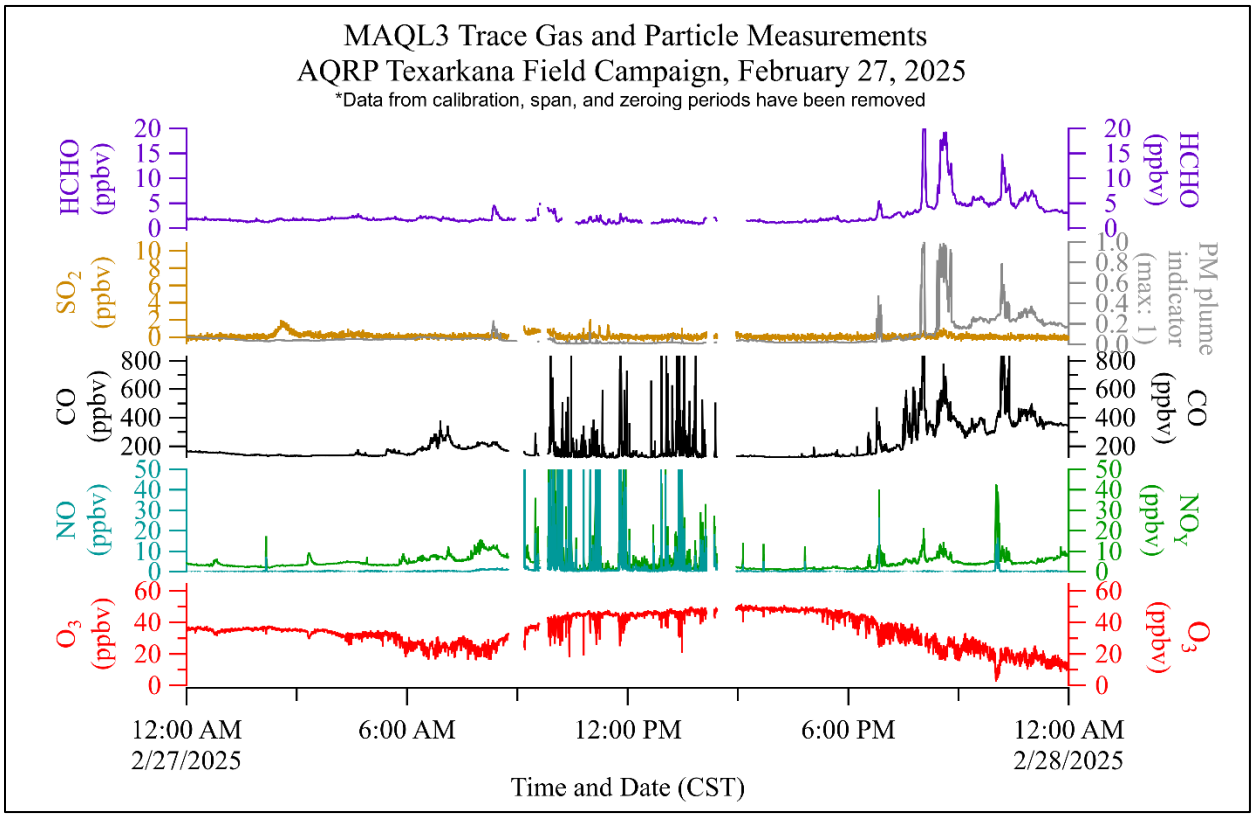

Figure 94. *Data summary of several of the MAQL3 measurements made during the Texarkana campaign. O_3, NO, NO_y, SO_2, CO, HCHO, and the particulate matter (PM) relative plume strength indicator (calculated from POPS instrument measurements) are plotted against Central Standard Time. Data was averaged to 10 seconds.*

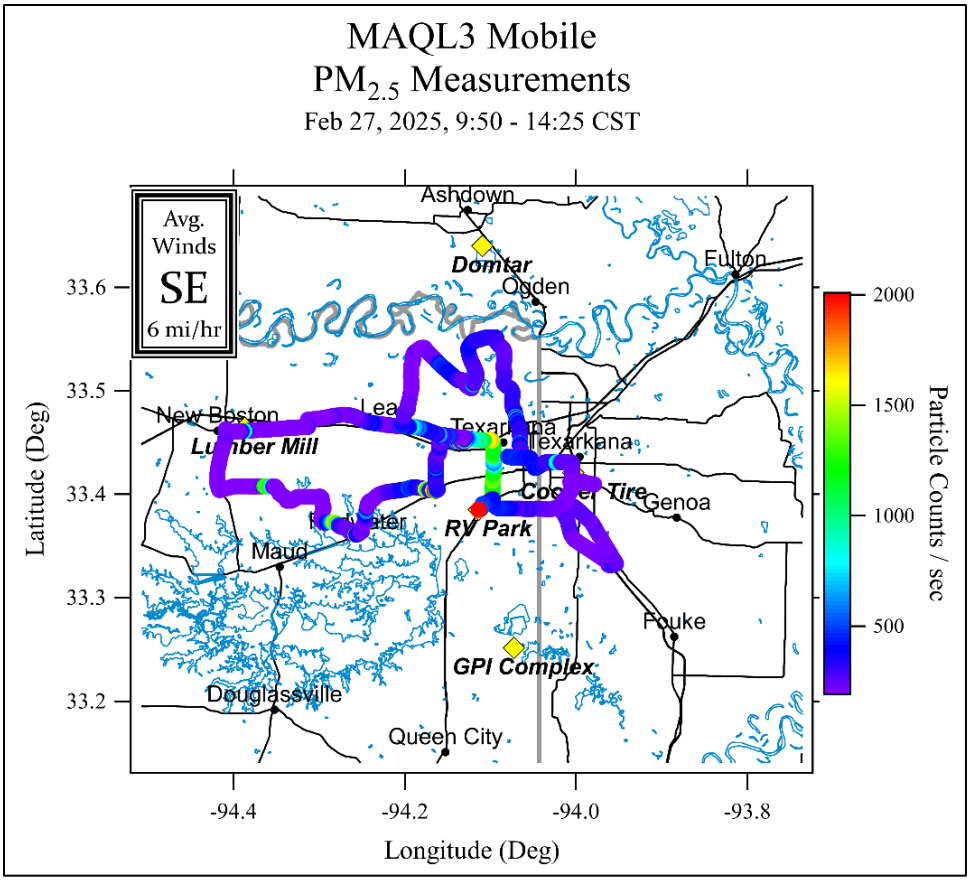

Figure 95. *The UH mobile lab sampling route for February 27, 2025, colored by $PM_{2.5}$ particle count per second measured by the MAQL3 POPS instrument. Average wind conditions (upper left), as reported by CAMS 1031, were calculated for the mobile sampling period (top of graph). The most recent tracks overlay older ones.*

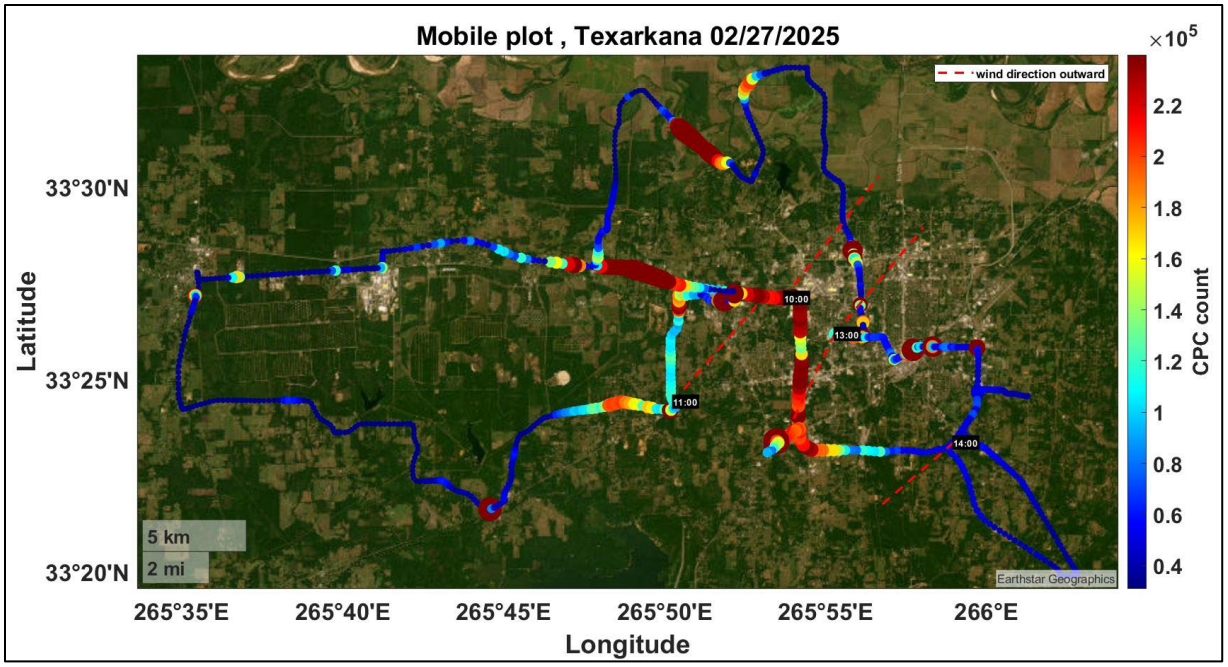

Figure 96. *The MAQL3 sampling route for February 27, 2025, colored by CPC particle count. Average hourly wind direction indicated by dash red lines, as reported by CAMS 1031, were calculated for the mobile sampling period. The most recent tracks overlay older ones.*

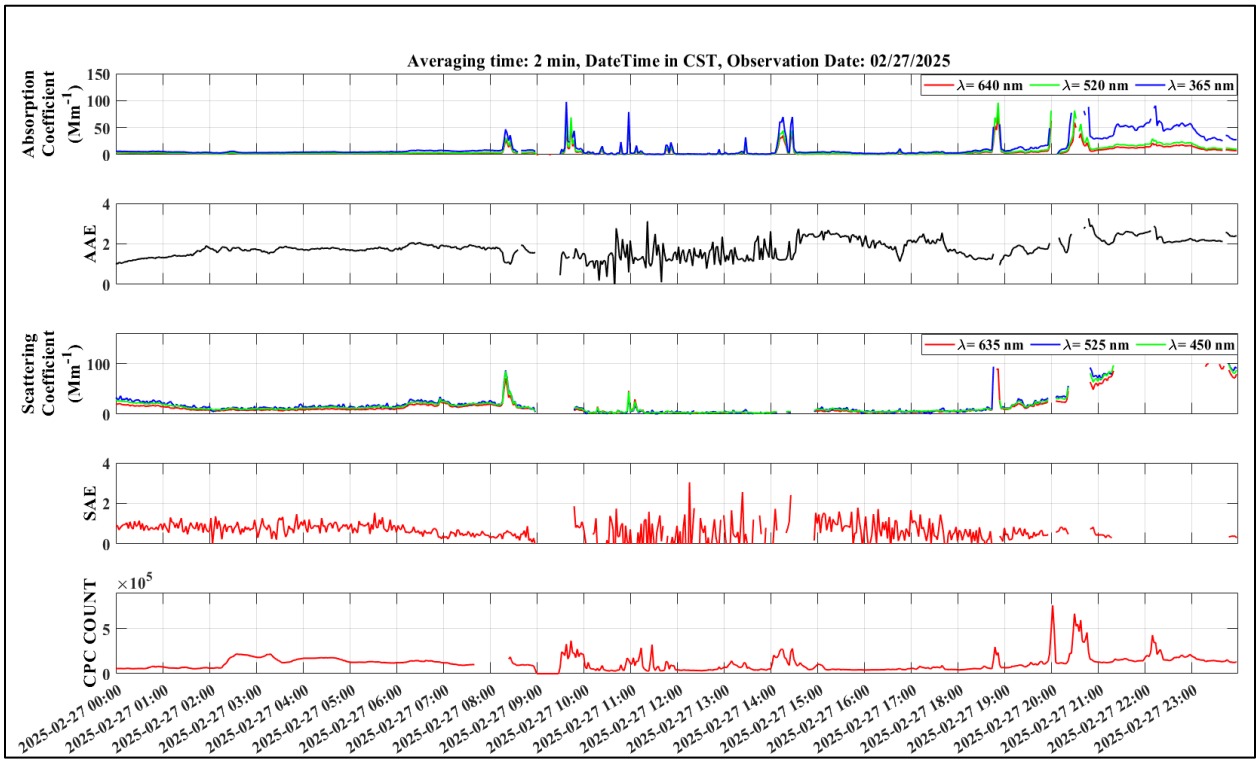

Figure 97. *Time-series data of select MAQL3 aerosol measurements made during the Texarkana campaign for February 27, 2025. Absorption and scattering coefficients, AAE and SAE (calculated values) and particle counts averaged over 120 seconds.*

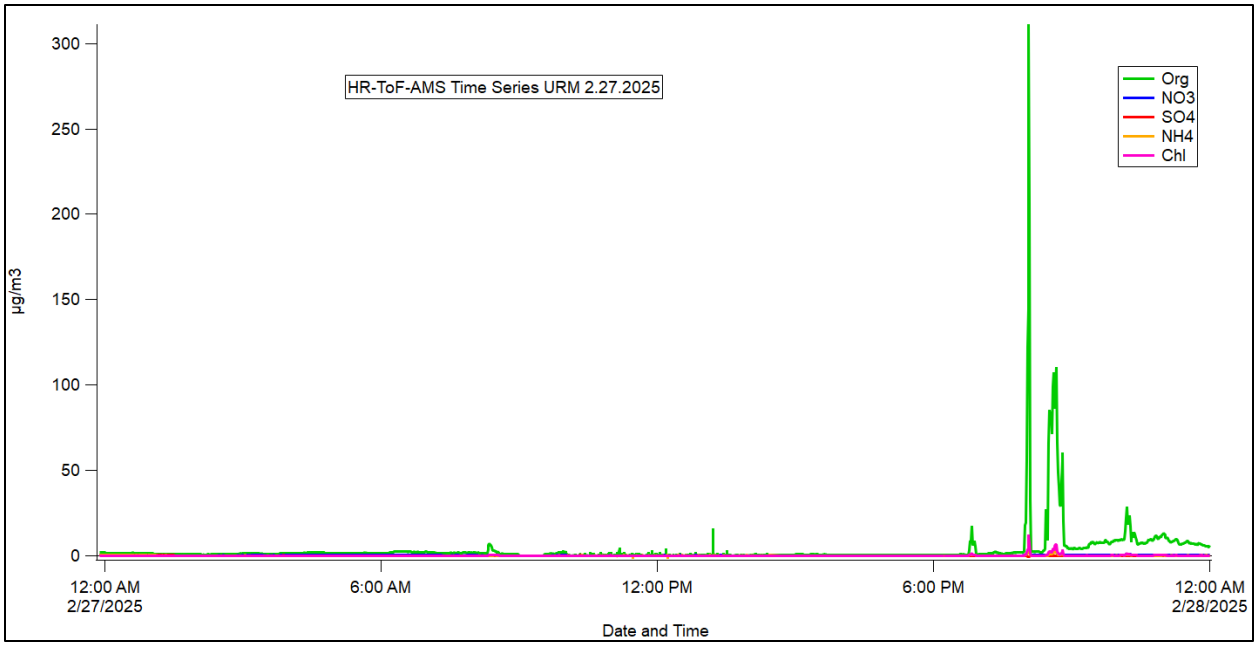

***Figure 98**. Time-series data of select HR-ToF-AMS species (Organics, Nitrate, Sulfate, Ammonium, Chloride) made during the Texarkana campaign for February 27, 2025.*

February 28, 2025

MAQL3 drove to a potential controlled burn plume near Red River Army Depot (RRAD), but the event appeared to have wrapped up. Some minor local yard debris burning was observed. Baylor had reported a large plume seen earlier during the drive from Waco. Before departing the RV park, Aerodyne sampled the area and obtained a GC sample while still within the biomass burning plume. MAQL3 then proceeded to Domtar, where successful stationary sampling was conducted in various parts of the plume. Significant train activity was also sampled before returning to the RV park.

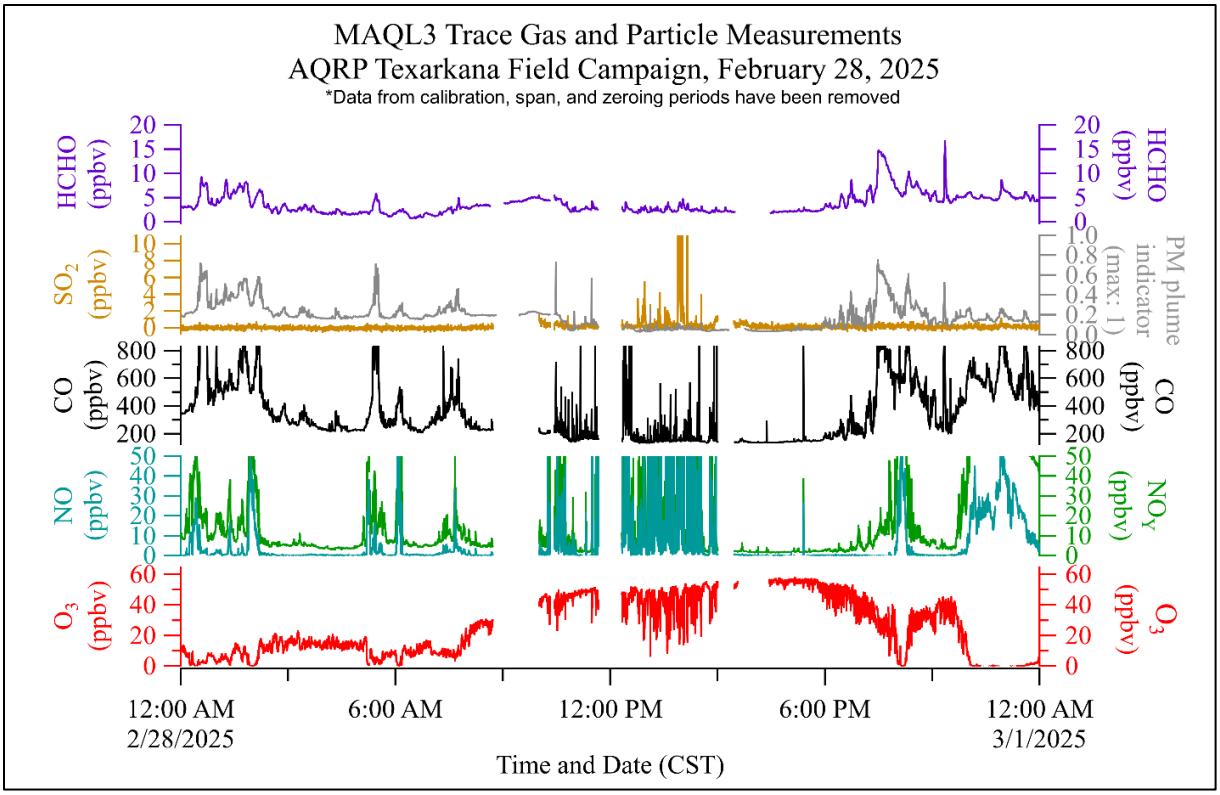

Figure 99. *Data summary of several of the MAQL3 measurements made during the Texarkana campaign. O_3, NO, NO_y, SO_2, CO, HCHO, and the PM relative plume strength indicator (calculated from POPS instrument measurements) are plotted against Central Standard Time. Data was averaged to 10 seconds.*

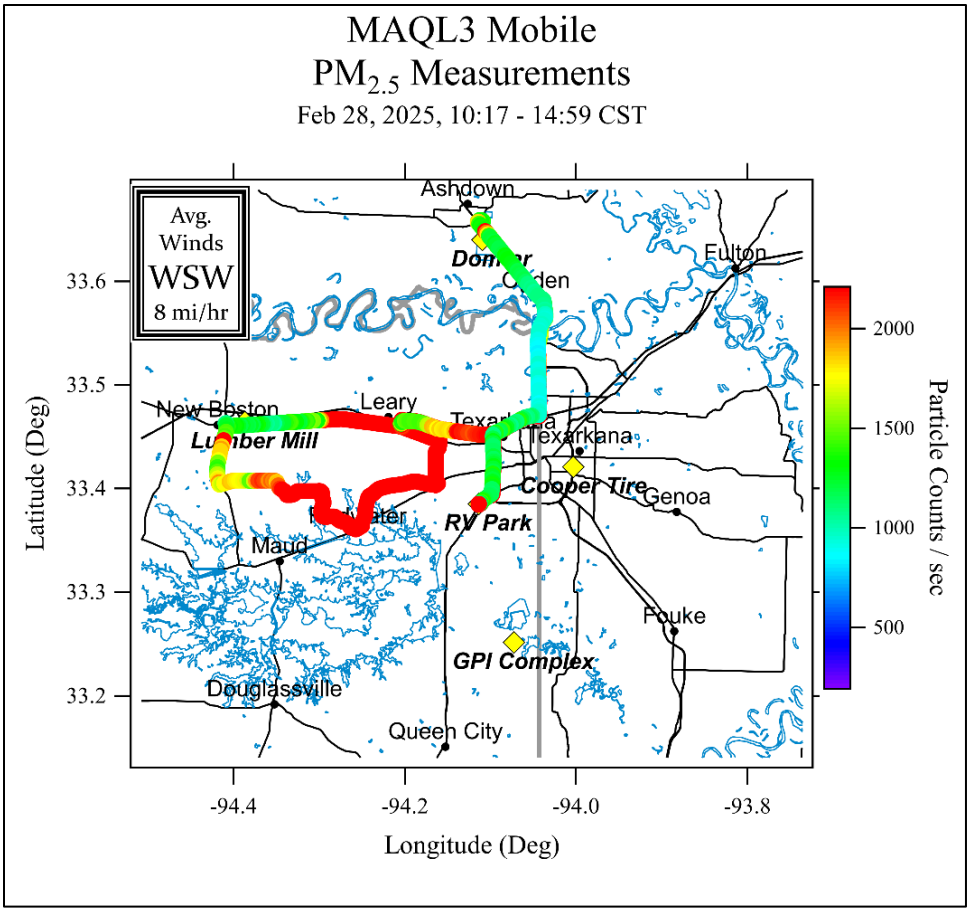

Figure 100. *The UH mobile lab sampling route for February 28, 2025, colored by $PM_{2.5}$ particle count per second measured by the MAQL3 POPS instrument. Average wind conditions (upper left), as reported by CAMS 1031, were calculated for the mobile sampling period (top of graph). The most recent tracks overlay older ones.*

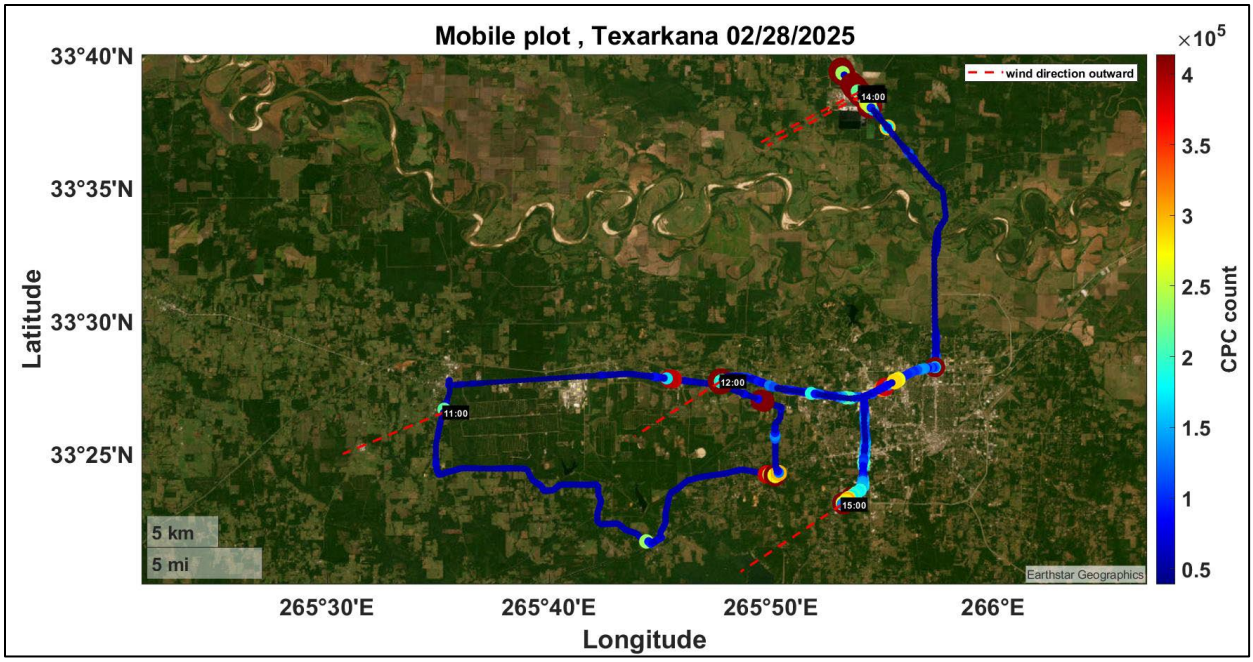

Figure 101. *The MAQL3 sampling route for February 28, 2025, colored by CPC particle count. Average hourly wind direction indicated by dash red lines, as reported by CAMS 1031, were calculated for the mobile sampling period. The most recent tracks overlay older ones.*

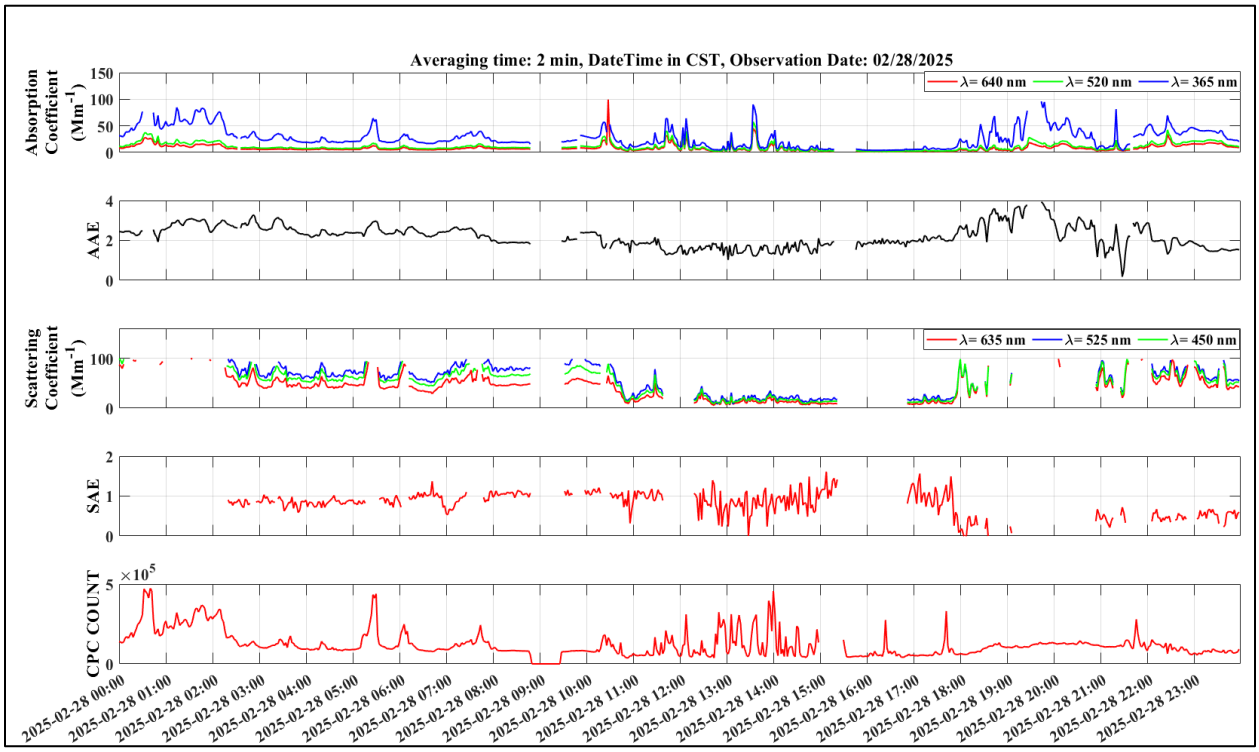

Figure 102. *Time-series data of select MAQL3 aerosol measurements made during the Texarkana campaign for February 28, 2025. Absorption and scattering coefficients, AAE and SAE (calculated values) and particle counts averaged over 120 seconds.*

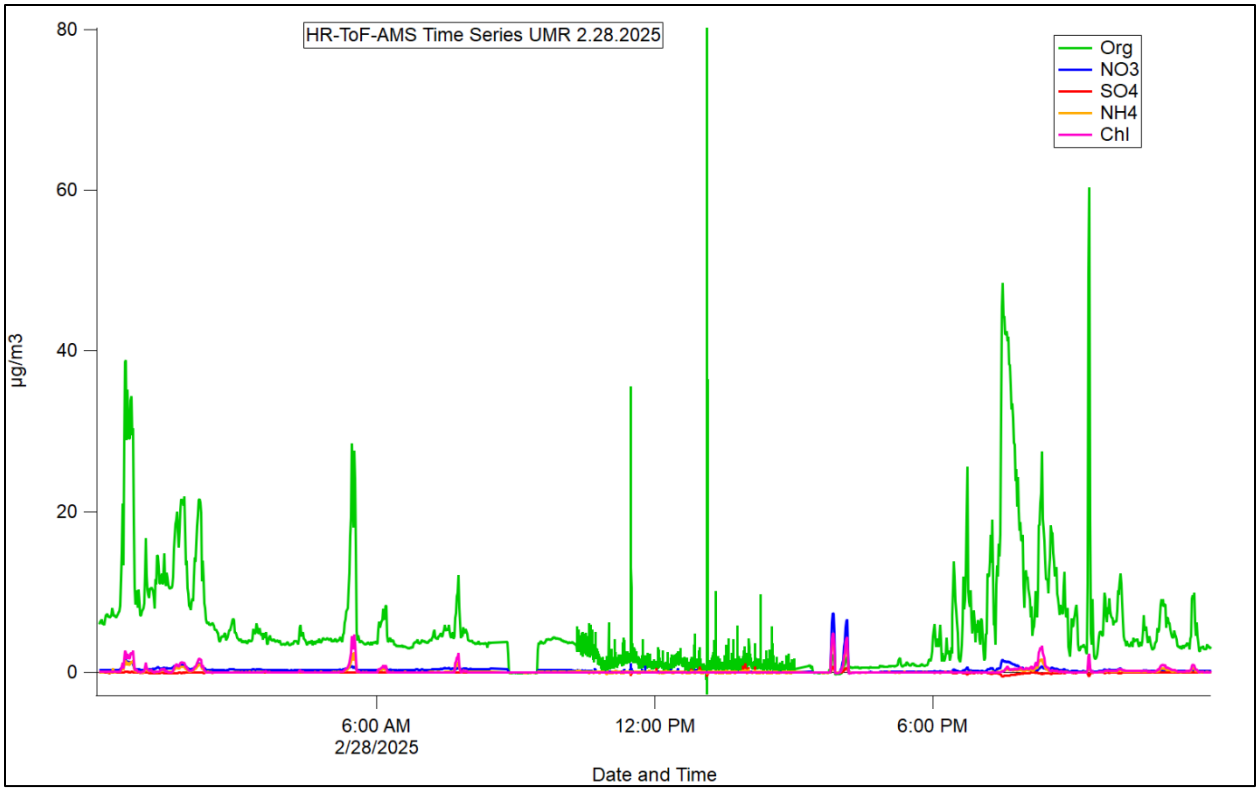

Figure 103. *Time-series data of select HR-ToF-AMS species (Organics, Nitrate, Sulfate, Ammonium, Chloride) made during the Texarkana campaign for February 28, 2025.*

March 1, 2025

MAQL3 went to the TCEQ monitoring site for a period to conduct co-location sampling, then proceeded south to GPI. Several close passes were completed near the facility, along with a few additional downwind passes along FM roads and Highway 59. The route continued north to the Cooper area, where the GPI plume was observed circulating within the town. MAQL3 then returned to the RV park.

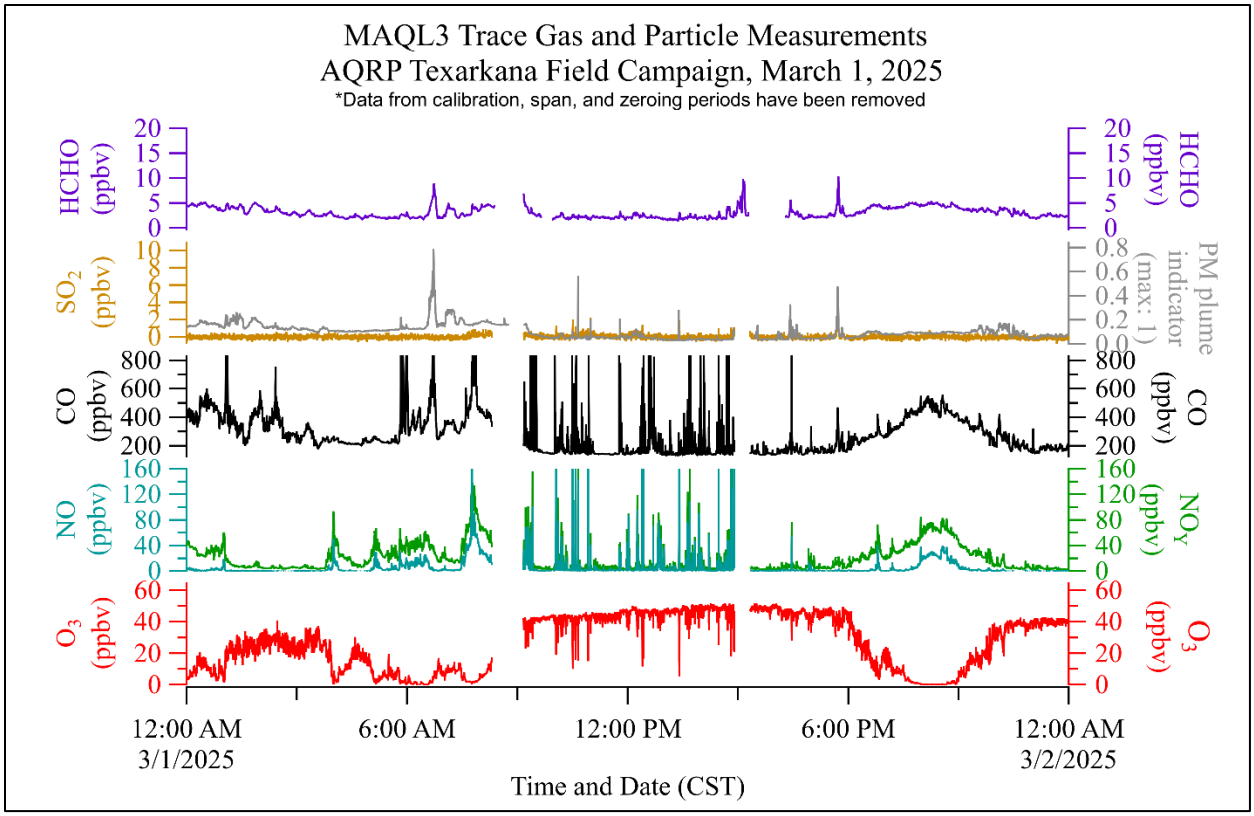

Figure 104. *Data summary of several of the MAQL3 measurements made during the Texarkana campaign. O_3, NO, NO_y, SO_2, CO, HCHO, and the PM relative plume strength indicator (calculated from POPS instrument measurements) are plotted against Central Standard Time. Data was averaged to 10 seconds.*

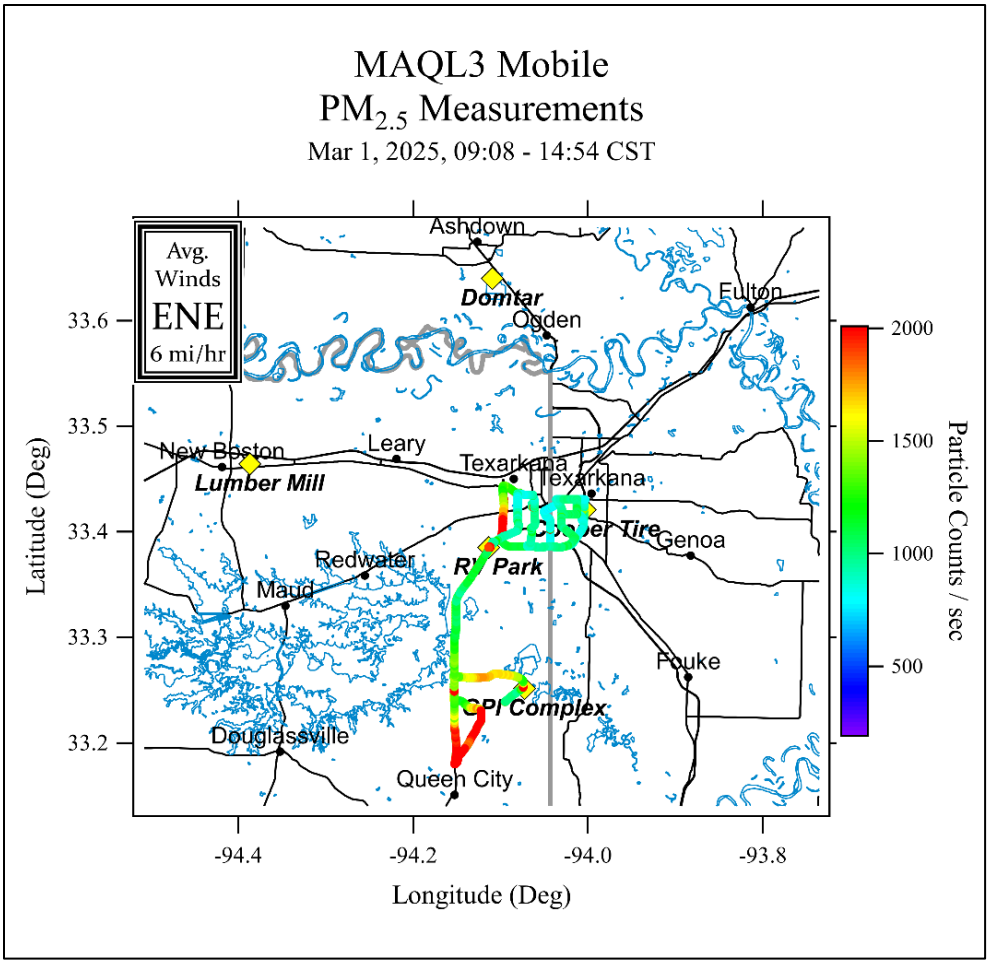

Figure 105. *The UH mobile lab sampling route for March 1, 2025, colored by $PM_{2.5}$ particle count per second measured by the MAQL3 POPS instrument. Average wind conditions (upper left), as reported by CAMS 1031, were calculated for the mobile sampling period (top of graph). The most recent tracks overlay older ones.*

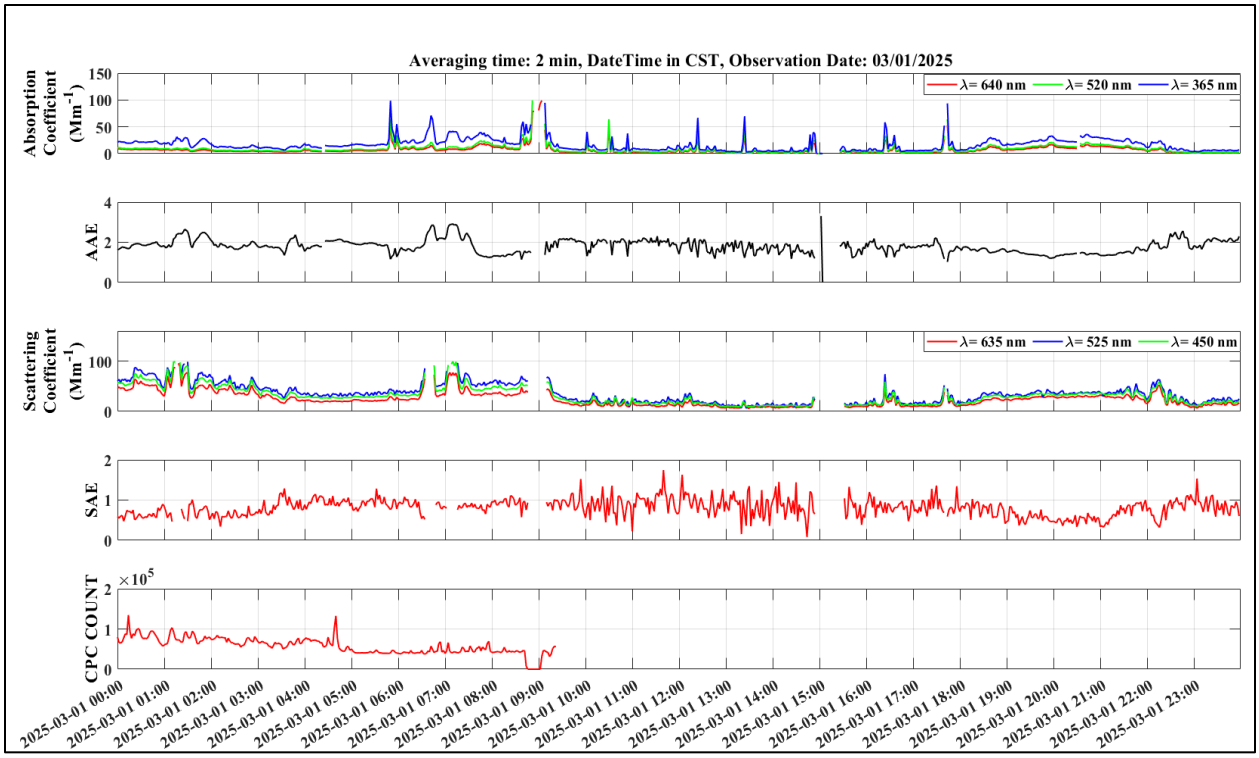

Figure 106. *Time-series data of select MAQL3 aerosol measurements made during the Texarkana campaign for March 1, 2025. Absorption and scattering coefficients, AAE and SAE (calculated values) and particle counts averaged over 120 seconds.*

March 2, 2025

The UH mobile lab continued stationary sampling at the RV park until late morning and continued sampling as it departed the Texarkana area.

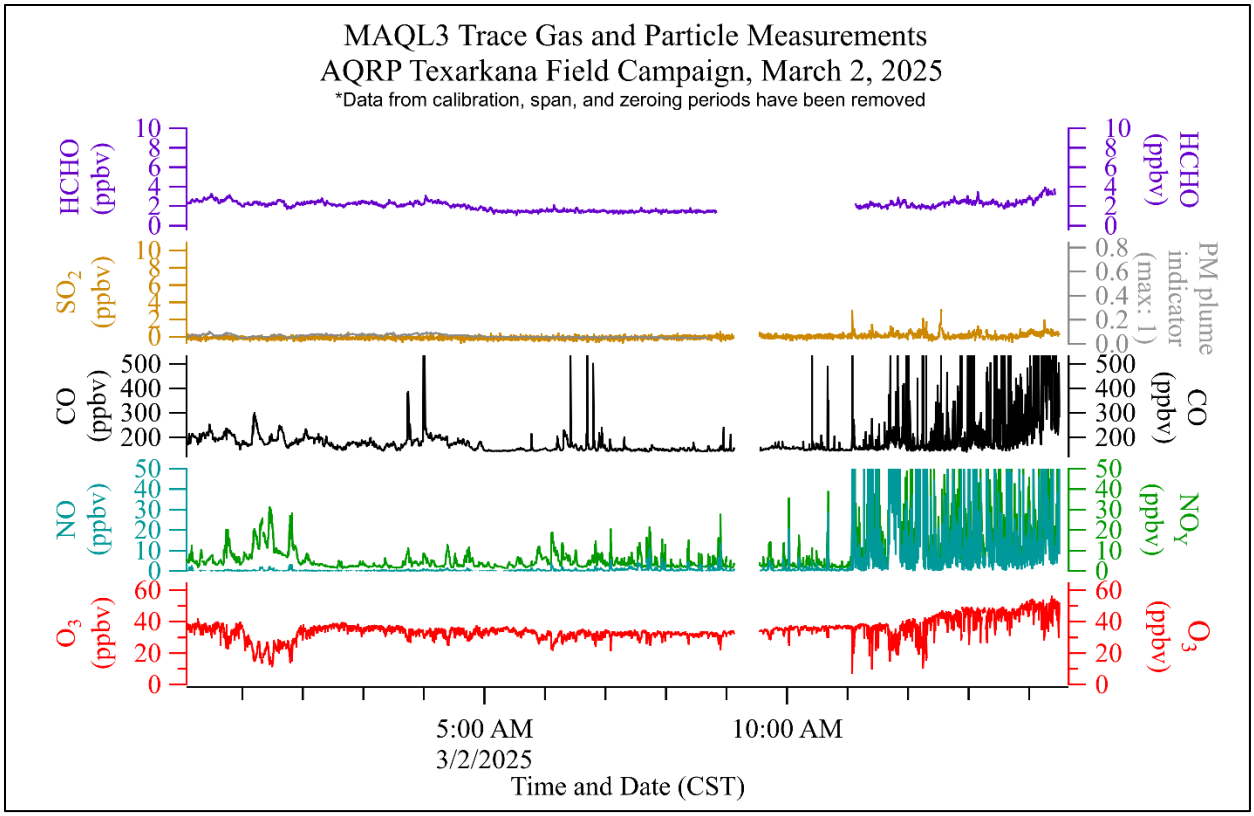

Figure 107. *Data summary of several of the MAQL3 measurements made during the Texarkana campaign. O_3, NO, NO_y, SO_2, CO, HCHO, and the particulate matter (PM) relative plume strength indicator (calculated from POPS instrument measurements) are plotted against Central Standard Time. Data was averaged to 10 seconds.*